The Dissertation Committee for Samantha Allison Moore Certifies that this is the approved version of the following dissertation:

Investigations of Laser-Induced Neuronal Guidance

Committee:

Mark G. Raizen, Supervisor

Ernst-Ludwig Florin

Wolfgang Frey

Jack B. Swift

Harry L. Swinney

Investigations of Laser-Induced Neuronal Guidance

by

Samantha Allison Moore, B. S.

Dissertation

Presented to the Faculty of the Graduate School of

The University of Texas at Austin

in Partial Fulfillment

of the Requirements

for the Degree of

Doctor of Philosophy

The University of Texas at Austin

December, 2004

Dedication

To my beloved husband, through whom I have come to believe in miracles.

Acknowledgements

I would like to thank everyone in the Center for Nonlinear Dynamics, members both past and present: it has been an honor to work with you. Especially significant, of course, have been the contributions of program designers Florian Schreck and Jakub Otwinowski as well as undergraduate research assistants Abe Peña and Alex Ramirez, for their dedicated, tireless and cheerful labors. I would like also to acknowledge the work of former group members Katrin Schmitt and Chris Kopech.

I am deeply indebted, as well, to scientists from many departments at the University of Texas at Austin who contributed to the success of this interdisciplinary endeavour, and especially to Wesley Thompson, John Wallingford, Jason Shear, Richard Allen, Rick Morrisset, Laurea Diaz, and Jerry Fineg. It is through the influence of UT Austin's IGERT program that my life has taken an exciting turn, and I wish sincerely to thank its leaders, Rebecca Richards-Kortum, Charlotte Harris, and John Wright.

Special acknowledgment goes to our overseas collaborators, especially Allen Ehrlicher, Björn Stuhrmann, and Josef Käs. Also, I am especially indebted to visitors Julie Theriot and Elisha Moses, to whom I extend great thanks for taking the time to see our experiment and for the inspiring conversations we shared.

I would like publicly to praise the heavens for the existence and kindheartedness of Mark Raizen, who not only accepted me into his research group and has generously seen me through to graduation, but also singlehandedly kept the University's biophysics program running during a crucial interim period.

Finally, my most heartfelt thanks goes to members of my family for their undying support and encouragement through some very trying times indeed.

Investigations of Laser-Induced Neuronal Guidance

Publication No._____

Samantha Allison Moore, Ph.D.

The University of Texas at Austin, 2004

Supervisor: Mark G. Raizen

One of the long-standing goals of neuroscience has been to look for ways in which to control neuronal growth. It has been discovered recently that placing a focused near-infrared laser spot at the leading edge of a neuronal growth cone elicits a turn in the direction of the laser spot [Ehrlicher *et al.*, PNAS **99**: 16024 (2002)]. Optical guidance has the advantage over conventional neuronal guidance methods that neither steric strain nor chemical gradients are necessary to its functionality. Although the success of optical guidance suggests potential therapeutic applications, our first priority is to decipher the mechanism underlying the phenomenon in order better to understand it. Several hypotheses are presented as well as preliminary evidence supporting biased diffusion as an appropriate model for the system.

Table of Contents

I. INTRODUCTION

1. An Integrative Approach

"Surely there is a time to submit to guidance
and a time to take one's own way at all hazards."

Thomas Henry Huxley (1825-1895)

Despite some historical divisions, physics and biology have come together in recent decades to bring the scientific community remarkable insights previously inaccessible to either discipline alone. From biological applications of nonlinear optics, such as multi-photon microscopy, to complex theories in polymer dynamics, biophysics bridges a gap between two subjects which, although complementary in many ways, still may seem to lie in very distant corners of intellectual Hilbert space.

This dissertation represents one small venture into biophysics research, specifically an examination of the recently discovered phenomenon of optical neuronal guidance [Ehrlicher *et al.*, 2002]. Originally inspired by the shared curiosity of two physics professors at the University of Texas at Austin (Raizen and Käs) as to whether laser light could direct the growth of cultured neuronal cells, this project has since included efforts from biologists, chemists, neuroscientists, and pharmacologists, both in the United States and in Europe. That which follows, however, is addressed to an audience of physicists, and accordingly, a bit of background information concerning the nature of the biological systems under consideration would be apposite at this juncture.

2. Neurons

2.1 The Function of Neurons

Neurons play a unique role physiologically as signal transducers in living beings. Communication among neurons occurs through both chemical and electrical signals, and which method a neuron employs depends on its location and function in the body. In vertebrate animals, neurons of the brain and spinal column constitute the central nervous system, and these cells are primarily interneurons, or neurons whose function it is to take chemical signals and convert them into electrical signals. Neurons in the brain interconnect to form a complex array of cellular structures which, as a whole, is capable of association, cognition, voluntary motion, and regulation of homeostasis in the rest of the body. The peripheral nervous system consists of both sensory neurons and motorneurons, which conduct information toward and away from the central nervous system, respectively. Sensory neurons include a wide variety of highly-specialized cells which produce electrical signals in response to variations in touch, temperature, sound, light, and chemical composition. The cell bodies of somatic sensory neurons reside within the spinal column, and neurites – long extensions emanating from the cell bodies – are the structures directly receptive to outside signals. Visceral sensory neurons, however, have their receptors located within organs and transmit signals in response to internal stimuli. Motorneurons, which transmit signals from the central nervous system outward to the rest of the body, are separated into three categories and are characterized by the type of control they exert upon muscles. Somatic motorneurons are responsible for voluntary movement, while autonomic motorneurons carry out involuntary actions. Sympathetic and parasympathetic motorneurons are dedicated to the involuntary

relaxation and contraction, respectively, of smooth and cardiac muscle (as distinct from skeletal muscle) in the body.

2.2 Some Structural Features of a Neuron

Neurons typically consist of thin, lengthy processes called neurites emanating from a central cell body, or soma, as shown in Figure 2.1. Neurites are named according to their function as either axons, the structures down which signals propagate away from the soma, or dendrites, the structures which receive signals from other neurons and conduct them to the soma. Before a neuron polarizes – or chooses, based on environmental cues, the directional orientations of its axon and dendrites – it extends many neurites into its surroundings which have not yet resolved into axons or dendrites.

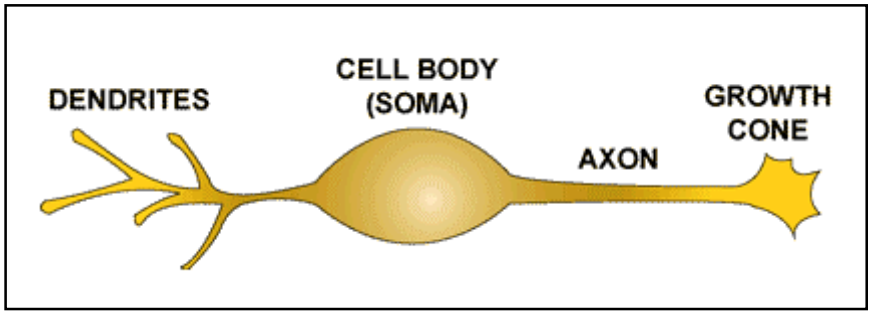

Figure 2.1 The Neuron. Author's rendition of the main structural features of a generic neuron. All processes emanating from the cell body, including both axon and dendrites, are referred to collectively as neurites.

Neurites provide a means by which the neuron gathers information about its environment at a distance from the cell body, and in order to translocate, they must have a means for advancement away from the soma. At the tip of an advancing neurite is a structure called the growth cone, which is a highly active (or motile) site first named by Santiago Ramón y Cajal [Ramón y Cajal, 1890]. The leading edge of the growth cone is the side which lies in the direction in which the neurite is advancing, and is characterized

by ruffling lamellipodia (thin, sheet-like structures, which appear lighter in phase) and sweeping filopodia (finger-like structures, which appear darker in phase due to high concentrations of proteins).

A fundamental internal structure common to all eukaryotic cells is the cytoskeleton, a network of polymerized protein subunits which give cells their shape and allow for cell translocation. There are three principal types of cytoskeletal filaments, distinguished by their constituent proteins: microtubules, actin filaments, and intermediate filaments. Microtubules are composed of distinct α- and β-tubulin monomers which form strands, and 9 of these heteropolymeric protofilaments are arranged in a tubular structure with two lone filaments in the middle of the tube (20 nm total diameter). Microtubules have a very high stiffness, which means that they provide the firmest structural support but are also the most likely to fracture under stress. Also, in conjunction with motor proteins, microtubules provide a means of transport for organelles to different regions of the cell. Actin filaments, often called microfilaments or F-actin (for Filamentous actin), are made of actin monomers, or G-actin (for Globular actin), characterized by a diameter of 7 nm. Actin filaments are termed semiflexible polymers and are considered to be one of the most dynamic components of the cytoskeleton [Lodish *et al.*, 2000], undergoing configurational changes essential to cell movement and serving as the primary determinant of a cell's elasticity. Intermediate filaments, as they are the most flexible of the three types of polymer, cannot provide structural support for the cell on the same order of magnitude as actin filaments and microtubules, so for our considerations concerning cell locomotion, the effects of intermediate filaments can be largely ignored.

Cytoskeletal polymers are usually in a state of dynamic instability, whereby monomers are actively added to or subtracted from the ends of the polymer chains. It is well-known [Lodish, 2000] that both actin and microtubule polymers are asymmetrical, favoring polymerization on one end (named, for this reason, the "plus end") and depolymerization on the opposite end (named the "minus end"). There are three stages in which polymers assemble: nucleation, elongation, and treadmilling. In the nucleation phase, a few monomers assemble into an oligomer, a process whose required energy is greater than that of elongation, in which monomers add to the growing polymer at a rate proportional to the local monomer concentration. When equilibrium has been reached between the rates at which monomers are inclined to add and subtract from a filament, a process called treadmilling, in which monomers are continually added to one end and subtracted from the other, takes place until the equilibrium position of the association and dissociation rate constants shifts. Monomers add to the plus end of cytoskeletal filaments through the hydrolysis of adenosine triphosphate (ATP), which serves as the currency of energy in cells. Through the dephosphorylation of ATP, energy is expended to add each monomer to the filament, but it is a concentration gradient (passive condition) which entices monomers to depart from the other end of the filament and repopulate the monomer pool.

The cytoskeleton plays a vital role in the extension, retraction, and turning of neuronal growth cones. The growth cone is characterized by three domains, as illustrated in Figure 2.2. The C-domain, or central domain, is the one closest to the neurite, defined by a preponderance of microtubules and associated organelles.

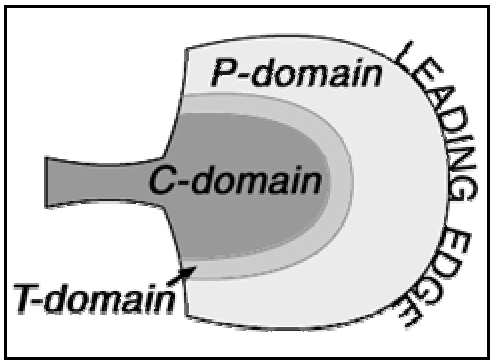

Figure 2.2 Growth Cone Domains. Central, Peripheral, and Transition domains each have differing constituent cytoskeletal elements.

During growth cone turns, the C-domain advances asymmetrically in the direction of the turn. The P-domain, or peripheral domain, is one in which actin networks dominate and in which there are not typically very many microtubules. Filopodia, which are located at the leading edge and which extend out past it, have actin bundles for their structure rather than actin networks, and this leads to their dark appearance in phase-contrast microscopy.

Different regions of the growth cone contain differently structured elements of the cytoskeleton, and the dynamic interactions of these regions determine the growth cone's behavior. First, the leading edge of the growth cone takes on two often coincident morphologies: filopodia and lamellipodia. Filopodia are composed of bundled actin filaments, whereas the actin filaments in lamellipodia are arranged in a network formation with the help of crosslinking proteins [Gallo & Letourneau, 2000; Smith, 1988], as illustrated in Figure 2.3. Microtubules also form bundles, located in the shaft of the neurite. As microtubules cross forward into the C-domain, however, they are more often defasciculated, but they (unlike actin) are not networked. Perhaps this is because actin filaments are narrow enough to be crosslinked by single proteins, whereas the broader microtubules would require either unusually large single crosslinking proteins or multiple proteins arriving simultaneously at the right place, both of which would seem extremely improbable.

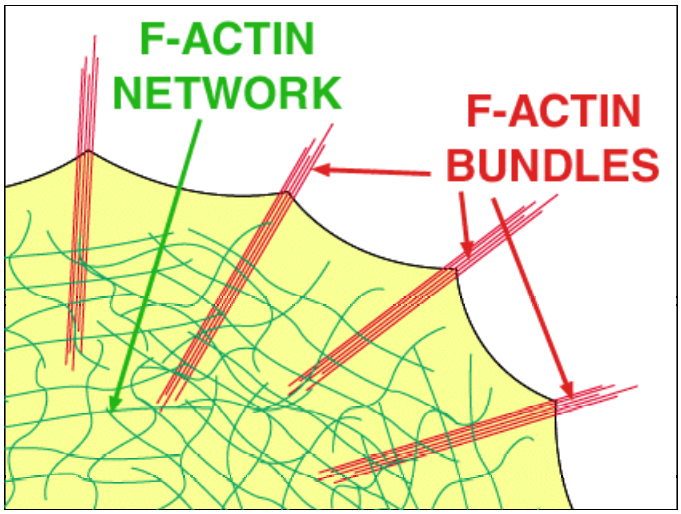

Figure 2.3 Author's Rendition of Actin in the P-Domain. Filamentous actin bundles (red) form the cytoskeletal basis for filopodia, and the filamentous actin network (green) lends structure and elasticity to lamellipodia as well as the body of the growth cone. Drawing is representational and is not to scale.

Single microtubules can extend all the way into the P-domain, there interacting with the actin network, and they can even enter filopodia, where they align with the actin bundles [Bush *et al.,* 1996; DiTella *et al.,* 1996; Gallo, 1998; Gordon-Weeks, 1991; Williamson *et al.,* 1996; Zhou *et al.,* 2002].

2.3 CYTOSKELETAL FUNCTION IN GROWTH CONE ADVANCEMENT

Microtubules and actin filaments both have multiple functions in the cell, many of which play a role, directly or indirectly, in the mechanics of growth cone turning. For actin, changes in the P-domain are governed by shifts in the equilibrium between two antagonistic actions: retrograde F-actin flow [Bray & White, 1988] and anterograde polymerization due to a forward flux of G-actin monomers [Gallo & Letourneau, 2000]. Microtubules also undergo both transport and polymerization, but the position of their equilibrium in terms of advance or retreat is determined primarily by polymerization and depolymerization. The distal end of a microtubule undergoes alternating periods of relatively slow polymerization followed by catastrophic (rapid) depolymerization, and these cycles are known as microtubule dynamic instability [Kirschner & Mitchison, 1986a, b]. There is a well-accepted, qualitative model for cytoskeletal actions associated with growth cone advance, whereby forward locomotion takes place in three stages: protrusion, engorgement, and consolidation [Goldberg & Burmeister, 1986; Aletta & Greene, 1988], each of which merits a bit of description.

Protrusion is enabled by the inhibition of retrograde actin flow and is limited by the maximal rate of actin polymerization at the leading edge [Lin & Forscher, 1993; Suter *et al.*, 1998]. There is evidence that actin filaments are coupled very closely to microtubules in the growth cone in this phase, as disruption of microtubules decreases the number of foci of actin polymerization [Rochlin, 1999], and also results in transient

hyperextension of lamellipodia in neuronal [Gallo, 1998] and non-neuronal cells [Rosaria & Swanson, 1996; Mikhailov & Gnudusen, 1998]. Inhibition of microtubule dynamic instability, too, can lead to failure of cell membrane material to move forward at the appropriate time [Zakharenko & Popov, 1998].

During the engorgement phase, the spaces made in the protrusion phase are filled with cell structures, mainly microtubules and some associated organelles. The extension of microtubules into F-actin networks has been seen both to hinder [Forscher & Smith, 1998] and to stabilize [Letourneau, 1979, 1983; Gordon-Weeks, 1991; Lin & Forscher, 1993; Bentley & O'Connor, 1994] their forward transport into the P-domain, so the exact nature of the dynamics here is not yet well understood. It is straightforward, however, that pharmacological disruption of microtubule dynamic instability results both in failure of microtubules to advance during this phase and also in a general reduction in axonal elongation [Tanaka & Kirschner, 1995; Gallo, 1998; Challacombe, 1997; Rochlin, 1996; Gallo & Letourneau, 1999b]. The advancement of microtubules to the P-domain is accomplished both by polymerization at the distal end and also by forward transport of polymerized microtubule fragments [Yu & Baas, 1995; Baas, 1997, 1999; Tanaka & Kirschner, 1991, 1995; Challacombe, 1997].

The final phase, consolidation, is perhaps the least well-understood [Gallo & Letourneau, 2000]. It has been observed, however, that during this phase the growth cone hesitates in its forward advancement and single microtubules form bundles as the boundary between axonal shaft and growth cone shifts forward to accommodate the new growth [Tanaka, 1991, 1995; Odde *et al.,* 1996].

2.4 NATURAL GROWTH OF A NEURON

The observation of neuronal growth in developing organisms like *Drosophila melanogaster* (the fruit fly, typically observed in larval stage) and *Xenopus laevis* (the

African clawed frog, typically observed in embryonic stage) has been the primary way in which the behavior of specific neurons has been studied. Many mechanisms of a growth cone's guidance toward its target have been elucidated by tracking the comparative growth of neurons in both normal and genetically-altered organisms. By deleting a genetic sequence G which codes for the expression of a protein P, and by observing any deviations from normal neuronal growth in such an altered organism, the role of protein P in the developing system can be studied indirectly. There is an extremely complex matrix of tissues, structures, and chemicals in insect, amphibian, and vertebrate systems through which neurons must navigate to their targets: the parameter space which describes these systems is absolutely enormous and, even in the present day, we have not come close to defining it fully, much less approaching any conclusions about causality.

There is a slightly simpler way in which to study the behavior of neurons, and that is to remove them from the animal, culture them in isolation from the myriad factors affecting their growth *in vivo*, and then systematically examine the neurons' responses to various stimuli in a controlled environment. However, it is not always as easy as that: cell culture, which will be described later in more depth, is far from an exact science and often requires adding undefined biochemical mixtures (such as serum, a blood derivative) to the medium in which the cell must survive. Since our experiments are with cultured cells, it is on similar experiments that I shall focus primarily in this survey of recent research.

3. Attempts at Neuronal Guidance: A Review

The impetus for studying laser guidance of neuronal growth is a desire to increase our understanding of their growth and development in organisms and of how we might manipulate their growth for the purpose of repairing damaged nerves. Guided neurons also have the potential to build controlled neural networks, from the study of which may come a deeper understanding of neuronal function in intelligent organisms. Additionally, large, controlled neural networks could someday provide a testbed for new drugs such that whole organisms would not then have to be subjected to testing to determine a drug's effect on cerebral or other neural functions.

Even the simple question of why growth cones turn has not been answered fully, since an understanding of directional changes in axon growth requires consideration of an enormous parameter space in order to be understood in general terms. Cell type, organism type, developmental stage as of cell extraction, number of hours in culture, and as many physical and chemical stimuli as researchers can imagine: these are just a few of the sets of parameters in the overall system state, whose ranges of values have never been considered simultaneously in a single experiment. It is considered a significant challenge simply to determine which cells live in overlapping parameter spaces such that their behavior can be compared. During the development of living organisms, it is even the case that the same axon must often react to the same stimulus in a different way in order successfully to complete its journey [Dickson, 2002].

A review of the more "standard" – which is to say, non-optical – methods of neuronal guidance is merited at this juncture. These experiments easily divide themselves by several criteria: by cell type (i.e., neurons from the peripheral or central nervous system), by organism from which the cells are taken, or by the types of stimuli

by which they are induced to grow or turn. It is this last sorting criterion, I believe, which best lends itself to description, and guiding experiments seem to separate into three kinds of techniques: topological constraints, substrate patterning with adhesive molecules, and the use of diffusable chemical cues in the culture medium.

3.1 TOPOGRAPHICAL CONSTRAINTS

If one seeks to encourage a neuron to grow (or not to grow) in a specific direction, one of the first things one may think of is building barriers or channels which would have the desired effect. For example, scratches may be etched into a quartz surface and then neurons plated thereupon, with the effect of the growth cones' orienting in the direction of the grooves [Stepien, 1999]. However, it has also been found that the neurites' preferred orientation is highly dependent not only on the cell type, but also on the age of the cells and whether the neurites in question are axons or dendrites [Rajnicek, 1997]. A series of experiments was performed by this last group in which they found a positive correlation between groove depth and neurite compliance to the groove direction for *Xenopus* CNS neurons. Perhaps their most remarkable observation, however, was that embryonic rat hippocampal neurons separated in development by just 2.5 hours (stages E16 *vs.* E19) had opposite reactions to the grooved surfaces: more of the younger neurons grew perpendicular to the grooves, while the more developed neurons grew parallel to them.

Another notable method by which the axis of neurite extension can be pre-determined successfully is through the magnetic alignment of collagen. When polymerized in a strong magnetic field, collagen fibers will form in the direction of the magnetic field, producing long channels through which neurites can then be sent to grow. When these collagen rods are grown and dorsal root ganglia are placed at one end of the

rods, the neurites from the ganglia extend preferentially in the direction of the collagen fibers due to the physical constraints induced by the polymer arrangements [Dubey, 1999]. In fact, there is a positive correlation between magnetic field strength during polymerization and degree of directional compliance of the neurites as well as depth of neurite penetration.

Physical barriers can also be made to limit the locomotion of cell bodies in the attempt to form neuronal circuits, as in the well-known "picket fence" method [Zeck, 2001], but even in these experiments, the neurites are left to grow in whatever directions they please. Combinations of lithography and laser ablation have also been used jointly to control the growth of neurons, but these efforts have met with limited success [Corey *et al.*, 1996]. Effects of surface topography on fibroblast orientation have also been observed to be dependent on groove width [den Braber *et al.*, 1996], but this effect was not observed for osteoblast-like cells [Duncan *et al.*, 2002].

Much of the success of these methods depends on whether the cells plated onto the substrates just happen to settle onto the correct places on the substrate, and thus there is always at least one crucial parameter which is completely out of the control of the experimenter. An additional drawback is the steric strain involved in a neurite's growing around a 90-degree corner, an effect not observed in neurons' natural behavior, as axons are inclined to grow straight and resist bending [Katz, 1985]. Also, especially with laser ablation methods, one must be mindful of the chemical alterations to the surfaces which can take place and produce unexpected results [Duncan *et al.*, 2002].

3.2 SUBSTRATE PATTERNING

Another way to guide neurite extension is to use short-range chemical cues in the form of patterned substrates. Short-range chemical cues are those which interact with a

cell's membrane receptors directly and which do not have to travel as messengers from one point to another. Finding ways to attach these proteins, or others which have a chemical effect on neurons, to surfaces has been of great interest to researchers.

Neurons readily adhere to surfaces coated with extracellular matrix (ECM) proteins, as these best mimic the cells' natural environment in an organism. Laminin and fibronectin, for example, promote cell adhesion and neurite outgrowth in both CNS and PNS neurons [Rogers, 1983]. Substrate-bound laminin promotes adhesion, outgrowth, motility, and locomotion in immortalized cell lines such as NG-108-15 [Smalheiser, 1989b], and laminin is more efficacious in promoting neurite outgrowth than either fibronectin or collagen [Smalheiser, 1984]. Preferential neurite extension along laminin pathways or stripes was observed as early as 1988 [Hammarback, 1988], and it has been observed that the width of the pathways has a large influence on eliciting patterns of neurite extension. There is a critical path width of about 5 microns, below which neurites will ignore laminin patterns and maintain large-scale isotropy in their extension [Clark *et al.*, 1993].

Poly-L-lysine (PLL), an amino acid polymer, is also widely used for the purposes of cell adhesion. Patterns of PLL have been used to direct neuronal adhesion and neurite outgrowth [James, 2000], but it has long been known that PLL promotes neurite extension at a significantly slower rate than does either laminin or fibronectin [Rogers, 1983]. When PLL and the cell adhesion molecule (CAM) L1 are patterned onto a substrate together, however, somata preferentially adhere to the PLL, while neurites preferentially grow along the L1 [Oliva, 2003].

If a substrate coating is too strongly adhesive, however, growth cones may "get stuck" and extend to a lesser degree [Forscher & Smith, 1988], and such a situation may even inhibit growth cone steering [Buck & Zheng, 2002]. There arises the question, then

of how the adhesive forces actually compare. It would appear as though, in comparing growth cones attached to untreated, PLL, laminin, and L1 substrates, in the first three instances the force required to detach a growth cone was similar, and only in the case of lamellipodia on an L1-coated substrate was there much variance (these growth cones had a lower required force) [Zheng, 1994]. Also in this study, it was found that the forces per unit area required to detach filopodia and lamellipodia from the substrate are fairly equivalent as well. Whether patterning, and its effective differential adhesion effects, can control neuronal polarity in and of itself is still unknown [Stenger *et al.,* 1998 J Neurosci Meth 82:167-173; Vogt, 2004]. There is more evidence that a chemical pathway not associated with adhesion may be responsible for polarity determinations resultant from crossing of a neurite from one coating to another [Esch, 1999].

3.4 COATED BEADS

Another way in which to elicit turning behavior from growth cones using short-range chemical cues is to coat microspheres with the protein of choice and to bring the spheres to the growth cone. In this way, the proteins coating the beads can interact with the cell's membrane receptors, but only at a specific location. Beads can be held either mechanically or with a laser trap, and the forces exerted by the cell on the bead can thus be measured.

Beads coated with nerve growth factor (NGF) brought in contact with a growth cone induce a turn in the direction of the beads, whereby it is noted that F-actin ultimately protrudes past the coated bead, but the turning effect vanishes in the presence of vinblastine or taxol, two drugs which interfere with microtubule dynamics [Gallo & Letourneau, 2000; Gallo *et al.*, 1997; Ming *et al.*, 1999]. However, when beads coated with brain-derived neurotrophic factor (BDNF) are used, actin filaments are stabilized

and the growth cone loses motility, although collapse via an NO^- pathway is inhibited [Gallo & Letourneau, 2000].

Another group used immunoglobulin-G (IgG)-coated beads to pull out tethers from cells mechanically, starting at one side of the cell body [Dai & Sheetz, 1995]. In this way, they found that the coupling of cell membrane to bead was far greater than that of cell membrane to cytoskeleton, as there was very little resisting force – only on the order of a few myosin motors.

Beads coated with either apCAM or ConA and brought to one side of a growth cone will cause the growth cone to turn in the direction of the beads and have some intriguing effects on the cytoskeleton [Suter & Forscher, 1998]. In the studies with ConA, the C-domain, complete with microtubules, advanced asymmetrically in the direction of the bead as the growth cone turned. In the studies with apCAM, there was an extension of the C-domain after a latency period of 10 minutes, and the force of the growth cone pulling back on the bead also greatly increased after this period. It was not until these events had taken place that inhibition of retrograde actin flow was observed.

3.3 DIFFUSIVE CHEMICAL CUES

Chemical cues often have long-range interactions with cells *in vivo*, by which they carry signals from other cells or tissues, and *in vitro* these may be simulated. These effects differ from short-range cues not only in the mechanism of action but also in the experimental parameters required. It is not required that substrates be patterned or that cells be directly manipulated, but only that the chemical compounds of interest be added to the culture medium in which the cells reside. Also, nearly all cell observation systems (ours included) are capable of medium changes with minimal perturbation to the cells, which means that multiple chemical cues may be introduced in succession or that a

chemical may be added to the system and then flushed out after a certain time has elapsed. Note that although the effects are called "long-range," the physical distance over which the cues may travel can be quite small compared to, say, the width of a growth cone: the designation of "long-range" signifies only that there must be travel of some sort through the medium between the place the chemical is released and the cell that receives it.

Laminin and L1, for example, can be effective both in the short-range (as in the previous section) or the long-range when added to cultures in solution, increasing growth cone motility and the rate of neurite outgrowth [Rivas, 1992; Doherty, 1995; Moore and Raizen, unpublished observations]. Similarly, netrins and semaphorins, when introduced to one side of a growth cone with a micropipette, will induce turning behavior, which is repulsive in the case of semaphorins, and can be either repulsive or attractive in the case of netrins [Tessier-Lavigne & Goodman, 1996].

The long-range effects of neurotrophins on growth cones have been studied extensively, and this class of molecules is known to produce cytoskeletal rearrangements through rho-family GTPases and other, downstream actin-regulating proteins [Paves & Saarma, 1997; Song *et al.*, 1997, 1998; Gundersen & Barrett, 1979]. These reactions must rely on specific signaling pathways, however, since – although nerve growth factor (NGF) exposure increases the presence of F-actin in growth cones – brain-derived neurotrophic factor (BDNF) stabilizes actin filaments in growth cones, causing loss of mobility.

In the presence of cytochalasins, a class of drugs known for capping one end of actin filaments and thus preventing monomer addition at those sites, F-actin networks devolve into actin aggregates (blobs) [Zhou, 2001], but actin depolymerization is not directly induced [Forscher & Smith, 1988]. Cytochalasins cause loss of F-actin from the

leading lammelae of growth cones, and in their presence, microtubules more readily advance from the C-domain to the P-domain [Forscher & Smith, 1988]. Additionally, the presence of cytochalasins in culture medium induces inhibited retrograde actin flow as well as reduced lamellipodial and filopodial protrusions [Buck & Zheng, 2002].

Another group of drugs whose effects on growth cones are of note are vinblastine, taxol, and nocodazole. Vinblastine inhibits microtubule dynamic instability [Baas, 2000, Buck & Zheng, 2002], so low doses encourage microtubules and their associated organelles to penetrate from the C-domain into the P-domain so that fewer microtubules are found in the axonal shaft and more are found in the growth cone proper [Tanaka, 1995]. High doses of vinblastine, however, lead to complete growth cone collapse [Tanaka, 1995]. Nocodazole, by contrast, actively depolymerizes microtubules, and the addition of vinblastine after nocodazole keeps microtubules from re-polymerizing [Gallo & Letrouneau, 1999]. Nocodazole acts as a repulsive guidance cue for growth cones, and higher doses lead to inhibition of growth cone advancement [Buck & Zheng, 2002]. Taxol, however, stabilizes microtubules and serves as an attractive cue for growth cone turns, and in some cases is known to promote microtubule polymerization [Buck & Zheng, 2002]. In any case, taxol interferes with normal microtubule dynamic instability, and in high doses can even inhibit neurite outgrowth [Tanaka, 1995].

Calcium ions are very important in the determination of cytoskeletal behavior, and regulation of Ca^{2+} ions in the growth cone is carried out by several classes of calcium channels. There are some which respond to voltage gradients, others to stretch activation, and yet others to the presence of other specific ion species. If extracellular Ca^{2+} is added to one side of a growth cone in normal culture medium, this induces an attractive turn, but when the cell medium lacks Ca^{2+} ions to begin with, this same introduction of Ca^{2+} to one side of a growth cone induces a repulsive turn [Zheng, 2000]. Moreover, when a

Ca^{2+} influx is allowed by the opening of ion channels, this leads to growth cone collapse [Zhou, 2001] through F-actin destabilization [Gallo & Letourneau, 2000], but removal of calcium ions from culture medium altogether generally increases the rate of neurite outgrowth [Zheng, 2000]. The presence of extracellular calcium ions has an effect synergistic with the presence of neurotrophins: a cocktail of netrin-1, acetylcholine, BDNF, and MAG elicits no turning response in the absence of Ca^{2+} and an attractive response in its presence [Song & Poo, 1999].

Cyclic nucleotides, such as cAMP and cGMP, constitute yet another class of molecules affecting growth cone advancement. Elevated levels of cAMP in growth cones stabilize F-actin and block calcium-induced depolymerization [Gallo & Letourneau, 2000], while also inhibiting retrograde actin flow and allowing organelle transport into the P-domain [Forscher & Smith, 1988]. The photoactivated release of caged cAMP with UV light is an interesting case, as pulsed release of cAMP induces attractive turns, whereas sustained photorelease induces repulsive turns [Munck, 2004]. Pulsed UV light by itself, however, has no effect on growth cones [Zheng, 2000]. Effects of cyclic nucleotides combine with those of neurotrophins, as a gradient of netrin-1 in the presence of cAMP elicits an attractive growth cone response, whereas in the absence of cAMP, the same stimulus elicits a repulsive response [Song & Poo, 1999]. Similarly, BDNF in the presence of cAMP results in attraction, while in the absence of cAMP it results in repulsion of growth cones [Song & Poo, 1999].

It is quite evident from all of these observations that, given the variety of growth cone reactions to various combinations of chemical cues, and given that similar stimuli under slightly different conditions can give drastically different behavioral results, it would be a nearly intractable problem to try to guide growth cones *in vivo* with diffusive chemical cues alone.

One issue that does not appear to have been addressed in the literature is that of how diffusable cues interact with the cells; that is, whether molecules floating freely in the culture medium connect with cell membrane receptors from the liquid phase or whether they first adhere to the substrate and then act upon the cells as short-range cues. For example, when preparing laminin-coated coverslips, one must let a solution of laminin incubate on the coverslips for 10-20 minutes so that the molecules adhere to the substrate, but using laminin as a diffusable guidance cue can require the same procedure in the presence of cells. It would be possible in this case for substrate-bound laminin to affect the cells and for solvated laminin not to have any effect, and yet the outcome of these experiments is considered to be due to the laminin in solution. One must be careful, therefore, in choosing the appropriate category for each observation and, as more becomes known about the mechanisms by which the observed effects occur, it would be reasonable to anticipate some possible future reclassifications.

3.5 MECHANICAL FORCES

It is also of interest to explore the effects of mechanical forces on neurites to identify any links these might have to issues of guidance. Tension may be applied to various parts of a neuron with a microneedle and a slight bit of suction, as described in [Zheng, 1991], and when this was done, the following results were obtained. When tension is applied to the side of an attached soma, an entire *de novo* neurite can be drawn out, and when a growth cone is attached but its soma is not, the soma may be moved away from the growth cone in order to lengthen the neurite. When the applied force (as measured by the deflection of the calibrated microneedle tip) is below a threshold value of 50-100 mm Hg, however, the neurite does not grow, but rather responds in a strictly viscoelastic manner. In other studies, when tension is applied to an axonal shaft

perpendicular to the direction of extension, like plucking a guitar string, the neurite will lengthen in response to the applied tension [Lamoureux, 1992].

Subjecting a growth cone's membrane to tensile force has been observed to result in the activation of stretch-activated (SA) ion channels [Sigurdson & Morris, 1989]. In these studies, when tension is applied to the cell membrane, the stretch-activated potassium ion channel has a higher probability of being open, which means that more potassium ions will be able to flow, which then results in the establishment of a voltage gradient across the cell membrane. This voltage gradient can then trigger voltage-sensitive calcium channels to open, leading to an influx of calcium ions, which then leads to a turn away from the source of the stimulus if it is applied asymmetrically to the growth cone. Although it is possible that mechanical membrane manipulation tears holes in the membrane through which ions may pass, experiments strongly suggest that ion channels are the mediators of calcium influx, as both extracellular calcium levels and calcium channel blockers abolish the effect in human neutrophils [Holm *et al.*, 1999].

A specific type of stretch-activated ion channel, the TRAAK potassium channel, was studied by transfecting immortalized COS-7 cells to express it [Maingret *et al.*, 1999], and these experiments met with the following results. Convex membrane curvature was required for activation of these channels, and the addition of the cytoskeleton-disrupting drugs colchicine, cytochalasin D, and trinitrophenol to the cells' environment increased the channels' response to stretch activation. Additionally, bringing the cell membrane potential to a more positive value induced stronger TRAAK channel response. It is interesting to note that, in experiments with fish keratocytes [Lee *et al.*, 1999], raising the membrane voltage actually inhibited the activity of stretch-activated calcium channels, so there is no universal correlation between voltage and mechanical ion channel response.

4. Principles of Optical Manipulation

4.1 Optical Forces

Arthur Ashkin first had the thought of using light to manipulate objects in 1969, when a back-of-the-envelope calculation revealed that the force imparted to a small object by a 1-Watt focused beam of light would be quite substantial. The first use of radiation pressure to move particles [Ashkin, 1970] led to the trapping of neutral atoms [Bjorkholm *et al.*, 1978] and other particles like the tobacco mosaic virus [Ashkin & Dziedzic, 1987]. In this last experiment, when some bacteria accidentally got caught in the trap and were "opticuted" by absorption of argon laser light (515 nm), Ashkin and colleagues were prompted to set up a trap on a microscope, and thus was born the field of optical manipulation in a biological context. Very soon afterward, it was found that a shift in wavelength from 515 nm to 1060 nm made a profound difference, trapping the organisms without damaging them [Ashkin *et al.*, 1987]. Since then, optical manipulation of biological objects has flourished in many directions, as in the development of an optical cell stretcher [Guck *et al.*, 2000, Guck *et al.*, 2001] and in the exploration of lipid membrane and vesicle dynamics with laser light [Bar-Ziv *et al.*, 1995a,b]. The principles of optical forces generally and optical tweezers specifically are illustrated in Figures 4.1 and 4.2.

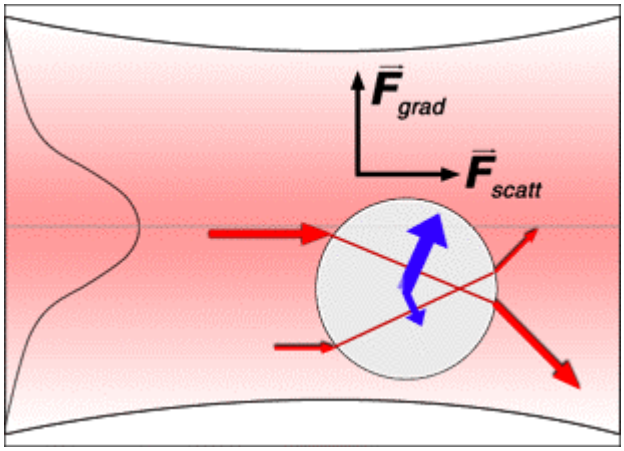

Figure 4.1 Optical Gradient Forces from a Gaussian Beam on a Particle Off-Axis. Momentum conservation dictates the forces exerted on a particle. Particle is assumed to have refractive index greater than that of the surrounding medium.

4.2 Optical Neuronal Guidance

The optical neuronal guidance project at the University of Texas at Austin was initially a collaborative effort between the lab groups of Josef Käs and Mark Raizen. The experiment arose from simple curiosity as to whether laser light could be used to alter neuronal growth patterns, and it was found to be the case that it worked [Ehrlicher *et al.*, 2002]. The first investigations were done primarily with PC-12 cells, and the experiment has continued with NG-108-15, GT-1, and primary rat neuronal cells.

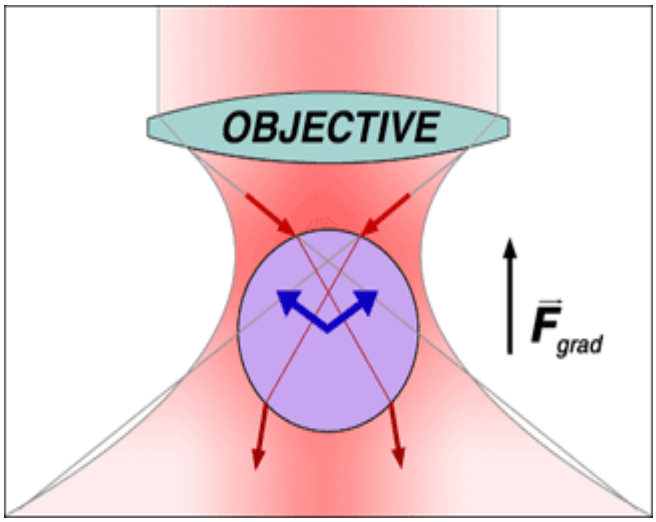

Figure 4.2 Optical Tweezers. Light is focused through an objective lens (such as that of a microscope) and an object is drawn in to the focus. In the illustration, light is traveling downward.

Although the experimental setup described below is similar to that of many optical tweezer configurations, tweezing large cell structures was not our goal. In fact, since the optical neuronal guidance endeavor originally followed a "guide now, ask questions later" approach, these effects were observed before a theory about the possible mechanism of guidance was formed, and the exact mechanism has still to be fully elucidated.

The preliminary hypothesis for the mechanism of optical guidance is that free G-actin (monomers) in the cytoplasm acquire, by virtue of their polarizability, a drift velocity from the laser light, thus making polymerization in the direction of the laser spot more probable by virtue of there being a higher monomer concentration there

[Stuhrmann, 2002]. The protein's polarizability is given by the Clausius-Mosotti equation:

$$\alpha = 4\pi\varepsilon_0 \, r_{monomer}^3 \, n_{cytoplasm}^2 \left(\frac{m^2 - 1}{m^2 + 2} \right) , \qquad (4.1)$$

where $m = n_{object} / n_{cytoplasm}$, r is the radius, and the n are refractive indices. As the radius of an actin monomer is 3.0×10^{-9} m [Lodish, 2000], n of cytoplasm is 1.37 [Drezek *et al.*, 1999], and n of actin is 1.59 [Suzuki *et al.*, 1996; Kratochvíl, 1987; Huglin, 1972], we obtain for actin monomers $\alpha = 5.83 \times 10^{-37}$ Cm^2/V.

We also assume a Gaussian intensity distribution for the laser focus, with beam waist equal to 1 micron, so the intensity profile looks like

$$I(r) = I_0 \, e^{-2r^2/w^2} , \qquad (4.2)$$

and the power, similarly,

$$P(r) = \int_0^\infty 2\pi \, r \, I(r) \, dr = \frac{I_0 \pi \, w^2}{2} , \qquad (4.3)$$

whereby we find that, with 100 mW of total laser power in a beam spot of 1 micron diameter, the peak intensity is $I_0 = 1.27 \times 10^{11}$ W/m^2. The gradient force imparted by the beam to any object off-axis is

$$\vec{F}(\vec{r}) = \frac{\alpha \nabla I(\vec{r})}{2c\varepsilon_0 \, n_{cytoplasm}} , \qquad (4.4)$$

We can then find the drift velocity for the monomer,

$$\vec{v}_d = \frac{\vec{F}}{k_b T / D} \quad , \tag{4.5}$$

where D is the diffusion coefficient for the monomers in cytoplasm [Popov & Poo, 1992]. We will neglect any scattering force which would want to push the monomers upward with the argument that the gradient force outweighs it by orders of magnitude. We can calculate the shape of the potential well to which the monomers are subjected; this is plotted in Figure 4.3 for laser powers between 40 and 120 mW and for three laser spot diameters. These plots show the importance of a tight laser focus to

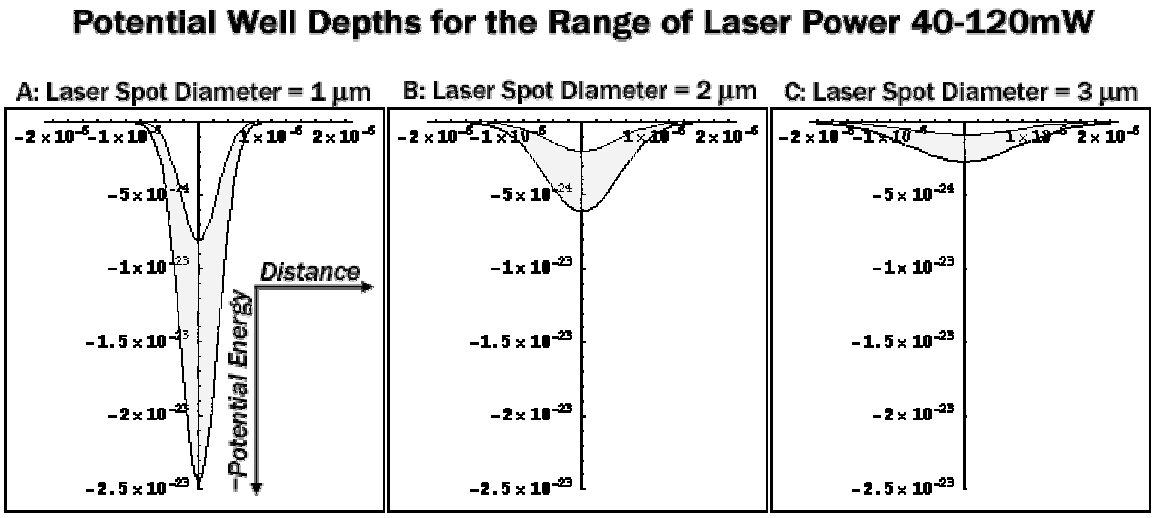

Figure 4.3 Potential Well Depths for Varying Spot Size and Laser Power. Potential wells for 40 mW and 120 mW are shown, and the shaded region contains all those that lie in between. Note the square dependence on spot size for a given laser power. Potential energy in [J], distance in [m].

getting good results if biased diffusion plays a significant role in optical guidance. This effect was evident experimentally when a small enough spot size was not attainable with

an air immersion objective lens (40X, numerical aperture (NA) = 0.6)†, whereas excellent focusing results were obtained with an oil immersion objective lens (40X, NA = 1.3).

In switching from an air immersion to an oil immersion objective lens, what we gained in ability to focus the laser beam to a tighter spot, we lost in depth of focus (the working distance of the new objective lens is 140 μm, representing a reduction by more than an order of magnitude). Since the objective lens units are proprietary configurations, their design is unavailable, but suffice it to say that the loss of depth of focus resulted in a reduction of the field of view by at least a factor of four. Inherent in the design of the experiment dishes (see Section 7.2) is a tendency for the bottom coverslip to be warped on the scale of a few microns, and the vertical displacement of cells in the field of view resulted in our being constrained to choose a very small (100 x 100 micron) field all of which could be in focus at one time with the higher NA objective lens.

† Some guidance was observed with the low NA objective lens, but these data are not shown.

II. MATERIALS & METHODS

5. Overview

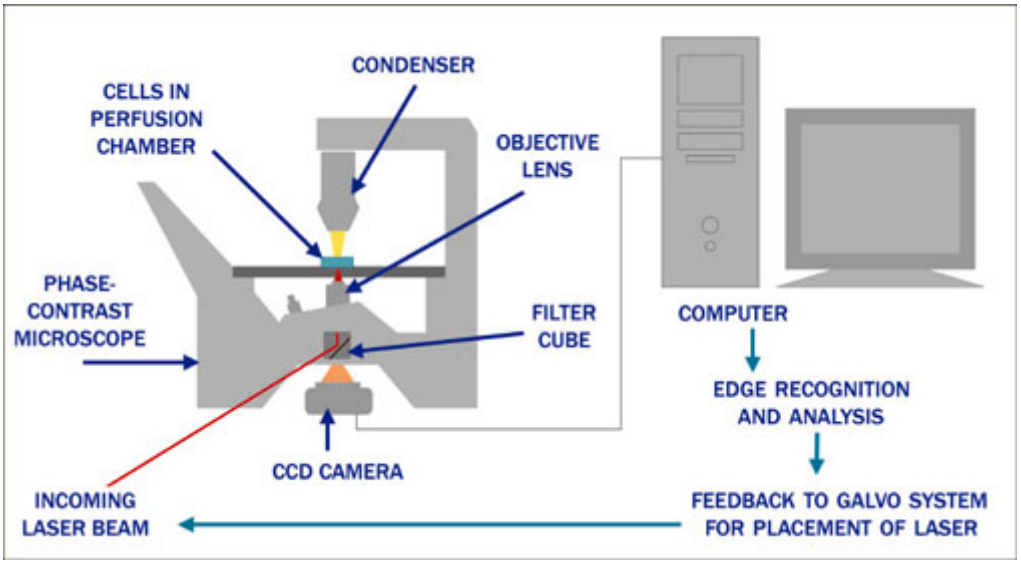

Figure 5.1 Experimental Setup. Images are acquired from the phase-contrast microscope while a laser beam is directed through the objective lens and focused at the plane of the cells. Cell and laser images are recorded by a CCD camera and a computer analyzes the images for automated guidance.

The basic elements of our experimental setup are shown in Figure 5.1 and a close-up schematic of the sample in Figure 5.2. Our microscope, a Zeiss Axiovert 25 (Carl Zeiss Microscopy Jena, Germany), has been modified to accommodate our devious imaging plans: namely, to allow images both of the cells and of the laser spot to be acquired in rapid succession. Light passes through the microscope condenser from a halogen source at the top of the instrument and is brought to a focus at the sample. The light then proceeds through the objective lens to form a magnified image of the sample (for a complete description of the phase contrast system, please refer to Section 8.2.3).

Simultaneously, laser light passes into the microscope from below the objective lens, is deflected upward, and is focused to a small spot in the sample plane. A very small fraction of the laser light is reflected back from the sample chamber and is recorded by the same camera as the phase-contrast image of the cells.

The laser spot is positioned with four mirrors mounted on galvanometers (GSI Lumonics, Billerica, MA), the precise positions of which are controlled from a computer through a National Instruments NI PCI-6733 PC interface card (National Instruments Corp., Austin, TX). A growth cone is selected by the researcher through the microscope eyepiece, and then the image is switched to the camera so that data may be acquired. The cell is monitored for 10-20 minutes before the introduction of the laser in order to determine whether it is sufficiently motile for an experiment, and then the laser is introduced for guidance. The laser spot is kept very near the leading edge of the cell, mostly within the cell, and is moved in conjunction with movement of the growth cone so as to hold its relative position. The leading edge of the cell typically continues to grow slightly past the laser spot, so the spot is continually moved back, the growth cone continues to follow, and thus the axon is guided from its original growth axis to a new one prescribed by the laser spot position.

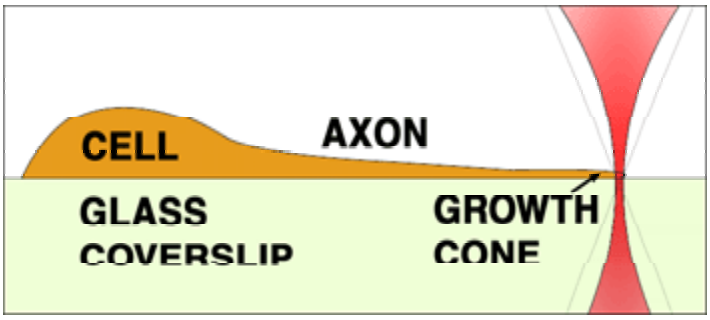

Figure 5.2 Schematic of Optical Guidance in Cross-Section. Note that the laser focus is kept slightly below the plane of the cell so that the growth cone cannot be tweezed off the substrate.

Our experiments have been performed upon a wide range of neuron and neuroblastoma cells and cell lines. The data reported here are for NG-108-15 cells, but PC-12 and GT-1 cell lines, as well as primary neonatal rat cortical neurons, have also

been investigated. Our present efforts focus on achieving results with primary *Xenopus* spinal neurons, and the scope of our experiments could someday be expanded to include *Aplysia* and *Helisoma* primary neurons for *in vitro* experiments and *C. elegans* organisms for *in vivo* experiments.

The neurons, especially those derived from mammals, must be kept within certain ranges of temperature, osmolarity, and pH in order for the cells to maintain normal functionality. It is crucial, therefore, to have a cell survival system capable of keeping all of these parameters within a normal range. Such systems are commercially available (Bioptechs, Butler, PA; Cell MicroControls, Norfolk, VA) but are very costly, so we have chosen to proceed with a system of in-house design and fabrication.

Digital image data are recorded at regular intervals and are saved (first to hard disk and later to DVD discs) for analysis. Also, every incoming image is analyzed by a computer program (written by Florian Schreck and extensively modified by Jakub Otwinowski) which determines where to place the laser spot for the next interval, and the laser position is adjusted accordingly. In this way, the optical guidance of neuronal cells has been automated, which has several advantages over manual guidance. First, and perhaps most important, the exact position of the laser spot during guidance is no longer left to human judgment, which eliminates both bias and error in laser spot placement and allows for more consistent data to be taken. Additionally, automation of the guidance process means that a researcher is no longer constrained to remain at the controls of the experiment with the task of adjusting the laser spot position for every new image acquired by the system. Still left to human judgement, however, is the initial determination of which growth cone to try to guide, and in which direction to try to guide it.

6. The Culture of Biological Cells

The scale of mammalian cells lies just below the smallest scales susceptible of visual discrimination, and single cells may be considered as individual units as well as functioning parts of the organs of which they are constituents. However, unlike many materials whose bulk properties are quite different from those of their constituent particles, individual cells will typically behave *in vitro* very much as they will *in vivo*, reacting similarly to chemical cues in both cases, for example.

There are two ways in which to gather cells for *in vitro* studies: either one must extract them directly from an animal (primary cultures) or one must find a way to keep them reproducing so that they can replenish their numbers (immortalized cell cultures). Primary cultures of fully-differentiated cells are sustainable, for a period ranging anywhere from days to weeks, depending on cell type and animal of origin, but all primary cells eventually undergo apoptosis, or programmed cell death. In order to establish immortalized cell lines, it is therefore necessary either to transform the cells genetically or to start with mutated cells (such as those from tumors) in order to have an infinitely self-replenishing colony. The method of genetic alteration is called malignant transformation, whereby normal cells are exposed to a virus carrying a gene sequence which, when integrated into the cells' normal genome, has the desired effects of suppressing apoptosis and promoting mitosis, or cell division. Once malignantly transformed, one cell can start an entire colony of cells identical to itself, called a clonal population. Such a population is called a cell line, since every cell in it can trace its lineage back to the first cell.

6.1 CELL TYPES: ESTABLISHED CELL LINES

Established cell lines (also called immortalized cell lines) are in many ways the most convenient variety to include in an experiment. Not only are they self-replenishing, but also they also obviate the sacrifice of an animal every time a new culture is required. Cells of this type can be frozen down, cryopreserved, and brought back to culture again years later with a high survival rate, and many cell lines can be purchased commercially from companies such as the American Type Culture Collection (ATCC, Manassas, VA). Additionally, since all cells in a clonal population have the same genome, results of experiments involving cell lines will generally be more consistent than those from primary cells.

However, because *in vitro* experiments are often performed with the purpose of reflecting cell behavior within organisms, established cell lines are further removed from the living organism than are primary cells. Not only are many immortalized cells either taken from tumors (unhealthy tissue) or malignantly transformed, but also cell genomes may be crossed, producing hybrid cells with part of their genetic code from one species and part from another. It is for these reasons that, in general, some scientific communities prefer work with primary cultures to that with established cell lines if the work is intended to represent, model, or predict events that occur in live organisms.

6.1.1 NG-108-15

The cell line most thoroughly investigated in our experiments has been NG-108-15. First created in 1977 by Bernd Hamprecht [Hamprecht 1977], these cells are a hybrid between mouse neuroblastoma N4 and rat glioma C6 clonal cell lines, specifically between mutants of these cell lies, N4TG3 and C6-BU-1, respectively. Hybrid cells are created by literally fusing two cells, one from each parent cell line, by introducing Sendai

virus inactivated by β-propiolactone to an environment containing both cell types. The cells are then exposed to hypoxanthine-aminopterin-thymidine (HAT) medium, which is toxic to the parent cells but not to the wild-type hybrid cells formed by their fusion. The NG-108 cell line is commercially available from ATCC and is in widespread use as a model for neuronal cells.

Of the many strategies available for stimulating NG-108 cells to extend elongated processes, the method with the highest ratio of degree of success to required effort is the approach of adding of dibutyryl cyclic adenosine monophosphate (cAMP) to the culture medium for extended periods of time. Other methods include (but are not limited to): serum deprivation, x-irradiation, exposure to hypertonic culture medium, and addition of NGF, DMSO, and other chemical compounds. All of these methods have in common that they deprive the cells of the ideal conditions they would need to reproduce, while leaving them healthy enough to ensure their survival.

6.1.2 GT1-1 and GT1-7

The GT-1 cell lines, established in 1990, were derived directly from a mouse hypothalamic tumor [Mellon *et al.*, 1990]. These fundamentally differ from NG-108 cells in that the GT-1s are from the central nervous system, whereas the NG-108s are from the peripheral nervous system. GT1-1 and GT1-7 are two subclones of the same GT-1 clonal population, and their morophological and growth properties differ very significantly from each other. Attempts at optical guidance of GT-1 cells have met with very little success [Schmitt 2002], perhaps due to their CNS origin, as CNS neurons cannot regenerate although PNS neurons can [Gordon-Weeks & Fischer, 2000]. Perhaps this is also partly due to the small size of their growth cones (1-2 μm in diameter), which leads to technical difficulties in guidance attempts. GT-1 cells are also more sensitive to

their culture environment than are NG-108s and serum deprivation of GT-1s does not lead to the formation of processes as long as those formed by NG-108s.

6.2 CELL TYPES: PRIMARY CULTURES

Although established cell lines are generally considered to serve as fine models for neuronal cells, it is still our long-term goal someday to apply optical guidance techniques *in vivo*, so we can get a better idea of how "real" cells would react by extracting some from an organism and investigating their behavior in culture. Unfortunately, this requires the sacrifice of the animal in question, and since primary neurons are already fully mature and are programmed to die after a certain time, primary cultures need to be replenished regularly with new cells in order for experiments to continue.

One can extract neuronal cells from almost any organism, so organisms are chosen primarily on the basis of their being easy and cost-effective to maintain. Rats and frogs fulfill this criterion, as they are regularly kept for a variety of other experimental purposes. Embryonic or neonatal animals are preferred to mature ones because full neuronal complexity has not yet been achieved at earlier stages of development and thus neurons are easier to extract in their entirety. In the case of rats, embryonic organisms are microscopic (and thus inconvenient to dissect), and fetal organisms require the sacrifice of multiple organisms at once (a pregnant female and many fetuses) – and thus are undesirable on that account – so neonatal rat pups are at the ideal stage for acquisition of primary neurons. For frogs, ova can be about a millimeter in diameter, increasing in size after fertilization, so embryonic organisms are quite amenable to microdissection and are thus the preferred source of neuronal cells.

The protocol for rat pup neuron preparation was generously provided by the laboratory of Richard Morrisset of the University of Texas at Austin College of Pharmacy, and the protocol for *Xenopus* was obtained from [Tabti *et al.*, 1991; Sive, 2000].

6.2.1 Preparation & Properties of Rat Neonatal Cortical (Pyramidal) Neurons

A rat pup 2-3 days old is sacrificed by decapitation and the cerebral cortex is quickly removed and placed in ice-cold MEM (with no L-glutamine)† in its entirety for 2 minutes. The brain is then recovered from MEM, placed on clean, chilled, and moistened filter paper, and the cortex is finely minced with a razor blade and placed into a solution of protease (digestive enzymes). The suspension of cortical tissue is kept in an incubator at 37 degrees Centigrade for 20 minutes and is inverted every 3 minutes to redistribute the settled tissue. The suspension is then centrifuged to get the tissue into a dense pellet, and the supernatant is removed. The sample is resuspended and centrifuged three times with trituration buffer to wash the tissue, and then the tissue is triturated with micropipettes of successively smaller diameters in order to dissociate tissue aggregates. The suspension is left to sit for several minutes, and gravity does the work of separating the larger aggregates to the bottom

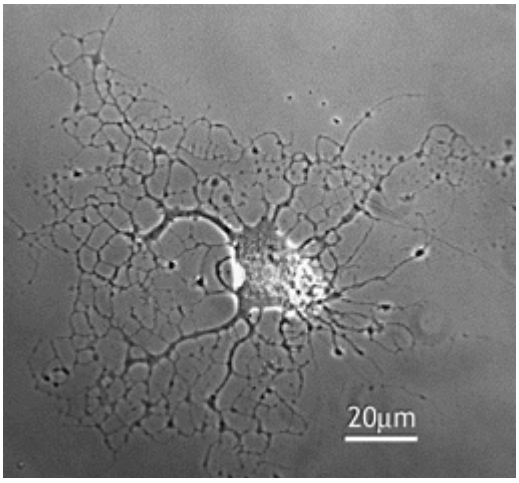

Figure 6.1 Primary Neonatal Rat Cortical Neuron in Culture. Densely networked processes with very small growth cones limited the feasibility of optical guidance for these cells.

† Precise formulations of buffers, media, and other solutions mentioned perfunctorily in this chapter may be found in Appendix A.

while leaving individual cells suspended near the top of the column. The cells can then be collected from the top of the suspension, placed into culture medium, and plated onto coverslips prepared with adhesion proteins. The culture medium should be changed during the first 24 hours and then subsequently every other day to refresh the supply of nutrients.

We found that neurons thus obtained did not typically display a polarized appearance, but rather a dense network of arbors arranged more or less symmetrically in a halo around the cell bodies, as shown in Figure 6.1. These networks of arbors grew further out from the soma with time, but the processes themselves got narrower and growth cones were extremely small (around 1 μm in diameter, about the same size as the laser spot). These cells turned out not to be good candidates for optical guidance, as discussed below.

6.2.2 Preparation & Properties of *Xenopus laevis* Embryonic Spinal Neurons

Xenopus laevis embryonic spinal neurons have some important advantages over neonatal rat cortical neurons. Foremost among these in my own mind is that in the embryonic stages these organisms do not have a developed nervous system and thus do not suffer during preparation as rat pups may. Also, since these cells do not come from mammals, they may be kept at or a little bit below room temperature and do not require an incubator for survival. The acutal dissection, however, is slightly more complex than that of the rat pup, mostly because of the small size of the embryo and the tough, thin, transparent vitelline membrane surrounding it.

The first step in this preparation is to sterilize the jelly coat sorrounding the embryo with 70% ethanol for 10 seconds, then transfer it into a petri dish containing 10% Ringer's solution. The embryo is released from both the jelly coat and vitelline

membrane in this dish before being transferred successively into 5 more dishes of 10% Ringer's solution to wash it, using a new, sterile Pasteur pipet for each transfer. Next, the embryo is transferred to CMF buffer for dissection, which consists of separating the neural tube and associated tissues from the rest of the embryo. The neural tissue (about an eighth of the total mass of the embryo) is kept in CMF buffer for 20-30 minutes following dissection so that the tissues become dissociated. The pigmented epithelial layer may be removed toward the end of the dissociation period, and then the remaining loose tissue is transferred to a dish containing culture medium. Tissue is aspirated into a narrow Pasteur pipet and then is dispersed into the medium. This produces a culture of both neural and muscular cells, but the two are easily differentiated by their morphological properties after they have adhered to the substrate.

6.3 WHICH CELLS ARE BEST CANDIDATES FOR GUIDANCE

From the thousands of cell types available in one way or another, we must choose those which most lend themselves to our particular experiments. Our primary criterion is that the cells have, or can be differentiated to have, a neuronal phenotype, with long processes emanating from the cell bodies. This narrows the field down to primary neuronal cells and neuroblastoma or neuroblastoma hybrid cell lines, and yet not all of these meet our criteria.

First, there is the issue of practicality, forcing one to ask which cells can be cultured in environments which are either currently available or constructed with relative ease. Primary whale neurons, for example, even if they were possessed of all other characteristics of cells ideal for our experiments, would be a sub-optimal choice. Length of neurite extension is an important parameter to take into account so that one does not end up with thirteen fields of view in the microscope separating the cell body from the

growth cone. The next criterion is that of cell size, and subsequently, growth cone size. If the diameter of a cell's growth cone is at most the diameter of our laser spot, as we found to be the case with 2- to 3-day-old rat primary cortical neurons, then such neurons do not work well either. Similarly, the growth rate of neurites for a given cell species must be reasonable for the timescales on which the experiments take place: for too fast a growth rate, there would not be enough data points per unit neurite growth, and too slow a growth rate would result in unnecessarily time-consuming experiments.

Additionally, we would like to work with cells which have been well characterized in previous research. One advantage of such cells is that there already exist protocols for their care and handling, so one does not need to spend valuable experiment time trying to find the optimal culture medium formulation, for example. Another very important advantage of characterized cells is that, since a baseline for normal behavior has been established for the cells, one may separate with certainty the effects of experimental conditions from the cell's characteristic behavior.

For the specific goal of establishing *in vitro* neural networks of characterized connection pathways, another desirable cell property would be the spontaneous formation of synapses. This is most readily observable in primary cells.

6.4 Modification of Cell Behavior & Morphology

The morphology of cultured cells can be modified by effecting changes in their environment, such as the availability of certain growth factors and the presence of chemical cues. Since cultured cells grow in flasks surrounded by culture medium, from which they take nutrients and into which they excrete waste products, altering the composition of the culture medium is sufficient to change cell morphology. This section will show how such alterations are achieved within the confines of parameters which

keep the cells in good condition. These survival parameters, in and of themselves, will be addressed in the following chapter.

6.4.1 Growth Medium

Established cell lines generally need a wealth of nutrients in order to proliferate, and these are contained in our standard growth medium. The choice of commercially-available medium to serve as the base of growth medium depends upon both the incubator conditions and the ideal pH for the cell lines in question. Three of the most widely used media are Dulbecco's Modification of Eagle's Medium (DMEM), Ham's F12 Medium, and RPMI 1640 medium, and occasionally DMEM and Ham's F12 are combined in a 1:1 ratio to provide the ideal solution. To the base medium is added a certain amount (typically 10%, but as high as 20% for some cell lines) of Fetal Bovine Serum (FBS) in order that certain nutrients, hormones, and growth factors be added to the mixture. Exactly what these are, however, nobody exactly knows: creating culture medium is far from an exact science, and rather is based on mixtures which historically have worked most effectively and which have continued to be used for decades.

In growth medium, immortalized cell lines are typically motile and actively dividing, so this medium is ideal for culturing progressively larger cell colonies. In fact, the cells divide so rapidly that one must perform a procedure called passaging, in which only a fraction of the cell population is kept alive to proliferate, on a weekly basis in order to keep the population at a reasonable level. If the culture becomes too crowded, then cells begin to compete for nutrients and surface area for attachment, and an exponential decay in live cell population results.

Cell morphology in growth medium can change rapidly as the cells undergo division, but otherwise is characterized by a flattened shape, broad lamellipodia when motile, and a lack of stable neurites. The neurites that do form are called "rapid-onset neurites" or "fast neurites" [Smalheiser, 1991] and are characterized by a high degree of plasticity and remodeling.

6.4.2 Starvation Medium

If the level of FBS, and thus of the cells' vital nutrient cocktail, is reduced by a factor of ten, then the cells acquire a different morphology in response. The rate of cell division slows significantly and neuroblastoma cells tend to grow longer neurites, become less motile, and have more rounded cell bodies. Such cells certainly are better candidates for optical guidance because of their distinct neurites and growth cones as well as their lesser motility. Optical guidance has found success with cells in this state, but there is one further step which renders the cells even closer in shape to neurons *in vivo*.

6.4.3 Differentiation

All normal cells in the body arise from pluripotent stem cells, which are wholly undifferentiated and unable to function properly as part of an organ or tissue. In response to specific chemical cues, however, stem cells develop into every kind of cell contained in the body, but in exchange, they relinquish their ability to divide and proliferate, and will ultimately die. This process of development, from a stem cell into a cell specialized for a specific function, is called differentiation.

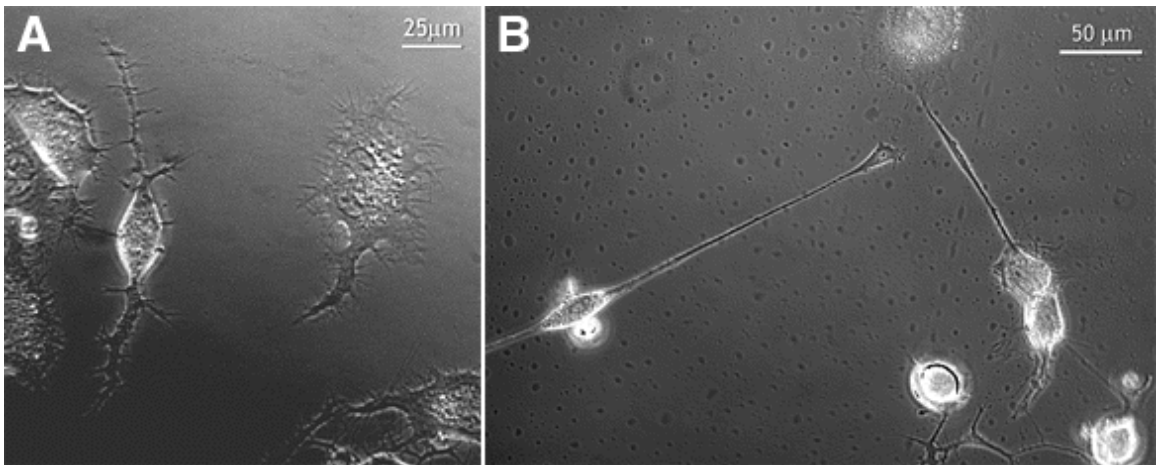

Figure 6.2 Undifferentiated (A) *vs.* Differentiated (B) NG-108 cells. Note the complete change in morphology from neuroblastoma to neruonal phenotype.

The malignant transformation of a normal, functional cell represents a step backward in the process of cellular differentiation, and this is required in order for a cell to be immortalized. When one starts, therefore, with a neuroblastoma hybrid cell line and wishes ultimately to observe a morphology similar to that of a functional neuron, one needs to induce differentiation through exposure to a specific chemical cue. In the case of NG-108 and PC-12 cells, the appropriate chemical cues are cyclic adenosine monophosphate (cAMP) and nerve growth factor (NGF), respectively, which can be added to the culture medium and unleashed upon the cells. A side effect of differentiation, as one might anticipate, is that the cells lose their ability to divide and regain their propensity to die, so new cells must be differentiated regularly in order to maintain a constant supply. Figure 6.2 compares a field of undifferentiated NG-108 cells to a field of differentiated ones, the latter of which have long neurites, growth cones, and cell bodies which are largely stationary. These cells are ideal for experiments in optical growth cone guidance.

6.4.4 Adhesion Factors

In vivo, cells adhere to one another in organs and tissues via extracellular matrix proteins, some examples of which are laminin, poly-L-lysine, and some peptide fragments from these larger molecules. *In vitro*, in the absence of these proteins, some cell types have a difficult time adhering to and spreading out on unfamiliar substrates, and so require the addition of a layer of adhesion proteins to the surface. The culture vessels in which immortalized cells are contained for proliferation are factory coated with adhesion factors, but it is sometimes necessary to add proteins to the plain glass surfaces of experiment dishes. Immortalized cells, such as NG-108s, do not typically need adhesion factors on their substrates and, in fact, the addition of laminin will often encourage cell bodies to migrate, resulting in neurites under tension with a higher likelihood of growth cone detachment.

7. Essentials of Cell Survival

7.1 What Cells Need

7.1.1 Sterile Conditions

Ensuring sterile conditions for cells is both imperative and difficult, as cultures can easily be destroyed by contamination and avoiding this requires constant vigilence on the part of researchers. It is typical for a laboratory involved with cell culture to have a separate partition or room dedicated only to cell culture, in which users must wear minimal protective apparel (gloves) and keep all surfaces generally clean. In the RLM building at this University, however, due to unusually high concentrations of mold in the ventilation system, it became necessary to build a cleanroom in which to culture cells, a schematic for which is show in Figure 7.1. The cell culture room was planned jointly by the lab groups of Mark Raizen and Ken Shih, with special efforts by Soyeun Park.

The room has several mechanisms by which sterile conditions are ensured. HEPA-filtered air is pushed into the room so that there is always a positive pressure within the room and a momentary opening of doors will not invite airborne contaminants inside. Separately from the inner cell culture room, there is a changing room in which users are required to don a clean, disposable lab coat, bouffant cap, multi-layer paper face mask, latex gloves, and shoe covers before continuing inside. The changing room is divided in half so that adjacent the entrance to the inner room the floor will not have been touched by shoes or any other unclean material from the outside. Every supply brought into the cell culture room is cleaned with 100% bleach prior to being brought from one half of the changing room to the other, and is then sprayed with 70% ethanol solution (30% millipore water) and wiped with a clean Kimwipe before being brought into the

inner room. Supplies that have been freshly sterilized in the autoclave may be cleaned only with 70% ethanol prior to entry, as their sterility has already been ensured.

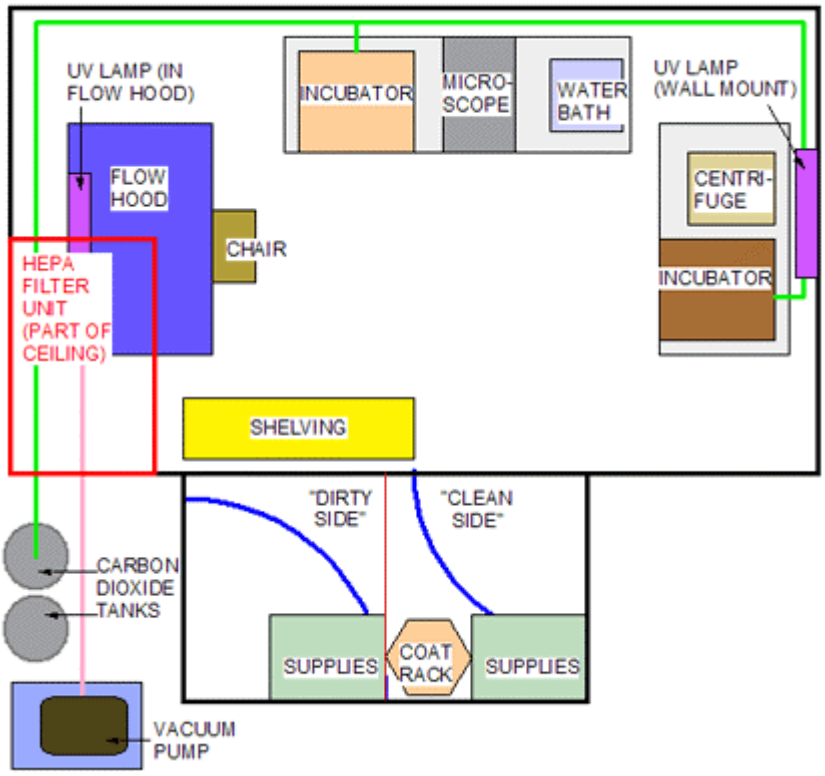

Figure 7.1 Cell Culture Room Schematic. Changing room and main culture room are shown, as well as outside accessories. Positive pressure is maintained in the culture room by constantly drawing air through a HEPA filter in the ceiling and into the room.

We use a Harvey SterileMax steam sterilizer to autoclave experiment dishes, millipore water, saline solution, and other items whose functional properties are left unchanged by extensive heat and pressure. Organic substances such as culture medium and serum cannot be autoclaved because of the denaturation of proteins caused by the heating process: proteins begin to denature at 42 degrees Centigrade, whereas the autoclave operates at temperatures up to 131 degrees Centigrade. For solutions which cannot be steam sterilized, we use sterile bottle-top filters with a pore size of 0.22 microns in their preparation and contain them in sterile glass jars with caps which can be fastened very tightly for storage outside of the cell culture room. Additionally, penicillin-streptomycin (antibiotic/antimycotic) may be added to culture solutions in order to curb the growth of microorganisms in the cell

environment [Elsner *et al.*, 2000]. However, this has the disadvantages of encouraging the evolution of resilient strains of bacteria, creating a slightly less hospitable living environment for the cells, and being able only to curb – but not to stop or reverse – the proliferation of contaminant organisms in cell cultures.

7.1.2 Temperature

The necessity of maintaining a sterile environment for the cells is a consequence of the growth and living environment that they need. Mammalian-derived cells thrive at 37 degrees Centigrade and only a short range of temperatures above and below this value. In addition, in order to keep water from evaporating and changing the osmolarity of the culture medium, the relative humidity in the cells' chamber must be kept at 100%. It is in warm, moist environments like that of the cell incubator that bacteria and mold prefer to proliferate.

During experimental runs, when the cells have been removed from the incubator and are placed on the microscope stage, temperature control is crucial. Special designs and procedures, described in following sections, have been employed specifically for temperature maintenance of the cells at all times.

7.1.3 pH

The purpose of a buffer system, in any context, is to guard against fluctuations in pH by providing a means by which ions can dissociate and combine with any surplus of hydrogen or hydroxide ions which might arise. The buffer system between carbon dioxide in a gaseous state and dissolved sodium bicarbonate in solution has been employed in cell culture for decades and is the standard and universal culture system for

mammalian cells. The most sophisticated part of a cell culture incubator, for example, is the CO_2 detection system which regulates the percentage of CO2 in the air with a precision of 0.1% by volume. The sodium bicarbonate in cell culture systems is found in the culture medium, and thus the pH of the solution in which the cells reside can be altered by changing either the amount of CO2 in the air or the amount of bicarbonate in the solution. As long as both bicarbonate and CO2 are present in the system, the cells' environment is protected from pH fluctuations due to nutrient usage or expulsion of by-products. However, from the moment the cells are taken out of the incubator, interactions between culture medium and atmospheric air begin to raise the pH of the medium, and if left unchecked, the pH can rise to toxic levels. One can see the challenge this presents, therefore, to those who might want to take cells from an incubator to a microscope setup and have them live for extended periods under observation.

We have developed a number of strategies by which to regulate the pH of the medium during the transition from incubator to microscope, and they are worth describing here for reference because this was one of the greatest challenges to our experimental setup. One strategy is to eliminate the air-medium interface altogether by sealing the cell chamber closed as soon as it leaves the incubator, thus trapping the dissolved gas within and not letting it escape; the main problem with this strategy lies in imaging, as dissolved gases will eventually manifest themselves in the form of bubbles pressing up against the top of the chamber and obscuring the microscope light. Another strategy is simply to change the culture medium as soon as the cells emerge from the incubator from their normal medium to one better suited to interaction with atmospheric air; there is great difficulty, though, in keeping the cells happy during this medium change, especially primary cells, which are especially sensitive to their environmentla conditions. A third strategy is to culture the cells in CO_2-independent medium

(Invitrogen, Carlsbad, CA) in sealed containers within the incubator so that they are exposed only to atmospheric air; the flaw in this method (aside from increased culturing awkwardness) is that the dishes often will not get sufficient humidity in their sealed containers, and the osmolarity of the solution will re-equilibrate at an unacceptably high value with evaporation of water from the culture medium. The only way in which we were able to sustain the cells on the microscope was essentially to bring the incubator-like environment to them: bubbling air from a tank of 10% CO_2 (balance air) compressed gas through warm water humidifies the gas, and then it is passed over the cells' normal culture medium. One must ensure a low flow rate for the gas – or pipe the exhaust out to a fume hood – in order to avoid displacing significant amounts of oxygen in the laboratory.

7.1.4 Confluency

Confluency is a measure of approximately what percentage of a substrate is covered by cells, and is most often measured by eye in the cell culture room. Cells in organisms are often quite close together, but when cells are in culture, their confinement to (quasi-)two-dimensional space limits their ability to spread out from each other, so it is especially crucial to monitor the cells' confluency to ensure that it does not get too high.

One of the many goals of cell culture is not to let one's cells become confluent, which signifies a confluency of 100%. In fact, even at overall confluencies of more than 90%, as confluency is never homogeneous throughout a culture vessel, there will be regions in which confluency is dangerously high. The danger of excessive confluency is that if cells are forced to grow on top of one another, they tend to lose the genetic trait of contact inhibition, whereby they are "programmed" not to climb atop each other. Once this genetic mutation has taken place, the cells will no longer act normally at reasonable

levels of confluency, will not spread out as desired, and will not be suitable for experiments.

Therefore, when cell confluency approaches 90% in a culture vessel, this is a signal that the time has come (the walrus said) to passsage the cells (sometimes informally referred to as "cell splitting," not to be confused with mitosis). Passaging denotes a procedure whereby one detaches all cells from their substrate, suspending them in a small amount of culture medium, and then taking a small fraction (typically around 10%) of the suspension and adding it to a new vessel with fresh culture medium. Most of the cells will then attach to the new substrate and begin dividing again, beginning at or around a confluency of 9%. This and other standard cell culture techniques are described in detail in the literature which accompanies ATCC cell delivery.

High confluency is only an issue, though, in immortalized cell lines, as primary neuronal cells cannot divide and thus their confluency is a monotonically decreasing function of time. Low confluency, however, can be problematical for both primary and immortalized cell cultures. The most plausible explanation for this problem is that in addition to releasing waste products, cells also release chemicals which are beneficial to other cells of their kind. This would make sense physiologically because such signals would encourage cells to migrate or grow in the direction of fellow cells that had already reached their designated target area, and cells going the wrong way, ending up where they were not meant to be, would have a greater chance of dying. When dealing with immortalized cultures, a confluency slightly below the lower threashold will likely be remediated as cells begin to divide, migrate across the substrate, and repopulate the culture vessel. However, with primary cells, it is especially important to ensure that cultures are plated at a high enough density, or else their medium must contain some of the beneficial by-products which cannot be produced by neighboring cells. Medium with

these special additives is called conditioned medium, and is easily obtained by placing new culture medium over a highly confluent dish of cells for a period of several hours and then recovering the medium to use elsewhere. There is also evidence that purified conditioned medium constituents, when patterned onto a substrate, guide the growth of neurites along their pathways, even if the conditioning comes from non-neuronal cells [Collins 1984].

7.2 Experiment Dish Design & Description: Structure & Function

Please refer to Appendix C for CAD schematics of the experiment dishes, as they are too large and numerous to be placed here reasonably. Although cell survival systems are commercially available, their high cost justified building an in-house system. In the process of describing our cell dish, it will be necessary at some points to recapitulate the dish's functional evolution to explain the presence of certain features which are no longer used or are used differently from what was originally intended. An earlier perfusion dish design is included at the end of Appendix C.

7.2.1 The Perfusion Chamber Idea

The first idea we had for a cell survival system was to construct a perfusion chamber, in which culture medium could continually be refreshed by adding it at one side and taking it out at the other at a constant rate. This would keep constant the amount of medium in the cell chamber but ensure that enough nutrients were available to the cells at all times. The perfusion would take place at such a slow rate (around 10 microliters per minute) that there would be only a very small perturbation in the fluid flow at the level of the cells. The idea was that diffusive processes, in their quest for maintaining equilibrium

throughout the fluid, would facilitate the exchange of nutrients for waste products to keep the cells viable and healthy.

Accordingly, the two flow antechambers (see Figures C.7 and C.8) were designed to cause a gradual horizontal expansion of the incoming fluid front to avoid a situation in which most fluid flow would be occur down the center of the chamber's width and only minimal, diffusive off-axis mixing would result. The two through holes at the end of each flow antechamber originally served the purpose of conducting culture medium into and out of the cell dish by way of a peristaltic pump. When used for an inlet and an outlet, these two holes held small stainless steel tubes for attachment of the silicone or tygon tubing which carried the medium. These stainless steel tubes, which even in the present incarnation of the cell dish serve as points of attachment for tubing, are each made with a 5-8 mm long segment of a hollow 18-gauge needle from which the sharp tip has been removed. With careful application of bending forces to the needle with a pair of fine pliers, the stalk of the needle usually can be cut with minimal compromise of cross-sectional profile at the ends of the resultant tube.

7.2.2 Central Well and Overflow Trough

Historically, the central well was filled with a pool of culture medium and was open at the top, allowing the medium to interact with the air. With this configuration, the atmospheric air would very quickly raise the pH of the medium to unacceptably high values, and the cells did not live long enough on the microscope for experimentation. Even if this problem could be circumvented, the requisite heating of the cell dish results in water evaporation and consequent disequilibrium in the medium osmolarity, which also then proceeded to kill the cells.

The next setup attempted was one in which a layer of mineral oil was placed atop the culture medium to inhibit evaporation, with the dish still undergoing perfusion. The overflow trough was created at this stage because of an inherent (and, as we found, ineluctable) mismatch in flow rates provided by the peristaltic pump to any two separate lengths of tubing. When minimized, the difference in flow rates could be tolerated for up to a few hours with a fair amount of consistency, but overnight runs were still impossible in this scenario. Ultimately, either the oil would overflow the central well (inflow greater than outflow) or all the medium, and then the oil, would be sucked out of the chamber (outflow greater than inflow). To save the microscope from inundation in cases of slight overflow, troughs were constructed around the border of the dish, which would buy the experimenter a bit of time. However, this situation was far from ideal, as the mineral oil could be neither sterile filtered (presumed to be due to its hydrophobicity) nor autoclaved (which apparently produces chemicals toxic to cells), so sterility could not be guaranteed. Additionally, in the best case scenario, there was a directionally isotropic lensing effect at the water-oil interface, which affected the quality of cell images. In case scenarios further from the best, the lensing effect would be anisotropized by the oil's coming in contact with a lower surface of one side of the central well, coating this surface with hydrophobic material and not allowing the culture medium to extend all the way to the edge of the well in that direction. The anisotropic lensing effect was just as bad as, if not worse than, the isotropic one, so a better way had to be devised of preventing (or at least significantly inhibiting) evaporation from the cell dish.

The overflow trough was still used in the next incarnation, in which a circular coverslip floated atop the culture medium so that minor fluctuations in the level of the medium would only cause the coverslip to rise and fall. This solved the lensing problem, confining the upper boundary of the liquid to the flat surface of the coverslip. However,

this did not solve the problem of unequal flows into and out of the chamber, although there was about twice as much leeway in the rising and falling of the coverslip so twice as much time could elapse before intervention was required to stop an overflow or underflow. At this point, the primary problem was the accumulation of bubbles beneath the coverslip. Although, by lifting one side of the coverslip, these bubbles could be let out, there was only about a 50% chance that even someone well-versed in this art form could successfully lift and replace one side of the glass without either breaking the glass or causing medium to climb up over the opposite side and sit on top of the glass. When the point of diminishing returns had been reached for our efforts, we completely revamped the dish by adding the following feature, the gas pockets.

7.2.3 Gas Pockets

The regulation of pH while the cells are on the microscope is a tricky proposition, mainly because of the difference between the air inside the incubator and the air outside it. The CO_2-bicarbonate buffer system is by far the most widely used for mammalian cell culture, but as soon as the cell dish leaves the incubator, atmospheric levels of carbon dioxide begin to raise the pH of the culture medium. Mammalian-derived cells are the healthiest in medium at a pH of 7.4, but the pH of medium in atmospheric air can rise to levels above 8.0. If the pH gets high, the cells become unhappy, and if the pH gets *too* high, the cells become *irreversibly* unhappy.

One remedy to this situation is to keep the culture medium isolated from atmospheric air, but this requires some discontinuity between the state of the dish in the incubator and the state of the dish on the microscope, and cells can be very sensitive to environmental changes. We wanted to minimize instability when moving the cells between the incubator and the microscope, and the best way we found to accomplish this

was to introduce pockets of 10% CO_2 gas into the cell dish which, by virtue of being in contact with the surface of the fluid, maintains the medium's pH in the same way the incubator does.

It is important, then, to ensure that the 10% CO_2 gas, which comes compressed from a cylinder and therefore completely dry, is adequately hydrated in order that it not cause evaporation of water from the culture medium. If this were to happen, the resultant imbalance in osmolarity between the cells and their hyperosmotic medium would result in shrivelled cells on a short timescale. Accordingly, we bubble the 10% CO_2 gas mixture through millipore water in two separate steps so that it becomes sufficiently humid before passing it into the cell dish on the microscope.

The flow rate of gas into the cell dish must be high enough to create a slight positive pressure in the cell dish so that atmospheric air cannot travel into the gas pockets, but not so high that it displaces a significant amount of oxygen from the lab. We have found that only a very low flow rate is necessary (less than 5 ml per minute), so that the CO_2 gas added to the atmosphere in the lab can be considered negligible.

7.2.4 Multiple Functionality of Gas Inlets/Outlets

The CO_2 gas is designed to flow into the pockets through two small inlets, to which silicone tubing can readily attach via small stainless steel tubes fabricated from 18-gauge needles. These inlets are placed at the corners of the gas pockets because they also serve as medium removal outlets for pre-experiment cell maintenance, which requires changing the cell medium every two days. The inner two holes to the gas pockets serve as gas outlets during the experiment and medium inlets during cell maintenance operations.

Since the stainless steel tubes through the outer holes are made by hand, it is always possible that their cross-section will turn out not to be entirely circular at every point along the tube, and this can sometimes constrict air flow. Uneven air flow leads to pH imbalance in the medium beneath: one gas pocket remains at the correct pH while the other gas pocket fills with atmospheric air and the pH of its medium rises to dangerous levels. To avoid this situation, one can place a small clamp on one of the two silicone tubes through which the gas flows so that the measure of flow constriction – and thus, flow rate – to both gas pockets in the cell dish remains the same. Failing this, another possible configuration is to drill one extra hole down into each gas pocket for the purpose of connecting the two gas pockets directly in order to abolish any disequilibrium.

7.2.5 Thermocoax Heating Cables and their Channels

Since mammalian cells need to be kept at or very near 37° C, it was necessary to find a way to heat the perfusion dish in order to keep the cells and their medium warm at all times. In the first incarnation of the experimental setup, a water bath supplied warm water to a volume of liquid surrounding the cell dish, but this setup had the distinct disadvantage that any slight leak in the water exchange system threatened to damage microscope optics and other hardware, and at one point this system did destroy a CCD camera in just that way. Another solution was deemed necessary.

Recent developments in materials technology have produced substances which are simultaneously electrically conductive, optically transparent, and biocompatible [Schmidt, 1997]. Such materials are an attractive option because of their capacity, if applied as a coating or a pattern on the coverslips of cell dishes, to evenly distribute heat to the cells from a small electric current. However, it has been shown that neurons respond to voltages by extending neurites in the direction of an applied electric field

[Borgens, 1997; Britland, 1996], about three times more rapidly than usual [McCaig, 1992], in response to as little as 3 mV / cm^2 [Patel, 1984], and even on biocompatible, conductive surfaces like polypyrrole [Schmidt, 1997]. Since we wish to have a cell environment which is isotropic with the exception of the laser spot, in the interest of minimizing the number of concurrent stimuli to the neurons, we figured that another approach was warranted.

We discovered that there exist heating cables of about 1 mm diameter which consist of two heating wires, insulating powder, and a metallic sheath [Thermocoax, Alpharetta, GA]. Because electric fields cannot exist outside of the metallic sheath, and because the dual-directional flow of current ensures that any magnetic fields will cancel each other out, these heating elements turned out to be the best way to heat the cell dishes.

Since the cell dishes spend most of their time in an incubator, we decided to construct them with rectangular symmetry so that the thermocoax heating cables could pass through them for the duration of the experiment but did not have to become an integral part of their structure. The pass-through holes for the heating cables are slightly larger than the cables themselves, and are typically loaded with vacuum grease prior to insertion of the heating cables. Vacuum grease serves the purposes of maintaining thermal contact between the cables and the dish (at least, better contact than would be provided by intervening air) and also increasing the ease of insertion of the cables into the dish.

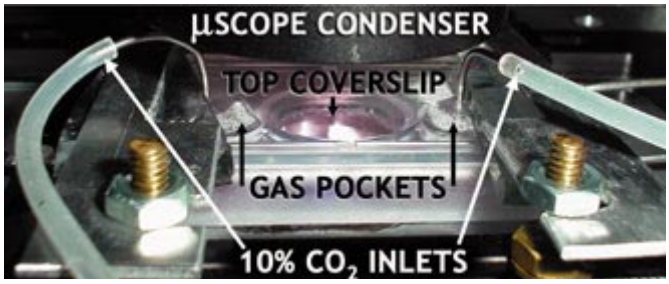

Figure 7.2 Cell Dish In Action. A view of the cell dish clamped down onto the microscope stage and connected to the carbon-dioxide gas supply.

The heating cables terminate in two wires on one end and a cap to connect the two wires on the other end, so that the current flows down the cable in one direction and then back in the other direction, dissipating heat as it goes. After the two cables have been inserted into the dish, they are connected in series with a power supply, and their temperature is regulated by a feedback loop with a thermocouple and a temperature controller [Omega Engineering, Inc., Stamford, CT]. In order to obtain the correct temperature for the cells and to allow for heat dissipation by the lexan dish on the way inward to the cells, the heating cables must be kept several degrees warmer than the desired cell temperature. However, with the help of an objective lens heater (see Section 7.3.3), the temperature remains constant to within one degree centigrade from the periphery of the cell chamber to the center. A photo of the setup is shown in Figure 7.2.

7.3 AUXILIARY CELL SURVIVAL COMPONENTS

7.3.1 Cell Transport: Getting Safely to the Microscope

Because the cells attach to such a thin glass surface, the glass cannot provide much thermal insulation during the trip from the cell culture room out to the microscope area, where the heating cables are prepared, and then onto the microscope stage. Additionally, for a short period it was required that we transport cells between buildings, so the issue arose as to how to transport the cells with minimal disturbance to them. The two most important factors in cell transportation are temperature stability and prevention of shocks to the system. For interbuilding transport, a thick-walled styrofoam container was filled with refrigerant/freezer packs which had been heated to 37° C in a water bath and cleaned with 70% ethanol. The container is suspended from the user's hand with four strands of approximately 1 m length x 1 mm diameter silicone tubing whose periods

of vertical and horizontal oscillation are far greater than those of a walking step. For cell transportation from incubator to microscope, a single heated freezer block beneath the cell dish maintains an adequately stable temperature. Visual verification is provided when one notes that the cell morphology as observed in the cell culture room and subsequently under the microscope are basically the same, without retraction of processes or detachment of cells from the substrate.

7.3.2 Microscope Enclosure with HEPA Filtered Air Inlet

In anticipation of the same kinds of problems which originally plagued the cell culture room and prompted us to build a cleanroom for the purpose, the microscope area was designed as an enclosure with an inlet for HEPA-filtered air, shown in Figure 7.3. A nitrile glove extended into the enclosure for contamination-free manipulation of the focus and stage position, and HEPA-filtered air was provided by a small, commercially available filter unit. Since one side of the area beneath the microscope stage was left open for the optics, pressure buildup was not an issue, and since the need to open the enclosure was rare, only a small positive pressure was necessary to keep out

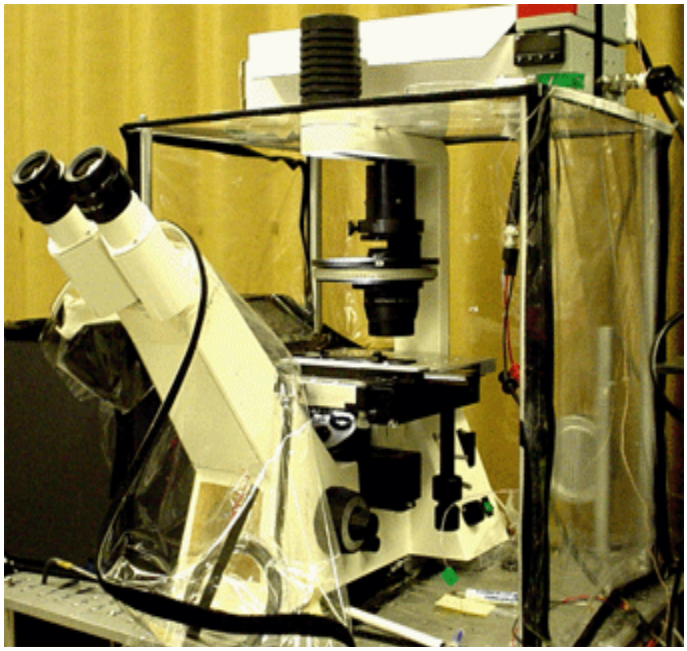

Figure 7.3 Microscope Enclosure with Front Pane Taken Down. The enclosure is made of aluminum rods supporting a plexiglas top, with clear vinyl siding attached to the rods with velcro so as to be removable.

contaminants. The housing managed to keep the microscope and nearby optics free of dust, even though it ultimately never needed to be used as the pure environment it was designed to be.

Briefly, the air from the filter unit travels through a modified dryer exhaust duct and then to an aluminum dryer exhaust vent which contains a bit of extra filtration material. To minimize high-velocity air flow around the sample area, which can lead to undesirable thermal effects, a piece of plexiglas can be placed about 2 cm in front of the air vent. This keeps a streamline of air from forming in the enclosure by inducing immediate turbulence for velocity dissipation. Combined with setting the filter unit for the minimum output velocity, this is a very effective method of ensuring steady-state temperature under these conditions.

7.3.3 Microscope Objective Lens Heater

An oil immersion objective lens is a mortal enemy to mammalian cell lines, since it becomes a very effective heat sink if not properly infused with warmth. As in the case of the cell dish, though, the objective lens was heated by the flow of water in the original incarnation of this experiment and so had to be changed. We turned once again to the effective thermocoax heating cable, and since this time we were designing a semi-permanent fixture for the objective lens, we could also make the heater with cylindrical symmetry so as to distribute the energy as evenly as possible. There is a single piece of aluminum which fits over the objective lens to within 0.005 inches, and attached to the aluminum cylinder with thermally conductive epoxy is a coil of heating cable. It is not appropriate to use a feedback loop with a temperature controller for this application, though, because if the objective lens were accidentally to overheat, the complex optics would be damaged. For phase-contrast microscopy, especially (see Section 3.4.1), even a

slight shift or warp in the objective lens has the capacity to ruin the image quality. The current to the objective heater, therefore, comes from a separate power supply, whose knobs are covered over to prevent accidental turning.

7.3.4 Light from Microscope Condenser

When first we were building the experiment, we found that filtering the incoming light from the microscope condenser down to a narrow span of wavelengths minimized chromatic aberration at the CCD camera and gave sharper images. Since, of the visible wavelengths, blue light carries the most energy per photon, and since we wished to minimize exposure times, a blue filter was chosen to sit atop the enclosure just beneath the microscope's illumination source. When the problem arose that the cells could only survive for a short time (a few hours) on the microscope – and given that other relevant variables (like temperature and pH) had been stabilized – we figured that perhaps the microscope light was contributing to the ill-being of the cells. The program was then modified so that the microscope light would be off by default, coming on only for the acquisition of the cell image.

At one point in time, however, we noted that the cells seemed to fare better and live longer when images were captured overnight at intervals three or four times longer than usual. Put together with our subsequent discovery that green light, at least, is known to be harmful to cells in culture [Langenfeld-Oster, 1993], this suggested that the microscope light was still contributing to their ill-being, and so decided to replace the blue filter with a red one. This has had the imperceptible drawback that chromatic aberrations are no longer fully eliminated by filtering but, supported by the rudimentary observation that the red-colored medium has a lower absorption of red light than of blue

light, preliminary indications are that cells undergo less photodamage in the current setup.

8. Laser Optics & Microscopy

8.1 DIODE LASERS

Several different lasers have been used in this experiment at one time or another, all with wavelengths in the near infrared. Argon-pumped Ti:Sapphire lasers of sufficient output power have been suitable here, though we found the power output from a 5-Watt pumped laser to be insufficient. A high-power Nd:YAG fiber laser was found not to function properly in our setup because coatings on the microscope optics prevented the needed light from passing through the objective lens without endangering the optics by undue absorption of power. Accordingly, in this incarnation of the optical guidance experiment, mindful of these constraints and to operate within the confines of cost and space, we chose to use diode lasers for our source.

For this application, we have the luxury of freedom from concern with the laser's linewidth, polarization, and superposition of modes (all of which are critical to atom optics experiments), so diode lasers are perfectly appropriate. However, we do need a Gaussian beam with radial symmetry so that guidance is never biased by an axis projected by the laser spot. There is certainly a threshold laser power below which guidance will not take place, around 60 mW, and to ensure that our experimental value would always greatly exceed this threshold, we decided to settle for no less than 80 mW of laser output in the plane of the cells. The main challenge to be overcome with diode lasers is that, in order to achieve high output power, diode lasers are often constructed with a linear array of diode elements, so the beam issuing forth is both highly divergent and near to a Gaussian intensity distribution only on one of the axes perpendicular to the direction of propagation. One can attempt to remedy this situation with a cylindrical lens and pinholes, but for us, this ultimately cost too much power and the approach had to be

abandoned. We were subsequently able to find diode lasers which have a nearly-circular Gaussian output profile by virtue of a minuscule lens incorporated into the diode (Blue Sky Research, Milpitas, CA). Two of these lasers, at 150 mW each, provide enough power to traverse the optics with a power of 100-120 mW in the plane of the cells. Most of this energy loss is due to the phase-contrast imaging system, whereby incoming laser light must be attenuated by a dark phase ring within the objective lens of the microscope (see Section 8.2.3).

Each diode laser has an independent current supply and temperature controller (Newport Corporation, Irvine, CA), and each is mounted on a TCLDM9-TECLD diode mount (Thorlabs Inc., Newton, NJ) and is kept at 20 degrees Centigrade. A spherical lens is mounted with slow-curing epoxy on each diode mount in order to collimate the light, since although the laser profile is nearly radially symmetrical, the initial divergence is still substantial (9 degrees). Standard grounding precautions must be observed at all times, and a maximum current limit observed, to ensure the safety of the diodes.

8.2 Optical Table Setup and Logistics

8.2.1 Laser Optics

A brief overview of the optics is shown in Figure 8.1. Since the light emanating from laser diodes is plane-polarized, light from two of them is combined using a polarization cube, with one diode mount rotated by 90 degrees. An optics mount with fine angular adjustment was required in order to maximize the power output of the combined laser beam. The spots from the two lasers were superposed iteratively in the near and far fields until optimal overlap was achieved. Then, the resultant beam was

directed through the optics and through the plane of the cells in a standard optical tweezer setup.

In order to obtain the smallest possible spot size for optical guidance, we wish to maximize the diameter of the beam entering the objective lens. The beam diameter is about 2 mm after the polarization cube, and we enlarge the beam diameter to roughly twice that diameter with a telescope consisting of two plano-convex lenses. Estimating the distance traversed by the beam on its way to the objective lens for this purpose can be tricky because of the multiple reflections required by the galvanometer-driven mirror system.

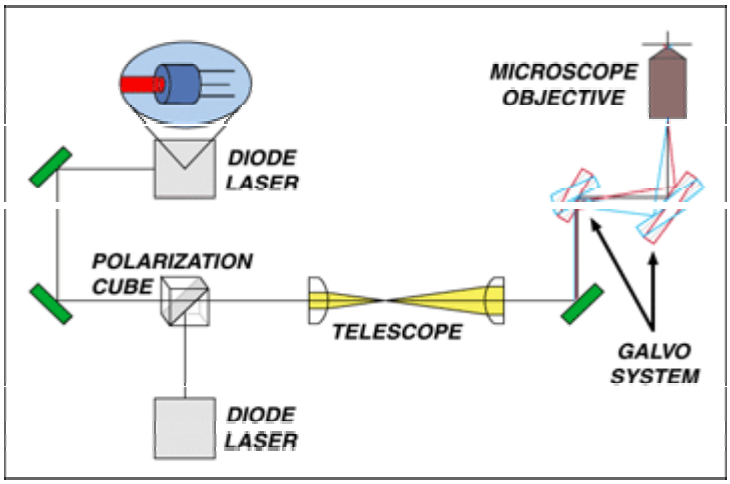

Figure 8.1 Optics Overview. The output of two diode lasers is combined and directed through the microscope objective. The beam direction system (only one axis shown) consists of mirrors mounted on galvanometers, by which the beam's incident angle is adjusted.

8.2.3 Table, Optics, Levels, Microscope

Phase contrast microscopy was first implemented by Frits Zernicke, who won a Nobel Prize in physics for this work in 1953. This type of imaging system, depicted in Figure 8.2, allows imaging of objects like biological cells, which are not perceptible under ordinary light microscopy. Objects which can be viewed using ordinary light microscopy are called amplitude objects, whereas ones that cannot are called phase

objects. Phase-contrast microscopy works by using the phase shift of light passing through a material to create an image.

At the time this experimental apparatus was assembled, the only available microscope was a Zeiss Axiovert 25 inverted microscope with phase-contrast air immersion objective lens (Zeiss LD Achroplan 40X, NA=0.60), but the lens was ultimately replaced by an oil immersion Zeiss Fluar 40X, NA=1.3. Switching the objective lens not only necessitated a change from Ph2 to Ph3 size rcondenser rings but also an entirely new condenser for the microscope as well. We acquired a Hoffman Modulation Contrast condenser (RG1, Modulation Optics, Inc.) to hold a Ph3 annulus. The filter cube was altered so that a dichroic mirror could fit in sideways to accomodate reflection of the laser up through the objective lens and transmission of the microscope image back downward to a CCD camera (Apogee AP9E, Apogee Instruments Inc., Auburn, CA). The camera had to be mounted underneath the microscope because of the large size of the unit, and so the microscope had to be raised up above the level of the lasers and optics to accomodate this configuration. The galvanometers and attached mirrors had to be placed on the upper level with the microscope to minimize the path length the laser would have to travel between the

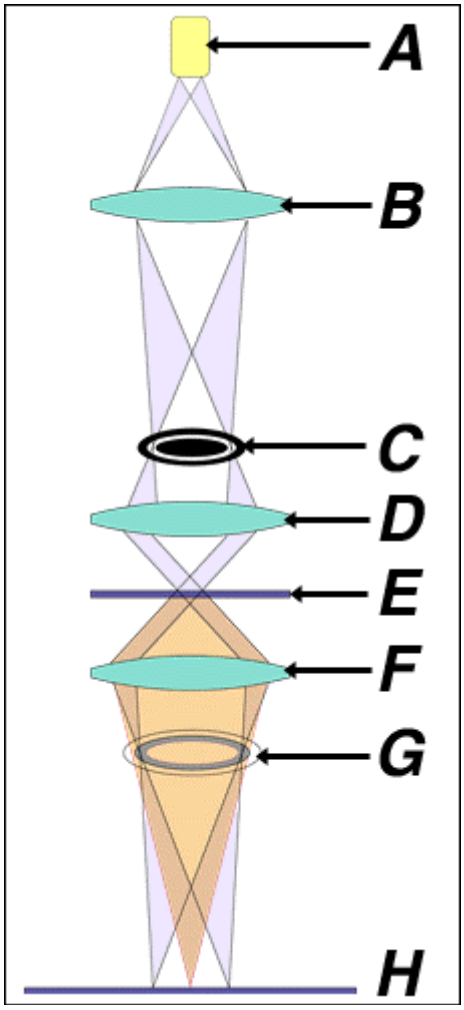

Figure 8.2 Phase Contrast. (A) Light source, (B) Collector, (C) Condenser annulus, (D) Condenser Lens, (E) Sample, (F) Objective Lens, (G) Attenuation Ring, (H) Image plane. Red light: phase shifted. Blue light: unperturbed.

positioning mirrors and the microscope (which ended up being about a half a meter in total).

8.3 BEAM GUIDANCE / GALVO SYSTEM

8.3.1 Rationale

For each axis perpendicular to the direction of laser propagation, we wish to have control over the point at which the laser spot arrives (always to be centered at the back aperture of the objective lens) and the angle with which it arrives at that point. We need two mirrors per axis, therefore, to comply with both of these spatial constraints (or two mirrors and one lens, but using four mirrors minimizes the chance of spherical aberration, which is important in designing a system for which one would like a wide field accessible to the laser). Each of these four mirrors must be adjustable in real time to allow repositioning of the laser spot at will, and the speed with which these adjustments can take place determines the granularity of the timescale of the experiment. Galvanometers with mounted mirrors are ideally suited to this purpose and are readily available commercially (GSI Lumonics, Billerica, MA).

8.3.2 Open-Loop Galvanometer System

The first system of galvos we attempted to employ were of the less costly open-loop variety. These galvos simply convert input voltages to output angles repeatedly at a rate determined by the user, with no feedback control. There are three basic modes through which a laser spot can be directed by galvos: step, raster, and vector scanning. For the multiple laser spots we wanted to have for guidance, step scanning is the most appropriate basic description of our fundamental needs.

The precision with which we needed to control the laser spot position turned out to be far more than this system could provide because of hysteretic effects inherent in all laser movements, most evident when the laser was "hopping" from point to point. The data acquisition program was modified to correct this problem to some extent by setting a fixed point to which the galvos would hop for a short time after each point set for guidance. This way, since every other laser position was the same point, the point immediately preceding every guidance point was the set point, and thus the hysteresis was mitigated somewhat. However, despite these adaptations, user control over the precise position of the laser spot was not consistent enough for successful manual guidance (much less automated guidance).

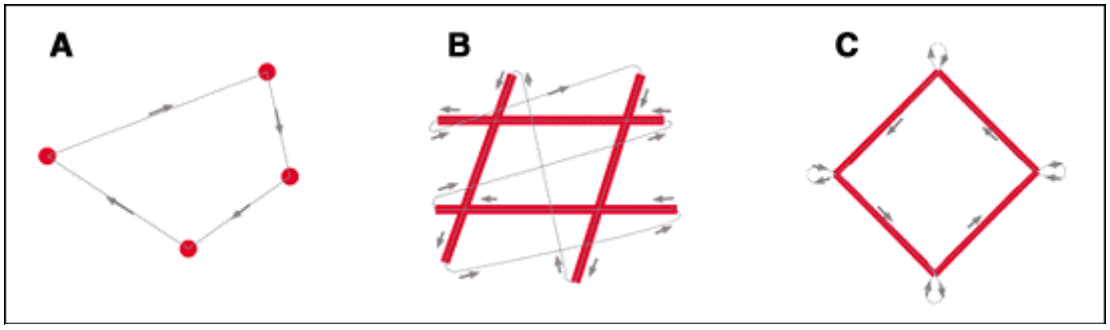

Figure 8.3 Three Laser Scanning Modes for Galvanometers. (A) Step Scanning, (B) Raster Scanning, (C) Vector Scanning. Thin, gray lines trace the path of the laser and bold, red lines represent times for which the laser is on in order to make various shapes (for general purposes, we assume the laser power is otherwise modulated).

8.3.3 Closed-Loop Galvanometer System

Closed-loop galvos (GSI Lumonics models M2S, M2ST, M3S, and M3ST), although considerably more expensive than open-loop models, offer a much higher degree of control over laser spot positioning. First of all, there is a feedback loop by which the actual position of the galvo is sensed and updated at a very high refresh rate (up to 100kHz), so the galvo is guaranteed to turn by precisely the correct amount for a

given voltage. Additionally, notch filters are programmed into the controller boards to take into account the exact moments of inertia of the specific mirrors mounted on the galvos (whereas with open-loop galvos, mirrors could be hand-cut and manually attached). Thermal control blankets are wrapped around the bodies of the galvos and the temperature of the instruments is controlled with Peltier elements to minimize zero drift by a factor of 12 over unregulated closed-loop galvos and by a factor of 20 over open-loop models. Wobble and jitter are reduced by an order of magnitude over open-loop models. The drawbacks to using closed-loop galvos are that mirrors cannot be exchanged (notch filters are specific to one individual mirror) and the degree of excursion is slightly lower than for open-loop galvos.

9. Data Acquisition

9.1 Calibration of Spot with Galvos

There are two calibration procedures required for precise control of the laser spot position. The first goal is to ensure that, for every combination of voltages for galvos 3 and 4 for which it is possible to direct the laser spot through the objective lens, another pair of voltages for galvos 1 and 2 is automatically determined, such that the laser spot is directed through the exact center of the objective lens's lower aperture. The second goal

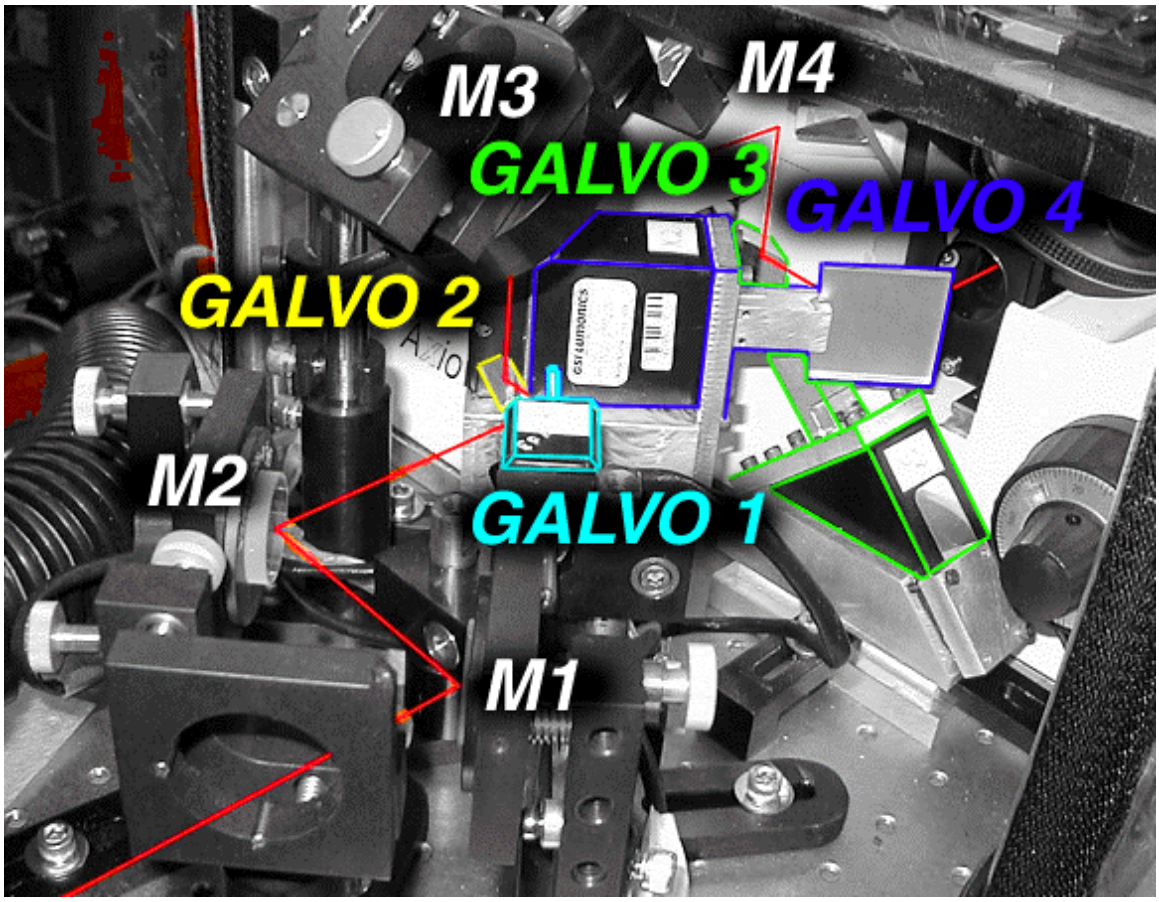

Figure 9.1 Galvanometer System Guides the Beam Path to Microscope. Path of laser: Lower-left corner, Mirror 1, Mirror 2, Galvo 1, Galvo 2, Mirror 3, Mirror 4, Galvo 4, Microscope Filter Cube.

is to calibrate user input to the actual laser spot position so that, when one specifies a target for the laser spot on the CCD image, the spot will show up within a reasonable distance of the point specified.

9.1.1 Coarse Adjustment

The goal of coarse adjustment is to ensure that, for every position of the pair of galvo mirrors 3 and 4 the other two mirrors will automatically be placed at the correct angles to ensure the beam's proper entry into the objective lens. This is accomplished by sampling a large number of points in the plane defined by the positions of the first pair of mirrors, and then manually adjusting the other two mirrors to position the laser spot. A piece of paper, thin plastic, or other translucent material must be placed on the objective lens turret in place of the lens so that the laser spot can be visualized in the correct plane with the help of an IR viewer (such as FJW Optical Systems). It is most ueful to employ a simple program in LabVIEW (National Instruments, Austin, TX) which interfaces directly with the galvo controller cards and provides a direct readout of the voltage values for each galvo. Two separate functions can then be fit to these data, one for galvo 1 and one for galvo 2, both as functions of galvos 3 and 4. These functions are fit using an nth degree polynomial function (where n typically equals 4) in OriginLab software (OriginLab Corporation, Northampton, MA). The resultant functions, when fit to the data points, establish three-dimensional surfaces for which there is a defined value for every coordinate produced by galvos 3 and 4 (and on a much finer scale than that of the points sampled).

9.1.2 Fine Adjustment

The ideal outcome for this step is that there be zero error between the user-specified laser position and the actual position of the laser spot, but unfortunately, so many sample points across the CCD image would be required to achieve this degree of precision that time prohibits it. The goal is to fit a function to the sample points to predict the position of the spot for any user-input points. Not only would such a function be highly nonlinear, though, but it would also fail to guarantee an exact result, even with a substantial amount of refinement. Our solution to this quandary is to sample a "reasonable" number of points (n = 20) across the CCD image, get the best possible fit with a fourth-degree polynomial function, and put in place yet another opportunity for the user to fine-tune the offset in the course of data acquisition.

9.2 Acquisition Parameters, Hardware Interfaces, and Requisite Setup

9.2.1 NI Controller Card, Galvo Board Interface

A National Instruments NI PCI-6733 PC interface card is installed for communication between the computer and the experiment; this card was chosen primarily for its eight analog outputs which control the galvos and filter flipper. Each galvo has its own controller board, a MiniSAX servo-amplifier with speed tuning module, thermal controller, and notch filter board specific to the mirror mounted on that galvo.

9.2.2 Timing of Microscope Light, Flipper, CCD Camera Exposure

The *Neuron* program is basically designed to take two pictures for every data point: the cell image and the laser image. The procedure for acquiring these images is typically as follows:

- Initial state, before acquisition sequence: microscope light is off, high-OD filter is out of the beam path, galvos are running at their specified intervals and locations to position the laser spot(s).
- Acquisition cycle begins: microscope light (through condenser) turns on, galvos redirect the laser into a beam stop and away from the sample.
- Camera shutter opens for a specified time (for the cell image) and the data are sent to the computer.
- Laser is directed back through sample; microscope light turns off; high-OD filter flips into the beam path.
- Camera shutter opens for a specified time (for the laser image) and the data are sent to the computer.
- High-OD filter flips back out of the beam path
- The cell edge is calculated from the cell image (with contrast optimized); the spline is adjusted accordingly; the new laser spot position is calculated; the laser is moved to its new position.
- Cell image, laser image, edge detection image, and spline are all combined for display and are saved to disk as separate image elements.

The typical time interval between acquisition points is 30 seconds, and the typical cumulative time for which the laser is either directed away from the cells or highly attenuated is typically under three seconds, so we have deemed that small period of "off" time to be negligible and have excluded it from consideration.

9.3 AUTOMATED GUIDING

The C++ program that we use for automated guidance was originally created by Florian Schreck in the summer of 2002 and subsequently underwent major modifications

at the hands of Jakub Otwinowski. Although the program is always being revised and updated with the addition of new features, the first version in which it was possible to automate optical guidance appeared in December of 2003. Since then, the majority of modifications have dealt with automating and simplifying the analysis of data already acquired.

For data acquisition, the two most relevant functions other than hardware control are the edge detection procedure and subsequent update of the laser spot position based on the edge information. Specific details about the program's user interface and the parameters available to be set can be found in Appendix B.

9.3.1 Overview of the Process

9.3.1.1 Goal for Laser Position

Exactly where to position the laser spot with respect to the edge of the growth cone is of primary importance, and Figure 9.2 shows some sample configurations. If the laser spot is contained entirely within the growth cone and is some distance away from the edge, as illustrated in Fig. 9.2 (A), then the laser focus is not at the cell's leading edge and guidance does not result (Käs *et al.*, unpublished results). In case (B), the entirety of the laser spot still lies within the cell, but the laser

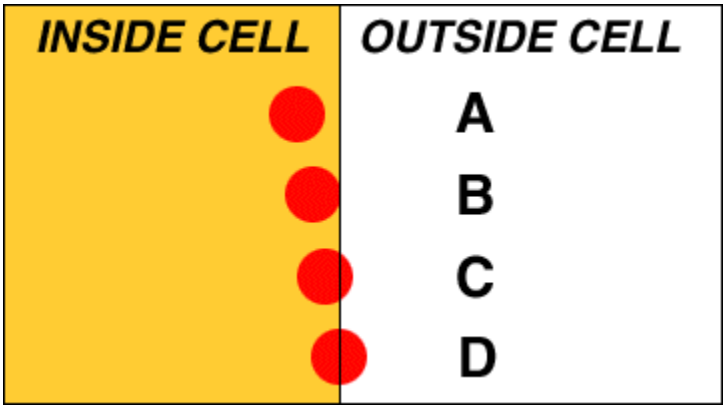

Figure 9.2 Laser Positioning. Positions B and C are considered preferable to positions A and D. Laser diameter ~ 1 micrometer.

focus is nearer to the leading edge and thus is able to result in growth cone guidance. Case (C), wherein the laser focus is even closer to the leading edge but some laser light is located outside of the growth cone, is also a suitable arrangement for guidance experiments, although some laser power is lost in exchange for having the focus closer to the edge. If the laser focus is directly at the leading edge, then half of the laser light is lost and such a configuration is again inconducive to guidance, as in Case (D).

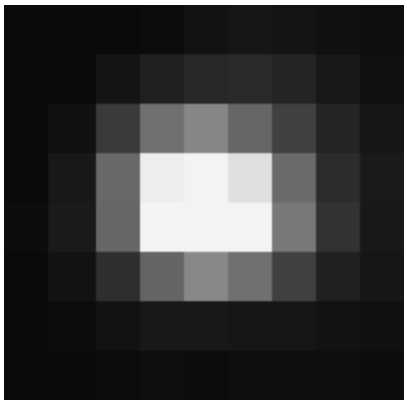

Figure 9.3 Laser Spot Profile. A magnified image of the laser spot in the plane of the cells, where each pixel spans 277x277 nanometers.

The laser spot profile, contrast-optimized for ease of viewing, is shown in Figure 9.3. Note its elliptical shape, just as the cross-section of the beam emanating from one of our diode lasers, and that the largest dimension does not exceed 1.5 microns. Additionally, the spot appears fairly Gaussian on both axes. Having the laser spot subtend so few pixels, however, may also have its disadvantages during manual guidance. In aiming for a cell-laser configuration as in Figure 9.2 (B) and (C), the user cannot err by more than a pixel or two in positioning the laser spot without a sub-optimal resultant cell-laser configuration. Although this problem of pixellation potentially could be rectified by further magnification of the image,† limited resources prevented an exploration of this avenue. Such a drawback underscores the importance of implementing automated guidance in our system so that the laser positioning is done by a computer and is not governed by the imprecision of human judgments. The means by which automation is accomplished is discussed in the following sections.

† With a numerical aperture of 1.3, the objective lens ensures that resolution is not the complicating factor here, but with an effective magnification of 32X, the image it projects can only be a certain size when it impinges on the CCD camera chip without the aid of additional optics.

9.3.1.2 Cell Boundary Determination

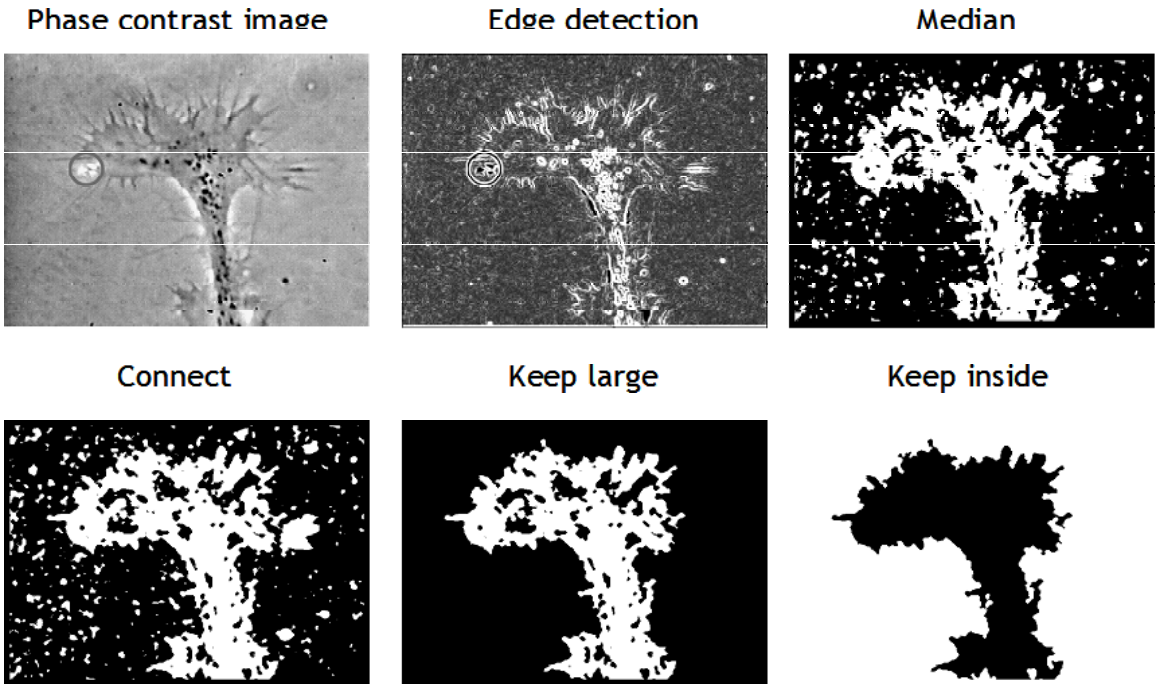

Figure 9.4 Steps in the Edge Detection Algorithm. A sample picture (upper left, progressing left to right before top to bottom), where there is a circle around the laser spot, is used to test the efficacy of the edge detection algorithm by tracking its progress at several steps along the path.

The computer must first create from the phase-contrast image input a determination of the boundary between the cell and its surroundings. Figure 9.4 shows a sample image for which a boundary computation is performed, illustrating the steps through which the computation proceeds in order to end up with a final result of two areas (black and white) differentiating the "inside" from the "outside" area.

The edge detection algorithm employed in the first step is a standard one, wherein for each pixel in the selected region an n x n matrix is created with that pixel in the center, and the direction of the greatest gradient of greyscale values is calculated. If this gradient is found to be greater than a certain value, as determined from user-defined

parameters, then this pixel is said to define part of an edge. Secondly, the resultant image is then thresholded, converting it to a binary (black and white) representation, according to a grayscale value set in the user-defined parameters. After thresholding, if there are two white pixels which are separated by a small number of black pixels, then these intervening pixels are filled in with white: this step helps to make contiguous the area "inside" the cell and to keep "inside" areas from being eliminated in the following step. Next, for each cluster of white ("inside") pixels, if the number of pixels it spans is less than a given value, then the whole area is changed from white to black – this ensures that small pieces of debris that may initially be detected are eliminated, leaving only the larger areas. The processes of filling gaps and keeping only the larger areas is repeated, and the resultant image is inverted for purposes of display and is saved as the "detection image" for the data point.

9.3.1.3 Spline Curve Determines Growth Direction

In order for the computer to be able to determine the ideal placement of the laser, the direction of guidance must first be specified. Before guiding begins, this direction is supplied

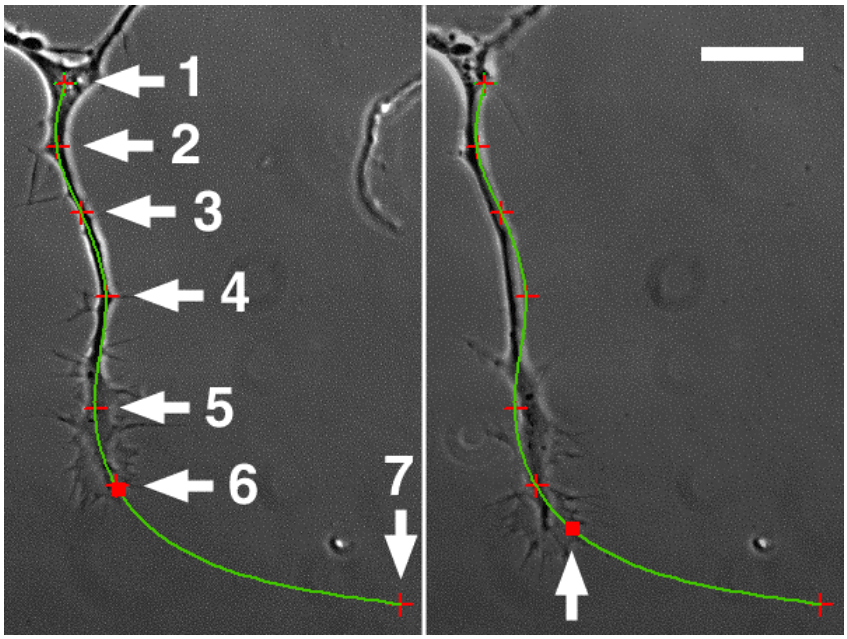

Figure 9.4 Spline Positioning. Spline points (red crosses), spline (green), and laser spot (red square) in images 20 minutes apart. Spline points are numbered sequentially and laser spot shift indicated in second image. Bar, upper right, 20 µm.

by the user in the form of a series of points, which are then automatically connected with a spline. This is usually most easily accomplished by viewing the phase-contrast image of the cell without the detection image calculated by the computer, as illustrated in Figure 9.4. Except in rare instances, only the last point on the spline lies outside of the cell, and the curve between the penultimate and last points (points 6 and 7 in Figure 9.4) constitutes the future propoesd trajectory of the laser as the growth cone follows along. In the latter picture of Figure 9.4, the automatic forward displacement of the laser spot is highlighted and, by virtue of the spline points' remaining fixed in position, one can readily observe the straightening of the axon from one image to the next with the aid of the spline.

Using spline curves for automated guidance trajectories has a distinct advantage over using straight line segments. A spline curve between the last two points, for example, begins tangential to the direction defined by the penultimate and antepenultimate points (points 5 and 6 in Figure 9.4) and continues changing its direction slowly until it is nearly a straight line at the last point. This gradual change in slope better follows the natural trajectory of a growth cone's turn, whereas a straight line assumes a sudden change in direction as happens when a growth cone bifurcates, and this behavior is not typically seen in optical guidance experiments. A straight line segment, therefore, is more likely to cause too rapid a directional change for the growth cone to follow and may result in a reduced success rate.

9.3.1.4 Intersection and Final Laser Positioning

The laser spot position is calculated by finding the intersection between the cell's edge, as determined in the cell boundary calculation, and the spline drawn through the user-specified points. Using this criterion for positioning, the laser spot position is

unlikely to change more than about a micron between data point acquisitions (usually 30 seconds apart), and this results in a smooth sequence of spot positions as "viewed" by the cell. Since the spline itself does not typically change unless one or more spline anchor points are moved over the course of an experiment, changes in laser position are determined solely by changes in the cell boundary calculation. Guidance will fail, therefore, for cases in which the boundary detection is rendered inaccurate.

In some later versions of the program, it was possible to have spline anchor point positions self-adjust to conform to the shape of the axon as it straightened, but in these program versions guidance would often fail because the spline points would shift in undesired directions and pretzel-like spline curves would ensue. However, one eventual improvement of the program was to allow for numerical measure of the growth cone's advancement along the spline by measuring the decrease in the distance between the cell's edge and the last spline point.

9.3.2 Changing Conditions and Human Intervention

The positions of the laser spot and of the spline points, in addition to many other program parameters, can be altered at any time in response to changing conditions. The most common changes are made because of axon displacement in an unexpected direction, a drastic shift in the median level of the cell image, or laser advancement into a region where fine calibration (or offset) is off by more than about half a micron.†

† There is some inaccuracy inherent in the calibration of the laser spot position to its intended position, as described in Section 4.1.2. During the initiation of guidance (before the growth cone has been seen to respond), it is after approximately half a micron's distance that the offset between the laser spot and its intended position becomes significant enough to warrant manual correction. After the initiation of guidance, the accuracy of this calibration becomes less significant, as the success of guidance depends on whether the growth cone follows the laser spot, which can be determined even if the laser spot's trajectory differs slightly from that which was intended.

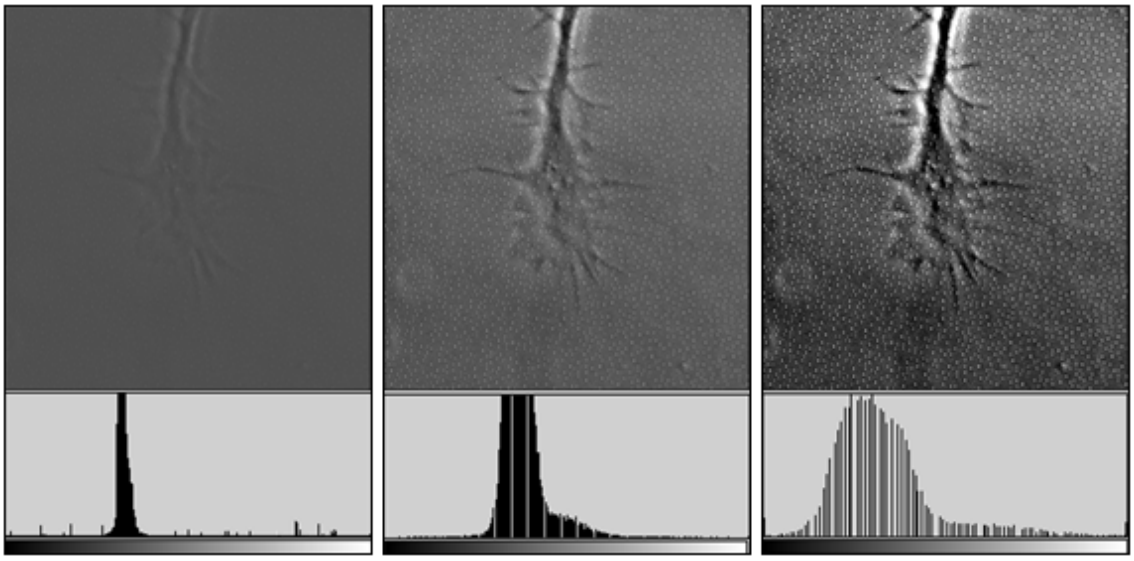

Figure 9.5 Contrast Optimization. Left: Incoming image from the camera and corresponding histogram of grayscale values (below). Middle: Contrast not fully optimized numerically, but rather optimized for ease of viewing, and corresponding histogram. Right: Contrast fully optimized numerically and corresponding histogram; note that a set of brighter pixels stands out and detracts from the clarity of one's perception of the cell boudaries.

When the leading edge of the axon translocates in a direction other than that of the laser spot, the growth cone advances past the spline and the laser and is left sitting at the side of the axonal shaft. If this is the case, then optical guidance cannot occur and manual intervention is required in order that the experiment continue. One must advance both the last and penultimate points in the direction of axonal growth in order to reset the guidance geometry for another guidance attempt, whether with the same guidance parameters or with an altered set.

The contrast of the cell image may be optimized based on a subset of the pixels in the total acquired image, a feature which (depending on the relative sizes of the acquired image and the chosen subset) can save a great deal of calculation time within each acquistion cycle. The subset of the total image is selected based on the region of interest defined by the growth cone one wishes to guide. The program begins contrast optimization by taking the histogram of grayscale values within the image subset and

performing mathematical operations whereby the histogram is "shifted" (with addends) and "stretched" (with factors) to span the domain of the histogram with minimal loss of data, and each pixel in the total image receives a new grayscale value according to the mapping determined with the image subset. A sample image with grayscale histograms is shown in Figure 9.5. In the first view, the raw pixel values acquired from the camera are displayed. To the right, the histogram of grayscale values is made to fit optimally within the range, but image noise obscures definition of the cell border by eye with this full numerical optimization. In the middle image, the contrast is optimized not numerically, but rather for the user's perception of the image, and the image appears clearer. Adjustment of parameters in the data acquisition program allows for precise control over contrast optimization.

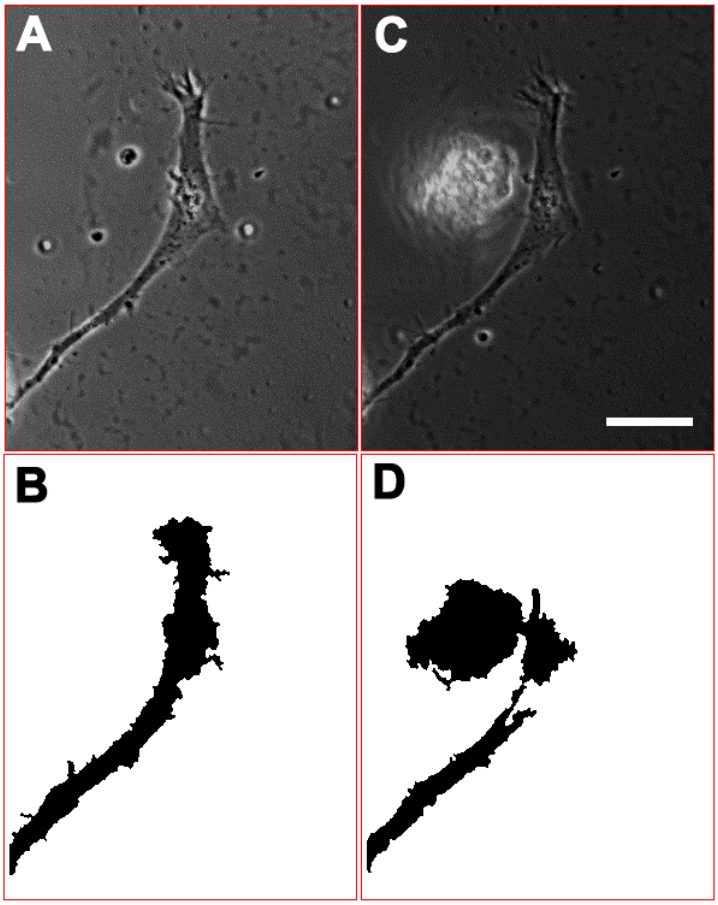

Figure 9.6 Interference from Cell Debris. With contrast optimization based only on the area shown, the introduction of a piece of cell debris shifts the grayscale values such that some definition of cell borders is lost. (A) and (B), Image before debris and corresponding boundary detection; (C) and (D), image with debris and corresponding boundary detection.

Problems with this scheme can arise when a piece of cell debris, for example, whose primarily bright pixel values skew the histogram to one side, results in loss of optimization for the final image. There also may be unfortunate results with the boundary detection algorithm, as illustrated in Figure 9.6, wherein a floating piece of cell debris throws off the contrast optimization and the subsequent boundary detection "misses" the entire leading edge of the growth cone. The main impediment to automatically correcting for this situation – by having the first calculation apply for all subsequent images – is that there are occasions on which a drastic shift in image quality serves as an alert that something has unexpectedly gone awry with the experiment, such as a surge in gas pressure displacing some cell medium. Additionally, the cellular landscape in a given field of view will change over time as axons grow and cell bodies translocate, and not updating the contrast optimization could result in subtle shifts of the grayscale values until the parameters used for optimization of the first image become no longer optimal.

9.3.3 Axes and Offsets

As seen in Section 9.3.1.1, the initial position of the laser spot with respect to the leading edge of the growth cone is very likely crucial to successful optical guidance, especially if the effect we observe is due to biased diffusion of protein macromolecules. Having the entire area of the laser spot well within the cell boundary is undesirable because it has been shown to inhibit growth cone extension (Raizen and Käs laboratories, University of Texas at Austin, unpublished data 2000-2002). However, having less than one-half of the area of the laser spot within the cell boundary means that only a very small percentage of the laser power is actually getting to the cellular material, so this is undesirable as well. For the initial stages of optical guidance, when the cell is first

exposed to the laser light, manual intervention is required to change the X and Y offset values (small adjustments to the galvanometer voltages such that the laser spot is translated a short distance in the directions of the X and Y axes). Once optical guidance has begun to take effect, however, subsequent small inaccuracies in the actual laser spot position are less important because the most relevant property of the laser spot is how much and in what direction it moves from one data point to the next. It has been observed that the trajectory followed by the growth cone may end up slightly different from the spline seen drawn on the monitor, but this does not affect the overall result of successful optical guidance for the growth cone in question.

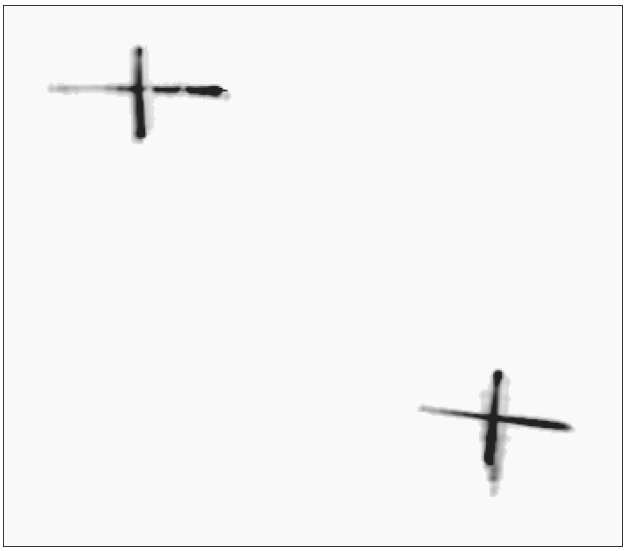

Figure 9.7 Aberrations Create a Need for Laser Position Updating. The result when the galvos are instructed to draw a vertical-horizontal line pair a one point (upper left) and then at a point 150 microns away (lower right).

The questions then arise as to why such small manual adjustments are needed and whether there is a way to correct automatically for the position offset. The most fine-grained calibration method currently available is the creation of a polynomial function to correct for changes in offset with respect to position in the field of view. This is done by taking a sampling of 20-30 points in the field of view, calculating the offset found at those points, and curve-fitting a correction function for all points in the field of view. Still, however, manual adjustments are nearly always requisite. One reason is that the sampled points are not dense enough to provide a reliable basis for a curve fit, but another reason may be that there is some degree of

rotation involved in the offset and that a polynomial function is not the optimal type of curve to fit. Figure 9.7 illustrates this problem: at two spots 150 microns apart, the galvos are instructed to raster one line in the vertical direction and one in the horizontal to provide a "set of axes" with which to define the surrounding coordinate space. At one of the locations, though, there is very visible rotation in addition to lengthening/shrinking of the rastered lines. Perhaps aberrations produced by the objective lens are in part responsible for this effect, but whatever the cause, there are several possible countermeasures to be considered. One solution would be to take a more dense sampling of offsets in the field of view, but these measurements are tedious when done by hand and our manpower is limited. One could automate the sampling process to some extent, but still the offset measurements would need to be done by hand. Further investment in programming could bring about a procedure whereby the computer would take the image of the laser spot, calculate its center, and automatically compute its offset, and this would be the ideal scenario. However, if something like this were implemented for the sampling procedure, one could also envision its being used during data acquisition itself, thus being adaptable to changes in the setup of the optics. This method would have the drawback of taking up more time per cycle with processing and thus slowing down the data acquisition process, but with a different hardware setup from our own, it might be the most reasonable way to handle the offset issue.

III. RESULTS & DISCUSSION

10. Results

10.1 SUMMARY OF ADVANCEMENTS

The new results derived from our experiments are attributable in large part to the evolutions of our experimental setup and procedures, several of which are described here. Having re-engineered the experiment in reconstructing it for our purposes, several significant advancements were made right away. First, the way in which we decided to introduce the laser to the system represents a dramatic advancement over that which was previously published. Instead of producing relative motion of the laser spot and the sample by moving the microscope stage, as was previously done, we chose to implement an optical system whereby the laser spot itself would be moved and the sample stationary. Not only does this arrangement enhance the physical stability of the sample in its not having to be translated constantly, but the heating elements attached to the cell dish and to the objective lens never need to move with respect to one another during the course of an experiment in our setup. This advantage reveals itself most readily in nearly eliminating any probability of sample or equipment damage due to failure of heating systems, especially when coupled with the fact that our system uses electrical heating elements instead of warm water circulation, the success of which is only as dependable as the weakest seal in the water conduits.

Our experimental progress can also be measured by the many ways in which problems with the previous experimental setup are circumvented in the current one. The most salient such feature in our experiment is the optics. Although the previous experimental apparatus produced a laser profile that could be roughly approximated by a

circular spot, there was always a characteristic "Maltese cross" pattern embedded in the profile, resulting in a very ill-characterized intensity distribution for the laser spot. The origin of this former problem remains unknown, but it never has been observed with the current apparatus. In fact, the laser profile we have obtained follows a very smooth, Gaussian intensity distribution, due in large part to the properties of the laser diodes themselves and the aspherical lenses used to collimate the outgoing beams. Our profile is elliptical in shape rather than circular – which would be the ideal profile to have because of its spatial isotropy in the plane of the sample – but because of its small size relative to the cellular structures to which it is introduced, the difference in beam spot width between the two axes is minimal. The diode lasers have the additional advantages of their compactness, low energy usage (compared, for example, to an Argon-pumped Ti:Sapphire laser), low cost, and zero maintenance. Using galvanometer-mounted mirrors for beam guidance means that the rate of switching the laser spot position is determined by the very precisely-controlled system of the closed-loop galvos, and this has automatically added a capability for multiplexing (having multiple laser spots – perhaps even guiding multiple neurons – at once) to the experiment. In fact, the progress we have recently made in the direction of understanding the mechanism for optical guidance could not have taken place were it not for the ability to have the laser spot "hop" from one point in the field of view to another.

Relevant also to this discussion is a brief revisitation of the enormous advantage of our capacity for automated neuronal guidance. The further automated these experiments can become, the higher the data throughput will be and the more successful the endeavor will be. Automation of the laser spot placement relative to the growing neurite is not only an advantage in time but also in the prevention of potential laser placement errors based on human judgment, concentration (or lack thereof), and

application of heuristics that may, through habituation, result in an overall bias into the data. The rate of data acquisition is so slow that the introduction of everything possible must be done to avoid errors in data-taking lest vast amounts of work be lost after close analysis.

Major strides forward were made in designing a cell dish for the microscope on which the cells could survive for numerous hours or even days. Our arrival, through many intermediate steps, at our ultimate dish design was the result of a continual process of design evolution, and a summary of that evolution is germane at this point. The reader may refer to Appendix C for technical drawings of early and most recent dish designs for reference to the structures named here. Our initial idea was to create a perfusion chamber through which nutrient medium could be supplied to the cells from one side of the dish and could be aspirated from the other side once it had flowed over the cells. This is illustrated in Figure 10.1.

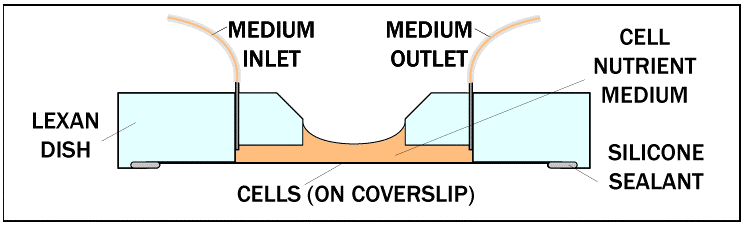

Figure 10.1 Original Cell Dish Design, with Perfusion, Cross-Section. A few millimeters of culture medium was to rest atop the cells at all times to ensure temperature stability. Lensing effects due to the meniscus formed by evaporation became the major impediment to using this type of dish.

The two main problems with this configuration were the amount of medium required to maintain a constant flow and problems with fluid evaporation, which would leave a fluid meniscus in the dish. The meniscus shape, of course, makes a lens through which the microscope light is bent, and thus the imaging system becomes severely flawed with time. Another consequence of evaporation is unwanted changes in fluid osmolarity and even microscopic crystalline mineral deposits being left behind in the medium (visible with the microscope, and at first mistaken, by their elongated shape, for some

rapidly-dividing bacteria of the *bacillus* family). In commercially available systems, these factors are controlled in large part by minimizing the surface area covered by cells or tissue in the flow chambers, but since the form and surrounding area of a growth cone are so largely contributory to its appropriateness for optical guidance, it was of significant importance to us to have a larger available area for cell plating per experiment dish. The ability to find multiple fields of view for guidance in a single experiment dish obviates the need to continue replacing samples on the microscope, an environmental stability of which the cells show their appreciation by refraining from apoptosing for longer periods of time. For this reason and for economical reasons, commercially available perfusion systems were not appropriate for our experiments.

In order to control evaporation of the cell culture medium and in order to discourage fluid surface curvature for imaging purposes, a coverslip was floated on top of the fluid surface, as shown in Figure 10.2. The desired effect of evaporation control was indeed achieved and the longevity of the cells on the microscope was extended significantly. However, this caused another problem to make itself known. The rates of influx and efflux of culture medium, although transported using the same peristaltic pump, may differ by a small amount and, left for a long enough time, this will either overflow or underflow the available volume. These

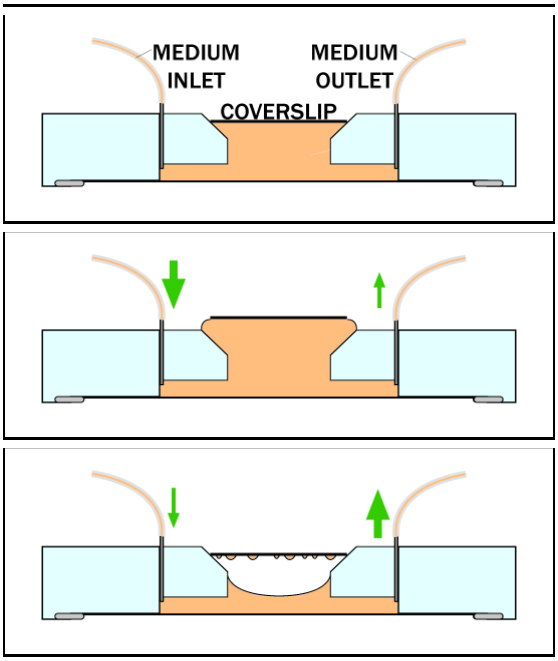

Figure 10.2 The Floating Coverslip Modification. A coverslip was placed atop the fluid surface to prevent evaporation during perfusion. Any disparity between the rates of inward and outward flow, however, became problematical.

conditions are shown in Figure 10.2. The disparity between inward and outward flow seems not to be a property of the pump or its channels, but rather of the tubing which carries the fluid. Since the tubing must be exchanged periodically for autoclaving and must be discarded when worn, we did not find a way to ensure consistently that the flow rates would exactly match. Working to minimize the flow rate differential has a low work-to-gain ratio because although the time before which problems are encountered can be increased, there is no ultimate solution to the problem.

It was then determined that perfusion of the culture medium was not absolutely necessary to the cells to ensure their long-term survival, but rather that periodic medium changes could suffice. With the silicone perfusion tubes disconnected, the small steel tubes onto which they attached are free for insertion of a thin needle for medium extraction and replacement. Eliminating perfusion also allows for one fewer heating element in the system, as there is no incoming medium to be heated before introduction to the cells. Replacement medium is most readily heated in a small centrifuge tube before being aspirated into a syringe for placement in the cell dish, just as it is replaced in cell culture procedures before the cells are brought to the microscope. The primary disadvantage to this arrangement is that eventually a gas bubble always forms beneath the coverslip. This must be in part due to dissolved gas from the medium, as the bubble-free period can be prolonged slightly by placing the

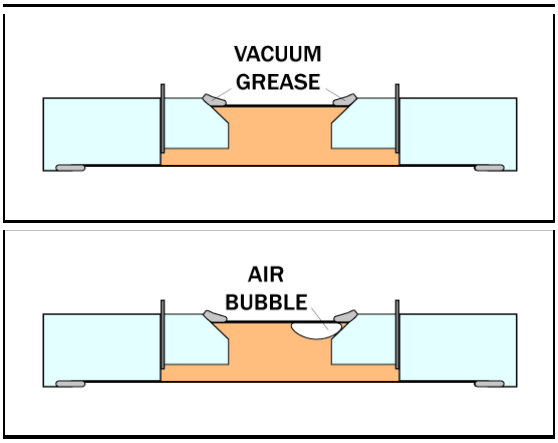

Figure 10.3. Elimination of Perfusion and Addition of Vacuum Grease Seal. Periodic medium changes replace perfusion and sterilized vacuum grease around the edge of the top coverslip eliminates evaporation. The cells survive for a longer time, but now dissolved gas in the medium becomes the limiting factor.

culture medium under vacuum for several minutes before its heating and introduction to the cell dish. However, it is quite possible that slight evaporation from the two steel tubes is contributory to the appearance of the air bubbles, as the problem was never eliminated entirely. Illustrated in Figure 10.3, this avenue was not fully explored because such efforts were preceded by the final modifications to the cell dish which brought it to its current state.

The final design of the cell dish is shown in Figure 10.4, its most notable feature being the addition of 10% carbon dioxide gas pockets above the surface of the medium on both sides of the cell plating area. Another feature, which greatly improved the imaging capabilities of the system, was the reduction of the height of the culture medium from more than 5 mm to about 2 mm above the cells. Additionally, the upper coverslip stays below the level of the medium on the sides (beneath the gas pockets), which means that any trapped gas bubbles will tend to rise to the sides and not interfere with the imaging process. In this experiment dish, cells could survive for several days on the microscope, provided daily medium changes and proper infection control. Environmental stability for the cells means not only that common cells (such as NG-108) could live for a longer time, but also that more sensitive cell types (such as primary cells) would have a better chance of survival for experiments.

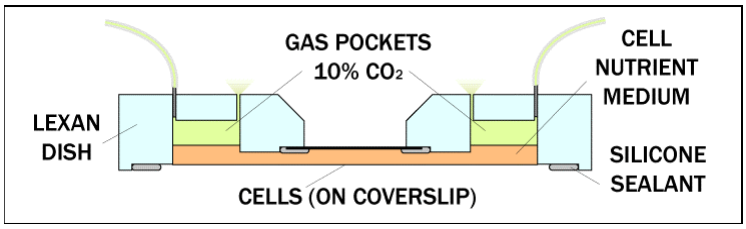

Figure 10.4 Final Experiment Dish Design. Note the thinner layer of culture medium to aid in imaging as well as gas pockets for pH regulation.

Several elements of the cell dish remained constant throughout the design development, primarily because it proved more time-efficient to modify existing

structures of the original dishes rather than to start with entirely new constructions. For instance, the two channels running lengthwise through the dish, which house the removable heating cables changed slightly in placement but never were fundamentally altered. The material out of which the dishes were crafted was always lexan, chosen because of its biological neutrality and its durability for purposes of repeated autoclaving and re-use. Silicone sealant was always the material of choice for attaching coverslips to the dish because of its biocompatibility, durability, fast curing, and fairly easy removal when adhered coverslips had to be exchanged.

The construction of a home-built cleanroom for cell culture (discussed in Section 7.1.1) completely eliminated infection of cultures, which previously could shut down experiments completely about once per year. Although a cleanroom is not required for all cell culture endeavors, the building in which our laboratory was located is known generally to contain high levels of particulate matter in the air, including mold spores, to which dishes could be exposed in transport during routine cell culture procedures.

The aforementioned advances in setup and environmental conditions have allowed us to begin exploring the phenomenon of optical neuronal guidance. As with any biological system, not only is the parameter space in question extremely large, but also one is not ever guaranteed to know what all of the parameters *are*. From lipid membrane and embedded proteins (of tens of thousands of species) to protein synthesis and transport, cell motility, apoptosis, and complex signal cascades involved in the regulation of all these processes, it is possible neither analytically nor computationally completely to characterize the activity in an entire neuron. Likewise, when an effect like optical guidance is observed, one cannot expect it to be readily apparent exactly which cellular mechanisms may be responsible for the behavior. Because of the complex nature of biological systems, then, it is essential for the experimenter to eliminate all possible

causes of variability in the system from experiment to experiment. Also, it becomes crucial to ensure that one is studying the effect of only one variable at a time. Combined with a slow rate of data acquisition, this means that one must persist in taking data on as specific an effect as possible for as long a time as possible, as opposed to hopping from one research idea to the next in the hopes of finding something strikingly new with each leap.

Since our laser spot profile is of such high quality, and because manipulation of optical properties of the system gives us a lesser chance of interfering unknowingly with the fragile biological equilibrium of the cells, we chose to investigate questions which could be answered by means of optical modulation alone. Our efforts are chronicled in Section 10.7, where our results are presented and some interesting conclusions can be offered.

10.2 Overview of Program Evolution

It is useful to outline the evolution of the data acquisition program from the first viable version to the last working version, which is tantamount to describing the steps leading from manual data acquisition to automated guidance. In the first working program version, there were two main impediments to automation: boundary-detection and optimization of contrast, when the entire field of view is the input parameter, were these two obstacles. First, since the grayscale values of one field of view can differ drastically from those of another just a short distance away due to objects like cell bodies, debris, and surface variegations, when the contrast of the image was optimized based on the histogram values for all of these pixels, new settings had to be effected at the start of every data run for there to be sufficient contrast to use the boundary detection algorithm. While this did not interfere with data acquisition *per se*, it consumed a great deal of time

each run and also relied heavily on human judgment. The major improvement addressing this issue was for the contrast of the entire image to be calculated based on the histogram values for only a subset of the pixels in the region. The region of interest, specified by the user, would contain an axon and perhaps part of a cell body, but would not greatly vary in content from one run to the next, thus also improving consistency of contrast optimization. In addition, considering for the calculation a set of pixels at least a factor of 10 smaller than the entire area required a significantly shorter time to compute and helped speed up data acquisition, allowing more data points to be taken in a given amount of time. An illustration of this problem and its resolution is given in Figure 10.5.

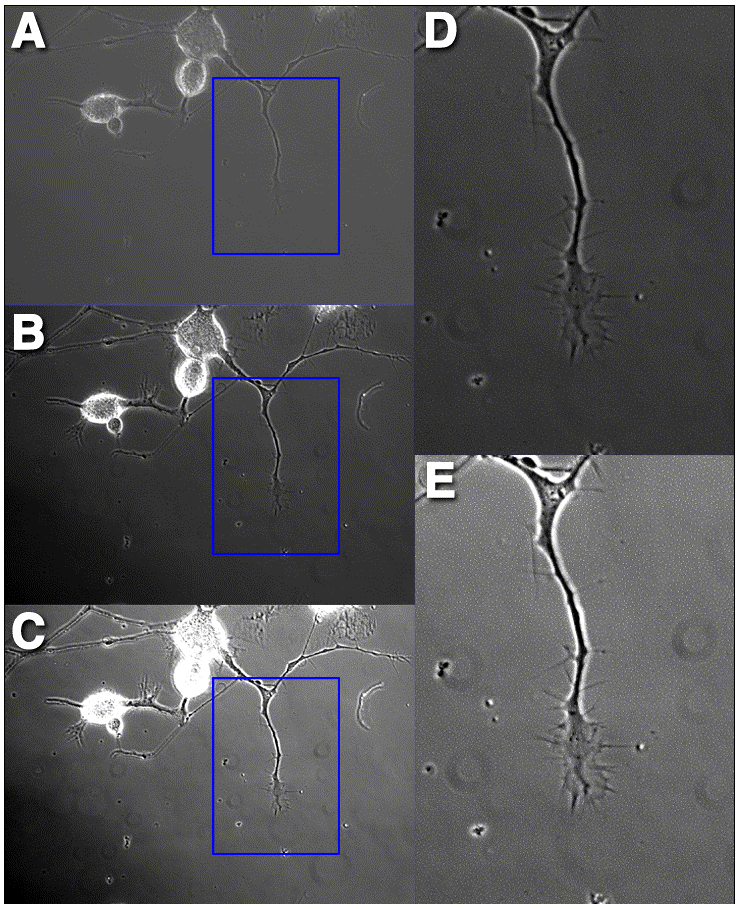

Figure 10.5 Contrast Optimization Based on a Limited Area. (A) A field of view with cell bodies and a long axon, raw output from the CCD camera. (B) Same field of view, with contrast optimized based on the histogram of grayscale values for the whole field of view. (C) Same field of view, with contrast optimized based only on the pixels enclosed by the blue box. This produces the best image of the growth cone. (D) and (E) are close-up views of the axon in (B) and (C), respectively.

The second major issue was that of boundary detecting only a small subset of the total image, which was primarily a problem of the computation time required. As the

boundary detection algorithm goes through at least eight steps, each of which must perform calculations involving all pixels and comparisons among them, analyzing the whole field of view is prohibitively time-consuming. As it is favorable to capture a large field of view in an experiment – because the behavior of cells neighboring the one of interest very often provides a gauge of the health of the chosen cell – it would be very disadvantageous simply to reduce the field of view in order to reduce acquisition time for each data point. Instead, it was necessary to implement an algorithm similar to the one above, whereby only a smaller region of interest is analyzed for boundary detection. Unlike the contrast optimization algorithm, however, which effected changes in grayscale values for all pixels in the field of view based on the values of a select number of pixels, the boundary detection algorithm both analyzes and operates on only a small subset of the total available pixels.

Other advances made to the acquisition program include improved hardware controls. These allow for more flexibility in the timing of multiple-spot laser positioning and provide more user options for control over optical elements of the system. The order in which steps in the acquisition cycle are performed was also optimized for fastest performance. Ultimately, the bottleneck for fast acquisition of data was due mainly to properties of the hardware, i.e. the data flow rate from the camera to the computer, rather than impediments caused by the software.

A good deal of effort was also spent on increasing the ease of data export and the analysis of completed experiments. One major shortcoming of the original program was that it only allowed for separate export of the cell, laser, detection, and spline images. During data acquisition, any number of these four separate images can be superposed to form a composite image, but there are significant complications associated with the export of composite images to files readable by a standard graphical program. Due to

restrictions imposed by the camera, incoming data from the CCD chip were always saved as Targa (TGA) files in a format not compatible with standard image software, but the separate image components could be exported, one at a time, for a sequence of data points, in Bitmap (BMP) format. The image components, if desired to be re-composited for display or analysis, had to be re-assembled by hand for each individual data point, which proves to be quite a task when there are hundreds of data points per run, and proves more cumbersome still when such steps are required for data analysis. Program advancements include the abilities to save composite images of any or all of the four image components, to save images in multiple file formats, and to make AVI animations of image sequences. Ultimately, there were impediments to efforts to combine the images any way other than to do so for display and then proceed with multiple screen-captures as the data advance. The time saved in this process far exceeds the raw difference in time between the two methods of export, as the latter method is performed automatically, allowing the user to concentrate on other tasks in the interval it takes the program to load, composite, display, capture, process, and save images from each data point.

Further improvements include the ability to measure axon extension numerically and to export these data to a spreadsheet file for analysis. The number in question can be either the straight-line distance between the intersection of the leading edge with the spline curve and the final point of the spline curve (smaller numbers signifying larger growth toward the final spline anchor point) or the same distance measured on the spline itself. The advantage to the latter measurement is that as the cell grows toward the final spline anchor point, if the middle spline anchor points can update their position, the spline itself will grow more and more straight as the growth cone advances toward the

final anchor point. To include the spline straightening phenomenon in the measurement gives a small added boost to the measure of growth as the leading edge advances.

10.3 DATA

Each data segment represents a point in the parameter space we explore, and two years' worth of design, construction, and data acquisition have yielded data enough to draw some simple but powerful conclusions. The data may be classified according to different sets of parameters, and each classification may suggest its own reflection of the system under consideration. Our data best lend themselves to classification on the bases of (a) duty cycle (percent of the time the laser is on the cell), (b) raw time interval for which the laser is on the cell, and (c) whether the laser power is attenuated or split temporally for the same time-averaged power on the cell. Appendix A lists a tabular compilation of the data segments considered for evaluation for our purposes.

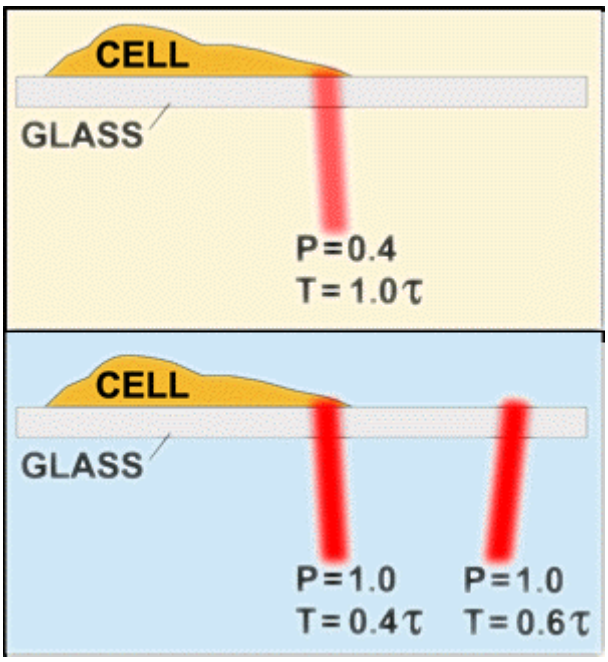

Figure 10.6 Temporal Profiles. Whether cells respond better to one of these mechanisms than to the other could be a clue to understanding the mechanism of optical guidance.

10.3.1 Criteria for Consideration of a Data Set

Although a vast amount of data was recorded, much had to be discarded as unfit for analysis because of the circumstances surrounding its acquisition. It is worthwhile to consider the criteria on the basis of which such decisions were made.

The experimental setup was constantly undergoing modifications toward optimizing the cell environment, and thus many data were lost through learning which arrangements did not work as well as planned. However, whether or not the cells are healthy enough for data involving them to be considered is something that can be determined only in retrospect because the time over which this becomes apparent is on the order of an hour or more. Such data can only be excluded in review, and roughly half of all the data gathered had to be eliminated for this reason. This is where having a full field of view including many cells is very helpful, as the criterion chosen for data elimination was whether more than half of the neurites from all cells in the area (about 300 x 400 microns) had retracted. If this was the case, then all data segments acquired within 30 minutes of the first neurite's retraction were disregarded.

Retraction of neurites, however, is not the only means by which cells express dissatisfaction with their environment. Sometimes growth cones will stagnate entirely, losing both translocation and motility. If the formation of lamellipodia and filopodia were halted, and if no changes in the shape of the growth cone could be observed, then these data segments were also passed over.

The third reason for discarding data is based on technical difficulties encountered during acquisition. On occasion, there would be too much cell debris in the area to obtain a viable edge detection image or debris would get caught in the laser focus. At times, there were problems with the acquisition program which allowed overwriting of critical files, so these data were lost. Other program-related problems also contributed to loss.

10.4 METHODS OF ANALYSIS

10.4.1 Defining Data Segments

With the imposing quantity of data needing evaluation and the distinct lack of personpower available to carry out the analyses, we were faced with something of a quandary. Subject to those constraints, we chose the simplest meaningful criterion by which to analyze the data: the binary distinction of whether or not, for each valid interval, guidance was successful. Although it is not uncommon for computer programs to be employed in the analysis as well as the acquisition of image-based data such as pictures of cells, fine-tuning the acquisition process was a higher programming priority for us than adapting algorithms for analysis, so manual analysis had to suffice. The data are organized as follows.

For each day in which data were acquired, there is a folder containing the data runs for that day, with each run separated out into its own subfolder. Within each run folder are stored the images associated with each time point at which data were acquired. For each run, there is one Run File containing an index of the acquired images and a record of global variable values. For each acquisition time point, there exists a small file containing the values of variables specific to that time point, e.g., laser spot position(s), spline point(s), and other information not conatined in the image files themselves. For each time point, there can also be up to three associated image files: cell image, laser image, and edge detection image. Typically, within one run there is no change in the field of view (position of the microscope stage); when a change does take place, the current run is closed and a new one begun.

Once all of these data are in place, each data run must be examined and divided into segments which can be analyzed independently. If, from Picture 46 through Picture 74, for example, the laser was on the cell at 40% power, and from Picture 75 through

Picture 99 the laser was hopping between two points, spending 40% of its time on the cell and 60% off the cell, then these two intervals (46-74 and 75-99) should be analyzed separately. There can be many segments within a single run, and once they are separated out from one another, those with parameters in common (regardless of which date or run) can be directly compared.

There are several events that qualify as demarcation points to separate one segment of a run from the next. First, and perhaps most obviously, there is the event of the laser turning on or off. Also, switching the focus of the experiment from one growth cone to another one in the same field of view is considered a delimiter. Next, if the laser intensity or the duty cycle or period of its hopping cycle is changed, this also divides one segment from the next. Another reason for separating segments is that one or more spline points have been repositioned such that the proposed trajectory of the growth cone has changed. It is not often that the interval between image acquisitions (time points) changes within a run, but such an event is also a delimiter. Events not considered delimiters are minor changes in the offset of the laser position, changes in contrast optimization parameters, and change in whether or not the edge is detected.

10.4.2 Drawing Correlations

In order to determine whether or not an attempt at guidance has been successful, several steps are required. First, one can eliminate right away any segments less than five minutes in length, as these intervals are always too brief to offer any conclusive evidence of optical guiding. Then, for the range of images which correspond to the segment at hand, the Neuron program can save a region of interest to disk, including any or all of cell, laser, edge, and spline images. In most cases, guidance is most easily recognized by superposing the cell and laser images, leaving out the edge and spline images. Once the

image sequence is saved as a series of bitmaps, the images can be opened and viewed as a time-lapse movie for the determination of whether guidance has taken place. This process is repeated for each segment (of each run, of each day) for which there are usable data until the information can be entered into a spreadsheet and correlations drawn with the help of sorting algorithms.

For the first pass, for each segment a conclusion is entered: "Y" for affirmative guiding, "N" for negative guiding, and "P" for possible guiding. One spreadsheet column is reserved for comments about the degree to which guidance is observed and any other notable effects. For example, there is a distinction between an instance in which a growth cone holds its position and one in which it actively retracts, both of which would be represented by "N" in the summary column, even though these are very distinct results. Similarly, there is a distinction between positive responses in which small and large amounts of growth were observed. Also, any other notable effects not directly related to growth cone guidance are noted, such as whether the cell body begins to translocate after the application of laser light.

The existence of a second pass over the data is functional in that any segment which is particularly difficult to analyze can be put off until the second round, rather than bogging down the analyst with time-consuming procedures which would have a low yield of statistical information. During the second round, all the segments for which a "P" was noted are gone over in greater detail, and a value of either "Y" or "N" is assigned to each segment for which there is not newly noted any reason why it should be disqualified. Additionally, and especially if there is only one person performing the data analysis, it is highly advisable that all segments be reviewed again quickly at the end of the analysis to confirm for each value recorded whether optical guidance was established. In the rare

occurrence that any original and confirmation values do not match, one more pass over the data will be required to determine which conclusion will be drawn.

It is preferable to perform data analyses at least monthly so that data sets do not build up to epic and/or disheartening proportions.

10.5 ANALYSIS PROCEDURES

10.5.1 How Growth Cones Behave Normally

We have observed at least five distinct states characterizing growth cone behavior, the most dramatic of which is simple collapse and retraction in response to unfavorable environmental conditions. The second is a state of leading edge ruffling without translocation, and the third is forward growth accompanied by similarly ruffling lamellipodia with little or no change in growth direction. Fourth, growth cone translocation is sometimes observed to occur

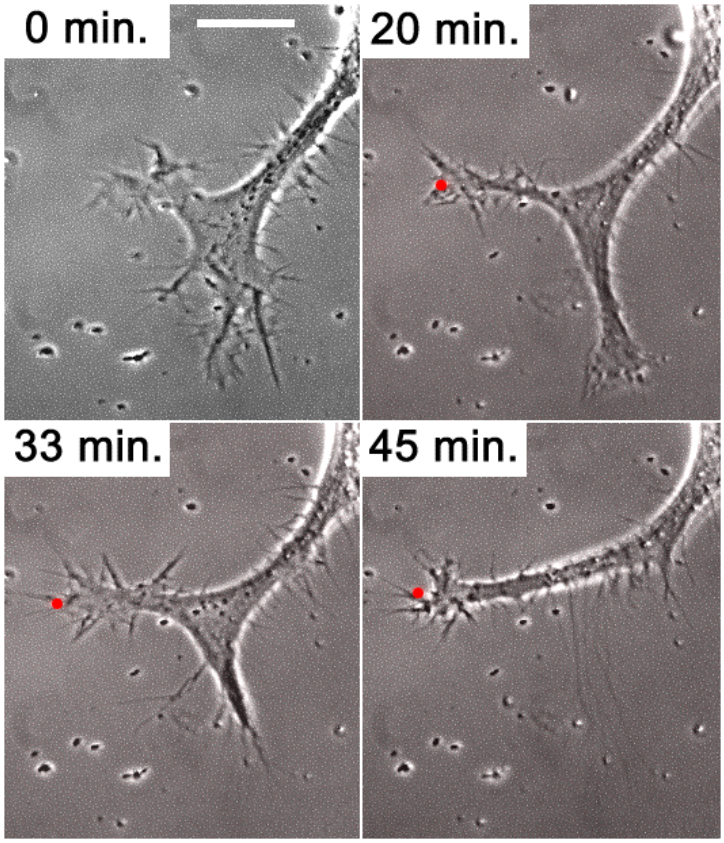

Figure 10.7 Natural Growth Cone Redirection through Bifurcation. Most drastic changes in growth direction for naturally growing axons are seen when the growth cone bifurcates and one of its branches survives. This sequence also shows optical guidance which, as is consistently observed, can be used to select which branch of a bifurcation will propser.

through filopodia alone, whereby the direction of growth can vary a bit more, as it is determined by the direction in which a filopodium is pointing at the time it anchors to the substrate. Fifth, a growth cone may bifurcate, with one or both branches possibly extending out at a large angle to the original direction of growth, ending ultimately in the dominance of one branch and a potentially significant change in direction for the axon. The final state in this description is a cycle of alternating growth and abatement (which can conveniently be named a "GRAB cycle"), which is more commonly observed in undifferentiated NG-108 cells and which results in neither net anterograde nor retrograde growth cone progression. A GRAB Cycle is shown in Figure 10.8, which illustrates its characteristic phases in successive panes: initiation, indentation, extrusion, extension, dissipation, and abatement (the last pane represents the same state as the first). As their designation suggests, these cycles may repeat themselves in one neurite over time, but they can also be expressed in more than one neurite of the same cell. These self-organized spatiotemporal patterns may be substrate-dependent and certainly they merit further study in another setting.

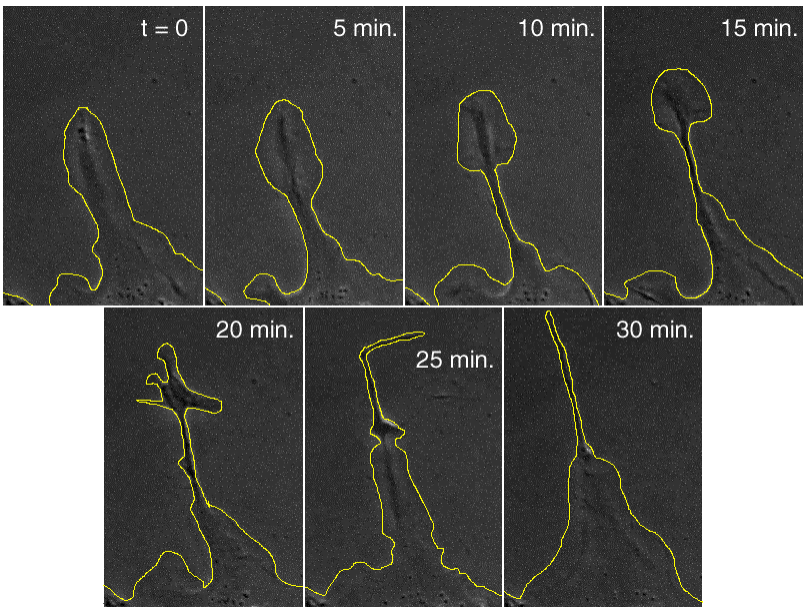

Figure 10.8 A GRowth-ABatement Cycle, or "GRAB Cycle." The outline of the neurite is highlighted for ease of viewing. The phases of the cycle are shown and may repeat in time: initiation (t=0 and 30 min.), indentation (5 min.), extrusion (10 min.), extension (15 min.), dissipation (20 min.), and abatement (25 min.).

10.5.2 Determinations of Successful Guidance

For the determination of whether a data segment represents a successful guidance attempt, if the data have been acquired with automated guiding, the procedure is as simple as measuring the position of the leading edge relative to the spline curve over time. The position points can be plotted and a linear fit determined, the slope of the resultant line indicating either advancement or retraction. (Quantitative measurements of growth rate are considered in the Section 10.5.3.) If the data have been acquired manually, however, a manual analysis is required to determine whether optical guidance has taken place. A series of time-lapse images is analyzed, and any non-transient extension of the growth cone in the direction of the laser spot (which always differs from the direction of initial growth) indicates success, whereas extension only in the original growth direction is recorded as non-responsiveness to the optical stimulation. For a preliminary analysis of the data, we have performed such a binary analysis on as large a number of data points as possible to determine the average rate of success of optical guidance. It should be noted that failure of guidance and failure of automation are treated as separate conditions although their coincidence may be high where automation has failed.

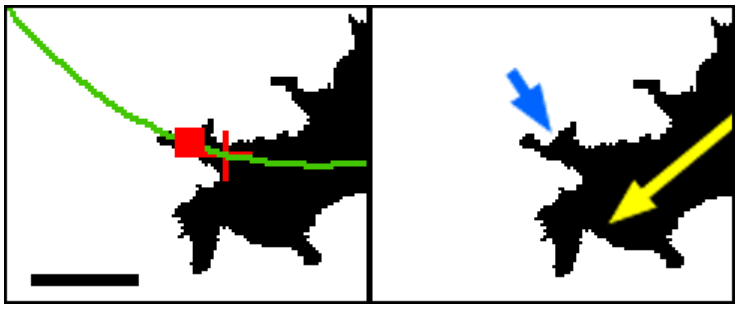

Figure 10.9 Successful Guidance Despite Straight Growth Cone Advancement. Here is an example of successful guidance: the cell did extend in the direction of the laser spot (blue arrow) despite failure of guidance to turn the entire growth cone (yellow arrow, highlighting straight growth direction). This case would be considered successful guidance. Bar, 10 microns.

In order to illustrate the criteria for determining the success or failure of guidance in a binary fashion, here are several cases and their outcomes. If, as shown in Figure 10.9, optical guidance fails to induce an overall change in the direction of growth cone advancement, yet still causes extension in the direction of the laser spot, this is considered a successful guidance attempt because of the evident influence of the laser. There are also times for which a distinction must be made between transient and nontransient extension of the leading edge. Types of transient extension include the sweeping of filopodia out from the growth cone and, failing to attach to the substrate at any point, their collapsing back into the bulk of the growth cone. Lamellipodial extension is usually non-transient, except in cases where extension is followed by collapse due to overall neurite retraction; these cases require inspection of an area quite larger than the growth cone, somtimes including other cells in the field of view if retraction becomes an issue and the health of the cells is in dispute. Any growth cone action within 30 minutes prior to retraction must be discounted, which emphasizes one's

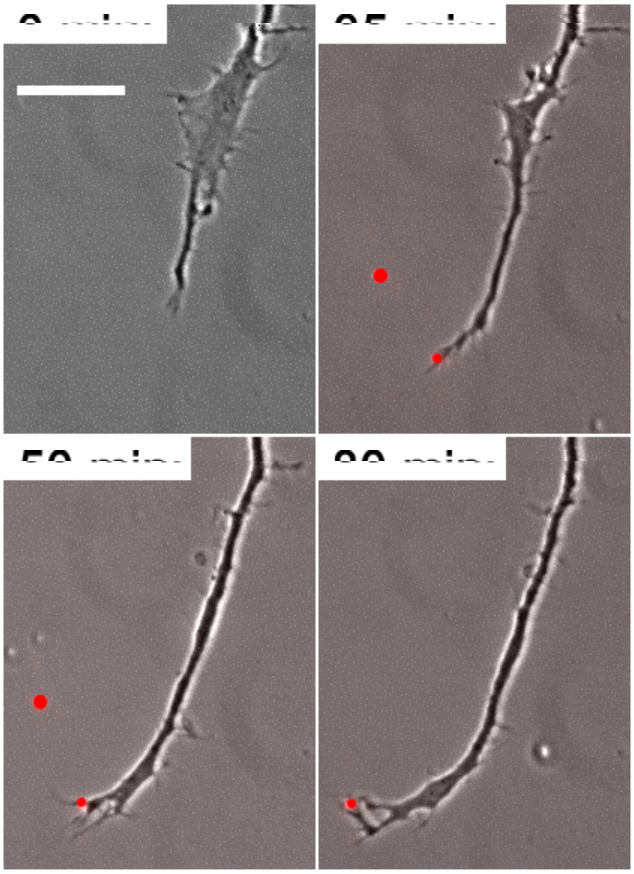

Figure 10.10 A Gradual Turn Induced by Optical Guidance at 0, 35, 50, and 80 Minutes. Such a gradual curving of a neurite is rarely if ever observed in nature and is the strongest indicator of optical influence. After a turn like this is executed, the neurite will straighten out to revert to a lower energy state. Bar, 20 microns.

inability to evaluate the success of optical guidance while the experiments are taking place. In addition, a growth cone in a GRAB Cycle (Figure 10.8) may at first appear to be advancing in the extrusion and extension phases, but further observation may see the rest of the cycle carried out. Laser influence over a GRAB Cycle is characterized by halting the cycle (at least temporarily) in the extension phase and causing further extension to take place.

Referring back to Figure 10.7, growth cones normally execute turns through bifurcation and the subsequent choice of one branch over the other. Such phenomena can certainly be exploited in the attempt to get a neurite to grow in a partucluar direction by biasing with the laser spot the branch whose path will ultimately be followed. However, natural turning phenomena are not necessary for a turn to be induced artificially by the laser. In fact, the strongest evidence for the influence of optical guidance is offered by neurites whose growth follows patterns not naturally observed, shown in Figure 10.10.

10.5.3 Rate of Growth Cone Advancement

TYPE	Rate (microns/hr)	Standard Error (microns/hr)	N Manual Measure	N Auto. Measure	N Total
Unguided (Laser Off)	21.7	0.9	5	2	7
Guided (Laser On)	7.8	0.2	0	12	12

Table 10.1 Growth Rates for Optically Guided and Unguided Neurites. Rates were determined using a weighted average of the values obtained. For unguided growth the majority of the rates had to be measured by hand, and a margin of error of +/- 8 pixels per measurement was assumed (4 pixels each for start and end measurements). For both automatic and manual measurements, the exact elapsed time was recorded by computer, rendering error from this source negligible.

In the paper initially published on optical neuronal guidance, one way in which laser influence was documented was by its acceleration of the rate of advancement of

growth cones [Ehrlicher *et al.*, 2002]. In our investigations, however, the opposite effect was observed, but there are several explanations for the discrepancy which will be detailed here. We found that the rate of unguided growth to be significantly higher than that of guided growth, as shown in Table 10.1. One major difference between our findings and those in the previous paper is that we observed primarily NG-108 cells while the cell type of closest focus in Ehrlicher *et al.* was PC-12. Additionally, our findings are different in that we have automatically measured optically-guided growth along the spline curve set as the direction for guidance: we do not compare straight-line unguided growth to straight-line guided growth because all of our guidance experiments involved redirecting the growth cone, so there existed no instances of successful guidance whereby the growth cone continued on a straight trajectory.

We must then direct our attention to reasons for an apparent slowing of growth cone advancement under optical guidance. One factor is that many of our optical guidance experiments were also experiments in the maintenance of cell viability over long periods of time, and because fast growth is associated with healthier cells and unguided growth is mostly measured before guidance is attempted, the probability would be that cells would tend to grow more slowly as experiments wore on in time, thus giving the appearance that guided cells grew more slowly. Also, our method of determining what growth states were guided and which were not were perhaps more reliable than those put forth in the previous publication, as we verified the effect of optical guidance (i.e. observation of a turn) while measuring the growth rate, and if this is not done (i.e. if turns are not observed during guided growth measurements), then there remains some uncertainty as to whether a growing neurite exhibiting the same directional behavior as that of an unguided neurite is in fact being affected by the laser at all. We can be most

highly confident of our measure of the rate of guided growth because these rates were all calculated with computer programs, leaving no room for human error.

10.6 When Automation Fails

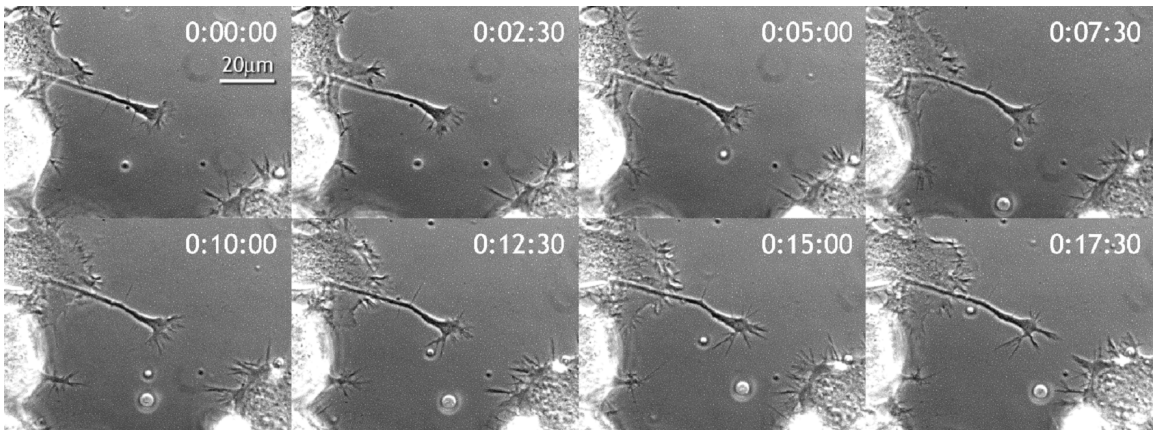

Figure 10.11 An Ideal Guidance Candidate Is Influenced by a Neighboring Cell. The growth cone in question then cannot be guided. Times indicated are in h:mm:ss format.

There are several reasons for which automated guidance may fail, many of which have been corrected but some of which are inevitable conditions of the experiment and must be worked around. In fact, there are conditions which impede the initial acquisition of data and upon recognition of which a run must be aborted. Figure 10.11 shows a time series of images of an axon which, at the beginning, seems like a good guidance candidate, but then gets too close to a neighboring neurite to be guided. It is important not to attempt guidance with an axon which might be "distracted" by other factors that might influence its growth rate and direction; this way, one can maximize the certitude of the laser's being the single, dominant influence on a given axon's growth. Additionally, Figure 10.11 underscores the necessity of allowing between 15 and 30 minutes to pass while observing a growth cone before attempting guidance: in the run that yielded the

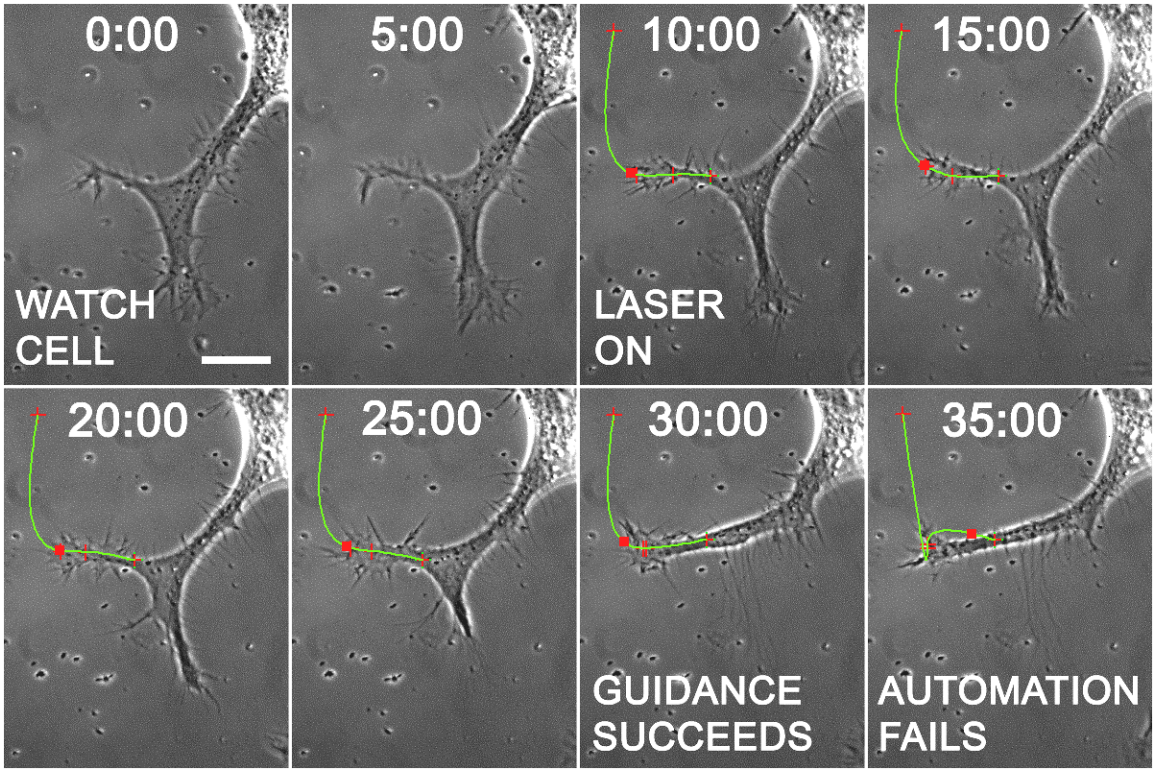

Figure 10.12 The Rise and Fall of Automated Guidance. The cell is first watched for a period to verify its viability. Next, Automated guidance succeeds in advancing a growth cone; the cell chooses to keep only the guided side of the initial bifurcation. In the last frame, however, self-adjusting spline anchor points cause the spline to curl, the laser spot to retreat, and guidance to fail. Times are in mm:ss, and bar = 20 microns.

figure, waiting a short interval saved effort from being spent on a neurite that turned out not to be a good candidate for guidance.

At one point in time in the program's development, we had decided to endow each spline anchor point with the capacity to adjust its position in a direction perpendicular to that of the spline. This way, the spline would ultimately conform better to the changing shape of the axon over time and would provide a smoother path down which the growth cone could be guided. Adding spline anchor mobility was a horrible idea, it turned out, as can be seen in Figure 10.13. By constantly recalculating their positions laterally across the axon, small changes in spline directionality lead to large

discrepancies in spline anchor positioning. In fact, the second spline anchor point actually overtakes the third in this example, causing the spline to twist around, the laser spot to move backward, and automation to fail. Figure 10.13 (C) and (D) also demonstrate a phenomenon which was initially quite puzzling to us: at times, the laser spot (red square) would seem to migrate off of the spline and become "lost at sea" in the surrounding pixels instead of being at the leading edge where expected. The laser spot's initial retreat from the leading edge is explainable from the changing trajectory of the point from (A) to (B), and any slight manual movement of the laser spot would cause it to "snap back" onto the spline, albeit still not near the leading edge. Ultimately, we found that the laser spot position on the spline was calculated before the anchor points were being moved and the spline curve recalculated, so the laser spot placement was always relative to the previous data point's spline curve. For large changes in the position of the spline curve, then, the laser spot would seem to hop off the spline.

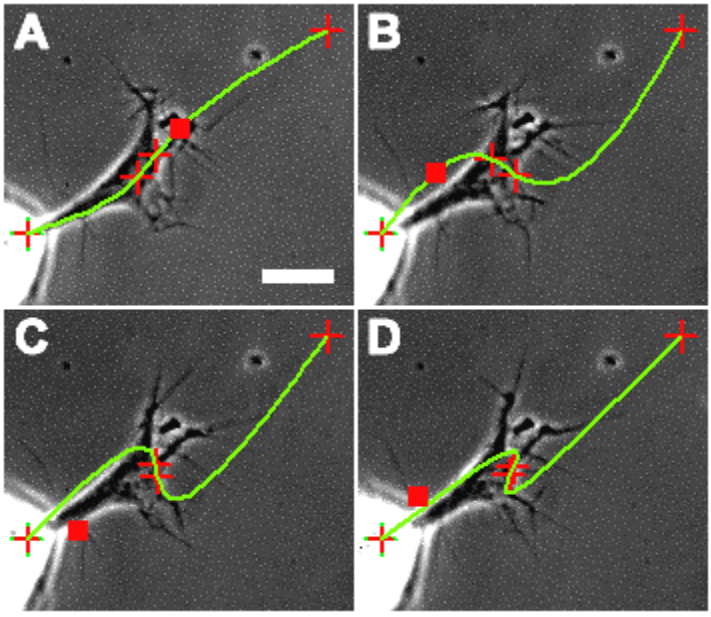

Figure 10.13 Automated Guiding Fails when Spline Points Auto-Adjust. In the time progression above (interval = 1 minute), problems are encountered when the positions of the two intermediate spline anchors and the laser spot are automatically adjusted. Bar = 10 microns.

Automated guidance falls short of manual guidance in very few instances, but those in which it does merit some attention. The most common such scenario is one in which the growth cone proceeds to grow along its initial axis without turning, leaving the trajectory of the spline sticking out the side of the neurite where no active growth is taking place. With manual guidance, one automatically corrects for these situations by always keeping the laser spot on the growth cone regardless of where the growth cone is located. It is for this reason that some guidance trends, such as whether application of a laser spot to an initially unresponsive neurite will eventually lead to guidance, are yet unavailable to be explored with our automated guidance program. One possible way to remedy this shortcoming would be to add to the program an algorithm that would 1) compute the initial growth axis from the boundary detection and 2) ensure that the spline

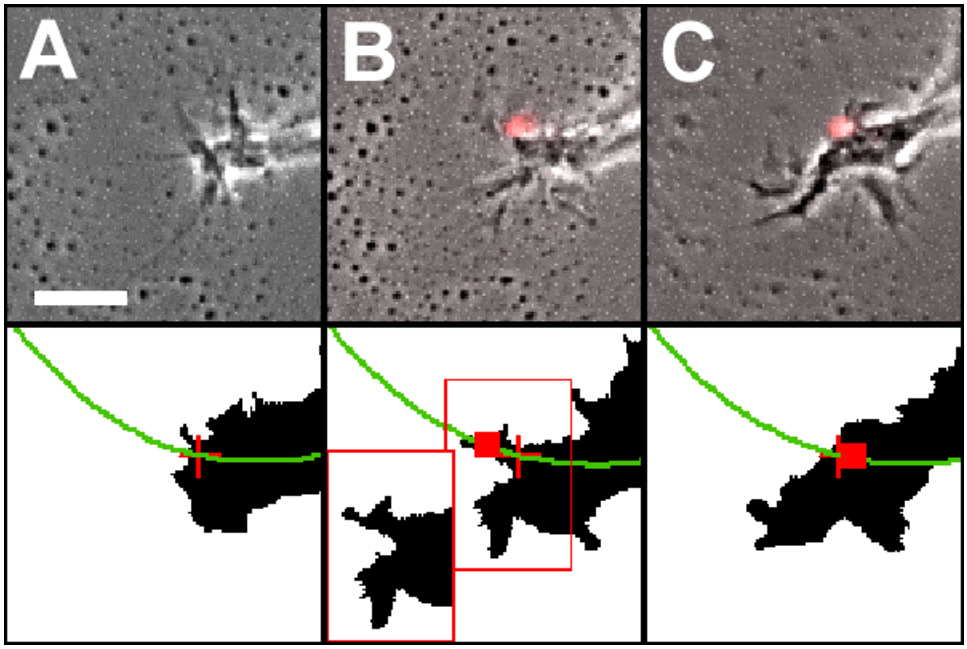

Figure 10.14 Automation Fails when Cell Grows Straight. Cell and detection images for 3 data points (columns) spaced 10 minutes apart. (A) Original growth cone position and boundary; (B) The growth cone follows the laser to one side (boundary without spline is depicted in inset), but the bulk continues to grow forward; (C) Growth cone has moved forward and has left laser spot behind, and human intervention becomes necessary. Bar, 10 microns.

extends forward each picture by a sufficient distance so that the laser spot will be no further than *n* pixels from the leading edge along the growth axis. One way to make sure the spline could adjust that way would be to move the last and penultimate spline anchor points forward along the initial growth axis until the condition for laser spot position is satisfied.

10.7 RESULTS

10.7.1 Data for Hopping *vs.* Attenuated Laser Spot

Many of the data were taken to determine whether, for the same time-averaged power, the cells better responded to an attenuated laser or an unattenuated laser hopping back and forth, on and off the cells. The situation is illustrated in Figure 10.15.

These comparative investigations began when two researchers in collaborating groups (Moore and Ehrlicher) independently remarked upon an ostensible trend: that of cells responding more successfully to a hopping laser than to a stationary laser. This discrepancy, if found experimentally, would point to a mechanism other than biased protein diffusion

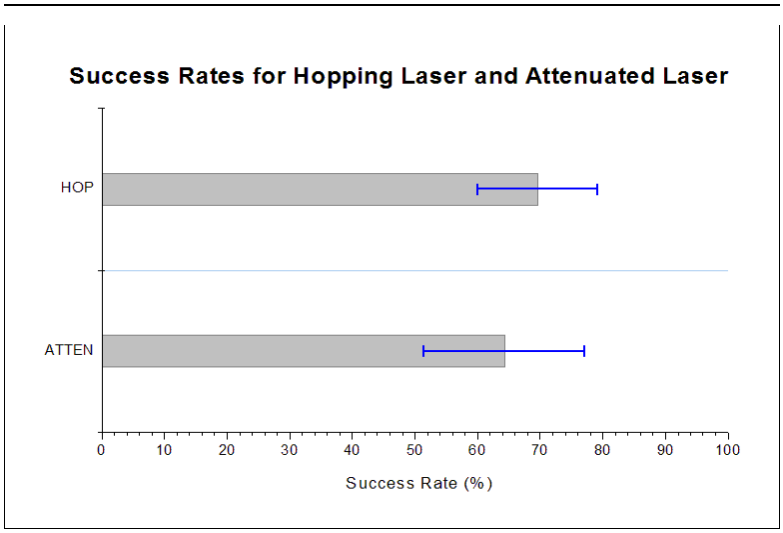

Figure 10.15 Guidance Success Rates for Hopping Laser versus Attenuated Laser: Same Time-Averaged Power to the Cell. The results are very similar, suggesting that biased diffusion cannot be eliminated from consideration as a mechanism for optical neuronal guidance

for responsibility in optical guidance because biased diffusion would be dependent only on the time-averaged laser power. With this in mind, we set out to show that a hopping laser would be more effective for optical guidance than an attenuated laser.

Generally speaking, if we are to compare data between the cases of hopping and attenuated laser guidance, as many other parameters as possible must be equalized for the two situations. In addition to consistency in the cell preparation and experimental protocols, the primary concern is to keep constant the time-averaged power in the two cases. This means, among other things, that only one value for time-averaged power can be studied at a time, so one must choose carefully with which value to begin. We chose 40% of the maximum laser power as our time-averaged value because previous experiments had suggested that this level of power was below the threshold for optical guidance. As is shown in Figure 10.15, however, we encountered an unexpected result from this investigation – that the mean success rate for hopping laser is very near to that for attenuated laser – a statistical analysis of which follows.

It would seem immediately evident from inspection that the two means are not significantly different, and since the sample sizes are unavoidably small, there are limits to what can be inferred from a more nuanced statistical examination. That the error bar regions overlap is sufficient grounds to say that the null hypothesis of equivalent populations (or equivalent effect from the two techniques) cannot be rejected – nor is it unimportant to be able to say this, since what evidence we have from hundreds of hours of observed neuronal growth definitely fails statistically to support the earlier conjecture that hopping yields greater success than attenuation – but since failure to reject equivalence is not the same as proof of nondifference (or proof that the difference is less than some critical value *d*), it might be worthwhile also to "run the numbers" in the most

obvious way, examining the standard error of the difference between means (SEDBM), which is defined (for proportional data) as:

$$\sqrt{\frac{p_1 (1 - p_1)}{n_1} + \frac{p_2 (1 - p_2)}{n_2}}$$

where n_1=23 is the number of cases available for analysis of hopping mode, p_1=16/23 is the proportion of successes for this mode, n_2=14 is the number of cases available for analysis of attenuated mode, and p_2=9/14 is the proportion of successes for this mode.

The actual difference reflected by the sampled difference has a probability dependent on the number of standard deviations, t, of falling within the interval (0.053 - tz) to (0.053 + tz). Since 0 is included in this interval for any useful value of t, we can again observe that the null hypothesis of equivalence cannot be rejected, but we can also observe with 80% probability that the actual difference lies in the interval from (0.053 - 1.28z) to (0.053 + 1.28z) = -0.15 to 0.25.

We can do considerably better, though, since we know (or can fairly safely presume) that, even if beam hopping provides no advantage over beam attenuation, we began by assuming that it certainly does no worse. So if we compute a smaller (0.84 rather than 1.28 standard deviation) confidence interval using this fairly reasonable assumption, we can observe with 60% probability that the actual difference lies in the interval from (0.053 - 0.84z) to (0.053 + 0.84z) = -0.08 to 0.18, but since we know that the difference is not less than (0.053 - 0.84z) (since beam attenuation is assumed not to do substantially better than beam hopping), we can add on the 20% of area under the graph to the left of (0.053 - 0.84z) and say that there is actually an 80% probability that the difference is not greater than (0.053 + 0.84z), or 0.187.

This is less dramatic than inferences that might have been derived from larger data sets reflecting the same proportions, but it certainly represents evidence in the direction of rejecting "beam hopping" as a more effective technique than beam attenuation, and disinclines us further to pursue that avenue of approach. The smallest achievable range with data sets of this size and success rates in the 70% range would have been the case with 16/23 successes for hopping and 10/14 successes (one more than attested) for attenuation. This would have yielded an interval of (0.018 - 0.16*t*) to (0.018 + 0.16*t*), not a vast improvement. It is worth noting that the standard error is at its maximal value with a 50% success rate, and minimal with 0 or 100%. 70% success in each case produces a fairly large standard error. To obtain a very small interval (of width < 0.10) with, say, 95% confidence for proportions in the 70% range of success would have required hundreds of data points for each experimental approach, not something remotely achievable with available resources.

10.7.2 Trends

Other than the comparison between cell response to hopping and attenuated laser spots, the data offer some additional insights. Two parameters whose effects we would like to compare are duty cycle and cycle period. To clarify, a few examples are listed in Table 10.2.

Position 1	Position 2	Cycle Period	Dwell Time On Cell	Duty Cycle
on cell, 40 ms	off cell, 40 ms	80 ms	40 ms	50%
on cell, 40 ms	off cell, 120 ms	160 ms	40 ms	33%
on cell, 80 ms	off cell, 80 ms	160 ms	80 ms	50%

Table 10.2. Illustration of Varying Parameters. All three cases (rows) may elicit very different responses from neurons.

Let us begin by separating data based on duty cycle. As illustrated in Figure 10.16, there is a general trend of an increasing success rate with increasing duty cycle, and this fulfills our expectation that an increase in time-averaged power would result in an increased guidance rate. Recall that this suggests as partial mechanisms for optical guidance those phenomena which depend on the time-averaged power to which the cell is exposed, such as heating or biased diffusion. Additionally, there had been some previous indications that there was a threshold value for the total laser power necessary to achieve optical guidance. Any threshold behavior would surely be revealed in this graph, as it also represents the total time-averaged laser power applied to the cells in attempts at optical guidance. Indeed, a threshold power between 30 and 50 milliwatts would be consistent with the data shown here. No explicit power-dependence experiments were carried out, but this should be an issue addressed in future experiments of this type.

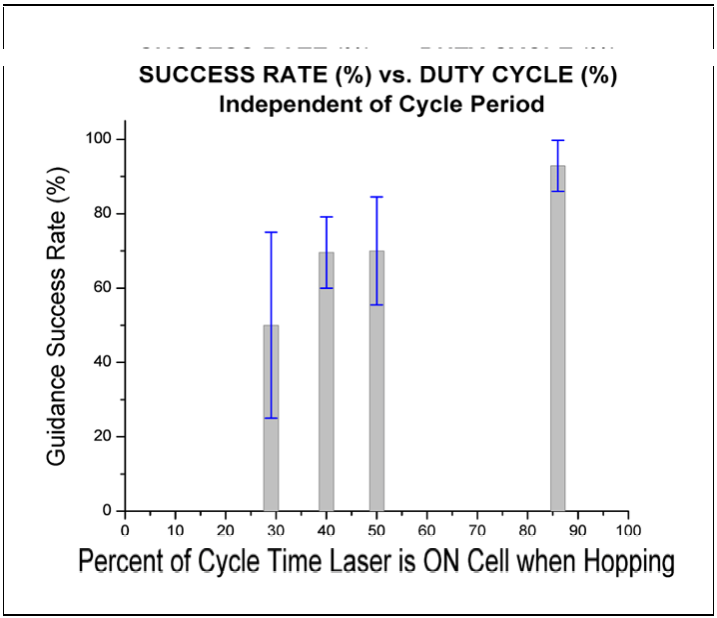

Figure 10.16 Duty Cycle without Consideration of Cycle Period. Note the general trend that success rate increases with an increase in duty cycle.

As a brief statistical digression, the error bars displayed in Figures 10.16 and 10.17 follow the usual convention of extending positively and negatively from the mean a distance equal to the SEM (standard error of the mean). For a mean that is actually just the proportion of binarily graded cases that are identified as "successes," the SEM is computed by the formula:

$$\sqrt{\frac{p\,(1\,-\,p)}{n}}$$

where n is the total number of cases and p is the proportion of these counted as successes.

Next, we approach a comparison based on the raw amount of time – not the percentage of time – for which the laser is on the cell per hopping cycle. This may initially seem an odd thing to consider, but the results are rather surprising: the rate of guidance generally seemed to hover around 2/3 except at 100 ms, as shown in Figure 10.17. There appears to be a single peak in guidance success here and, given the larger sample size, there can be greater confidence in the rate determined for this point.

Certainly, this result suggests that perhaps there are forces other than biased diffusion (or other phenomena which rely for their function on the time-averaged power of the laser light) that are contributory to the optical guidance effects we observe. A time constant of 100 milliseconds has been associated with potassium channel activity, both in the activation/deactivation of the channels and in bursting behavior, whereby the current passed by the channels oscillates rapidly at a high amplitude before returning to quiescence [Bossu *et al.,* 1996; Nisenbaum *et al.,* 1996]. More recently, though, a 100-ms timescale has been associated with the activity

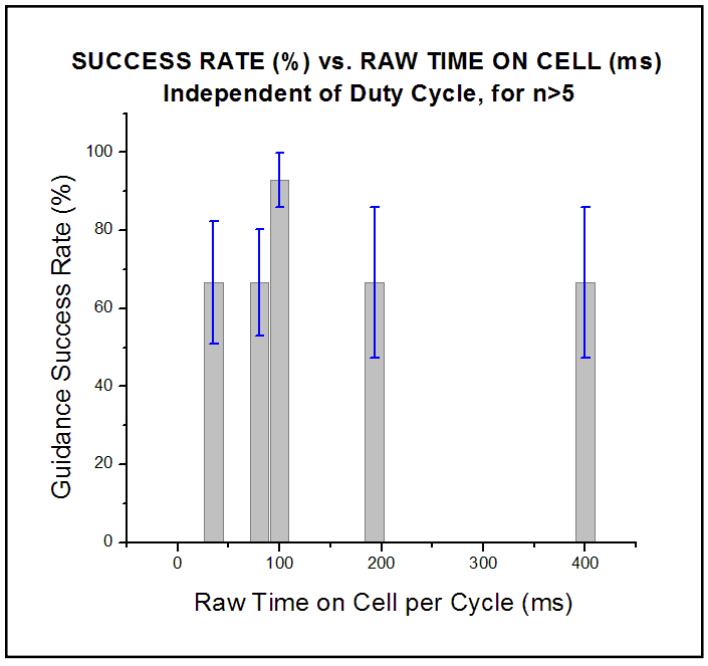

Figure 10.17 Laser Dwell Time on Cell without Consideration of Duty Cycle. The graph suggests that cells may respond more strongly to a dwell time of 100 ms than to surrounding values.

of stretch-activated cation channels [Pellegrini *et al.,* 2001], and the mechanical stimulation of stretch-activated channels could possibly be a contributor to the effect of optical guidance.

11. Discussion

11.1 Candidates for the Mechanism of Optical Guidance

We have shown that, between temporal patterning of the laser and attenuation to achieve the same time-averaged power to the cells, there is no universal rule governing which mode has the greater effect: in a counterexample, comparing the effect of 40% irradiation at full power with that of constant irradiation at 40% power, we obtain similar results in both cases. It follows that biased diffusion, which relies upon time-averaged power for its effects, cannot be ruled out as a mechanism of optical guidance.

However, there appears to be a peak for the case of temporal patterning in which the laser is on the cell for 100 ms every cycle (with duty cycle from 40-91%), and this could be an indication that – although in the aggregate the results for hopping appear similar to those for attenuation – there may be a great deal of variability within the set of results for hopping.

Localized heating has not been ruled out experimentally, for this too could rely on the time-averaged power applied to the cells. This issue was addressed in [Ehrlicher *et al.*, 2002], but a very thorough study on heating in optical traps was also carried out by [Peterman *et al.*, 2003]. This latter group measured laser-induced heating through measurements of Brownian motion of polystyrene and silica microspheres in both water and glycerol, and performed simulations that further supported their experimental evidence. They concluded that, for experiments in water-based solutions (of which cell culture medium certainly is one) and for laser powers on the order of 100 mW (which is the approximate laser power in our experiments), the temperature increase in the laser focus would be approximately 0.8 ºC. We can take this figure as an upper bound for the range of temperature variations possible in our experiment for several reasons. First,

their laser wavelength was 1064 nm, whereas ours is 810 nm, and the Lambert absorption coefficient of water drops from 34.13 m^{-1} for their wavelength to 2.32 m^{-1} to ours, both calculated as per [Hale & Querry, 1973]. Second, Peterman et al. found, both in experiments and in simulations, that heating increased with increasing distance from the lower glass plate in their chamber (roughly proportionally), as glass has a higher thermal conductivity and a lower absorption coefficient than water. In our experiment, the laser spot is exactly at the glass-water interface, so heating in our experiment would be even lower. Third, the Zeiss oil immersion objective lens used in Peterman *et al.* had an NA = 1.4, whereas ours had an NA = 1.3, which means that in our experiment, the laser light is focused less tightly than in theirs, thus making the peak intensity of the light lower in our experiments *ceteris paribus*. In light of this evidence, the likelihood that heating could be the mechanism of optical guidance seems, if not minimal, far smaller than originally considered.

11.2 BIASED DIFFUSION: BEYOND ACTIN?

The mechanism of biased diffusion was introduced in Chapter 4, and with it, a model for calculating the actin monomer drift velocity. In [Ehrlicher *et al.*, 2002], it was estimated that the monomer drift velocity was roughly equal to the rate of neurite extension, but the high variability of the dipole force with dependence on laser power suggests that the correlation between induced drift velocity and the rate of neurite extension is not necessarily strong. Also, if we consider the model of retrograde actin flow, it would seem that the monomer drift velocity would have to be substantially greater than that of neurite extension in order that enough monomers be supplied to the leading edge.

Actin, however, is not the only cytoskeletal polymer in the cell, and interactions between actin and microtubules in neurites play an essential role in growth cone turning (see Section 2.3). The microtubule monomer α-tubulin has recently been characterized in electric dipole moments and refractive index, with calculated $p_\alpha = 566D$ and measured n=2.85, respectively [Schuessler *et al.*, 2003]. Using Equation 4.1 and the knowledge that a tubulin monomer has a diameter of 4 nm, we obtain $\alpha = 7.0 \times 10^{-36}$ for tubulin, over a factor of 12 larger than α for an actin monomer. The force on a tubulin monomer, as well as its induced drift velocity, all increase proportionally to α, so there is a much greater effect on the monomers for the same laser power. Note, though, that microtubules are heteropolymers and have both α and β subunits, and only for the α of these are the properties known well enough to produce a calculation.

11.3 MEMBRANE EFFECTS

There have been experiments to show that it is quite possible to pull away part of a neuron's cell membrane into a tether, and with very little resistance from the membrane [Dai & Sheetz, 1995b]. This suggests that there are parts of the neuronal cell membrane not tightly bound to the cytoskeleton and thus available for mechanical extension out from the cell. In the above work, the following forces were hypothesized to be at work: tension from the membrane itself along the axis of outward deformation, bending stiffness of the lipid bilayer (non-negligible when the membrane has high curvature), and a viscous damping force from a combination of membrane viscosity and shear between bilayers.

Lipid membrane instabilities in response to laser tweezers have been found to produce pearling states (large fluctuations in tube diameter) in tubular lipid bilayers [Bar-Ziv & Moses, 1994; Bar-Ziv *et al.*, 1998]. If an instability at the leading edge of the

growth cone were to be induced by the laser spot, then it is possible that the membrane would extend outward with little resistance, leaving room for cellular components (e.g., actin meshwork, actin bundles, microtubules, or organelles) to flow into the newly vacated space. Additionally, it is plausible that transmembrane proteins, such as those involved in cell adhesion, might be either tweezed or encouraged through dipole force to move toward the center of the laser spot. A higher concentration of these proteins at one side of the leading edge might result in increased incidence of cell-substrate adhesion and thus a propensity for turning in the direction of the laser spot. Since many transmembrane proteins are in fact connected to the actin cytoskeleton, if such proteins were tweezed and caused to accumulate at one side of the growth cone, this would pull on the actin network and perhaps either encourage it to extend forward or provide a force counteracting its retrograde flow.

11.4 MECHANOSENSITIVE ION CHANNELS

The cell has many kinds of transmembrane proteins in addition to proteins that link to the cytoskeleton and/or mediate extracellular adhesion, and a large class of these proteins are ion channels. Ion channels differ in three ways: in which ions they let pass, in whether by default (i.e., in resting state) they are open or closed, and in what way(s) they are activated (switched away from their resting state). One particularly interesting type of ion channel is called a stretch-activated (SA) and mechanosensitive (MS) channel. Channels of this type were discovered accidentally when one group found that, in making patch-clamp voltage recordings of patches of cell membrane, an increase in pressure applied to the membrane resulted in a voltage spike: this was due to one or more SA ion channels opening and letting ions flow through [Sachs, 1986]. It was hypothesized that these channels, in order to be so sensitive to membrane tension, must

be connected to a large area of the cell membrane and to the underlying actin network. Exposing the cells to cytochalasin, which inhibits actin polymerization, increases SA channel sensitivity [Guharay & Sachs, 1984]. The proposed reason is that the actin filaments connected to a given SA channel normally help relieve the tension on other membrane proteins which pass this tension on to the SA channels; when the actin filaments cease to be attached, the other membrane proteins exert their full tension force on the SA channels, thus causing increased SA channel sensitivity.

It happens that SA ion channels are sensitive to both membrane tension and voltage, but chemical messengers do not play a role in their activation. Depending on which species of ion(s) they let pass in the open state, their activation can cause either membrane hyperpolarization or depolarization. Subjection of the cell membrane to a sudden and significant change in voltage often results in a signal cascade which can end with many different results, among them a propensity for growth cone turning. It is possible, then, that if the membrane were distorted by the presence of the laser spot, this could lead to the activation of SA channels and a chain of signals producing the effect of optical guidance.

11.5 CELL TYPES OTHER THAN NG-108-15

11.5.1 GT-1 Cells

GT-1 cells are another type of immortalized cell line, and these were subjects of guidance experiments long before automation was in place. These cells were derived from a mouse hypothalamic tumor in 1990 [Mellon *et al.*, 1990] and thus originated from the central nervous system. One would expect in general, therefore, that they would not be as easy to guide as the NG-108 hybrid cells, each parent cell of which was derived from the peripheral nervous system. The two clonal populations of GT-1 cells used in our experiments were GT1-1 and GT1-7 cells, and both of these cell lines were generous gifts of their creator, Dr. Pamela L. Mellon.

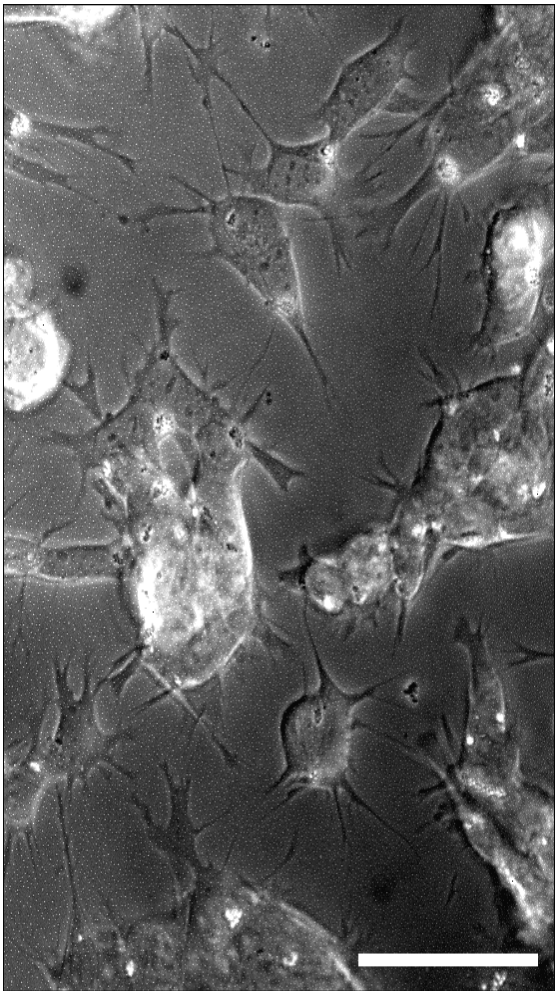

Figure 11.1 GT1-1 Cells. These tend to grow in clusters and, although they do have processes, are not polarized as neurons are. Bar = 50 microns.

The property for which GT-1 cells are most frequently studied is their release of gonadotropin-releasing hormone (GnRH), which is involved in studies of the female reproductive system and is particularly relevant to issues of fertility [Vitalis *et al.,* 2000; Weiner *et al.,* 2001]. Networks of GT-1 cells in culture exhibit waves of action potentials accompanied by pulsatile release of GnRH, and the patterns emergent from these systems

have been characterized both qualitatively [Weiner *et al.,* 1993] and mathematically [Gordan *et al.,* 1998]. The subclones GT1-1 and GT1-7 differ in size (10-50 microns *vs.* 20-80 microns in diameter, respectively), rate of population doubling in culture (3-4 days *vs.* 1.5 days, respectively), and general morphology in culture (growth into clusters *vs.* growth into networks, respectively). GT1-1 cells are more motile, require a poly-l-lysine or laminin-coated substrate for attachment, and tend to grow shorter neurites. GT1-7 cells tend to want to stay virtually immobile on a substrate and do not require an adhesive coating to attach, and these cells tend to look more polarized, with more pronounced neurites.

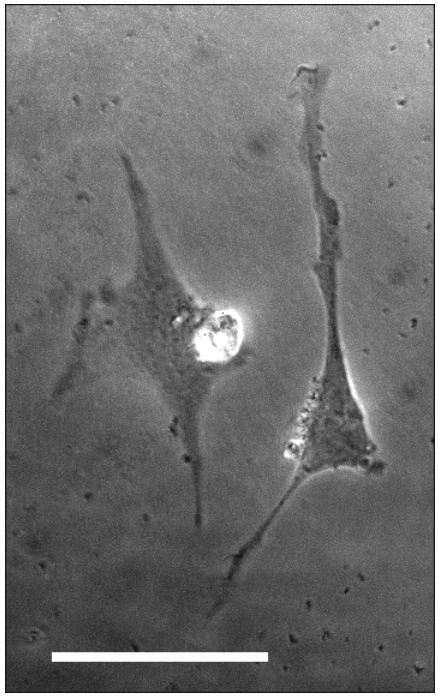

Figure 11.2 GT1-7 Cells. These cells are much larger and have a polarized morphology. Strongly adherent to the substrate, these cells are less conducive to optical guidance. Bar, 50 microns.

For experiments, the GT-1 cells were cultured in starvation medium for at least 12 hours prior to their use in experiments in order to encourage neurite-like process emergence from the cell bodies. Perhaps it was the slower timescale on which the GT1-7 cells appeared to grow, or perhaps the experimental conditions were more difficult for these cells to tolerate, but in any case, there was no evidence of guidance of this subclone. For GT1-1 cells, although one analysis of some initial results determined that no guidance was observed (Schmitt, 2002), further observations suggest that there does exist some evidence for the optical guidance of GT1-1 cells. One would expect GT1-1 cells to respond more positively to guidance than GT1-7 cells because, generally speaking, cells very strongly attached to their substrates are much less likely to be incited to movement

by any stimulus, whereas for motile cells more growth and motility reactions to stimuli are observed [Suter *et al.,* 2000]. However, GT1-1 cells are clearly not the ideal cell type for guidance due to their propensity for the formation of cluster-like cell colonies with neurites not always clearly defined. Figure 11.3 shows an instance in which optical guidance was observed for GT1-1 cells. All frames in the figure are five minutes apart in time, and in frames (A) through (D), the cell cluster is being observed without any laser

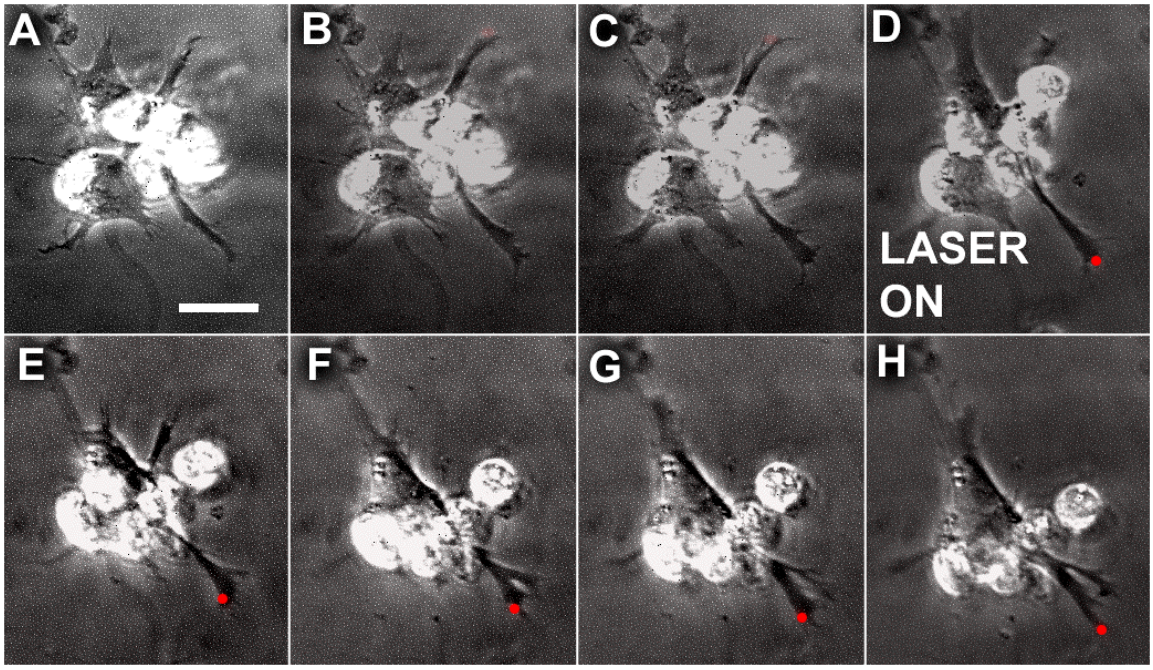

Figure 11.3 GT1-1 Cells React to Optical Guidance. In this sequence of pictures, spaced five minutes apart, the cell is observed until frame D, in which the laser is turned on. Between frames A and D, there is shape change in the neurite but no extension. The neurite clearly extends in the direction of the laser spot between frames D and H, however. Bar, 20 microns.

guidance attenpted. Frame (D) marks the time at which the laser was turned on, and the neurite is guided through frame (H). Before laser guidance was initiated, the guided neurite changed shape but did not extend, as can be clearly seen by comparing the neurite's outlines at frames (A), (D), and (H), as in Figure 11.3. During the observation period (from Frame A to D), there is some lateral movement and growth cone broadening

visible, although there is no significant advance of the leading edge. During the guiding period (Frame D to H), there is pronounced forward movement, accompanied by soma translocation and a bifurcation. The guided branch of the bifurcation shows a higher rate of translocation than its unguided counterpart of the same neurite. Additionally, an additional unguided neurite is visible in Figure 11.3 pointing toward the upper-right corner of the first row of frames. Before guidance, this neurite does not show a great deal of change, but once guidance has been established, this neurite retracts. It is very typical for sister neurites to a guided neurite to retract over the course of optical guidance, showing that the cell seems to favor the guided neurite by eliminating other neurites whose growth would compete for cellular resources. Translocation of the very bright cell bodies in the images is not particularly relevant for our purposes, as these somata are not attached to the substrate, but rather are clustered around the cell of interest by chance. The somatic translocation of the cell of interest is most easily visualized by comparing the relative amounts of cellular material visible in the upper-left section of the cell in Frames A, D, and H of Figure 11.3.

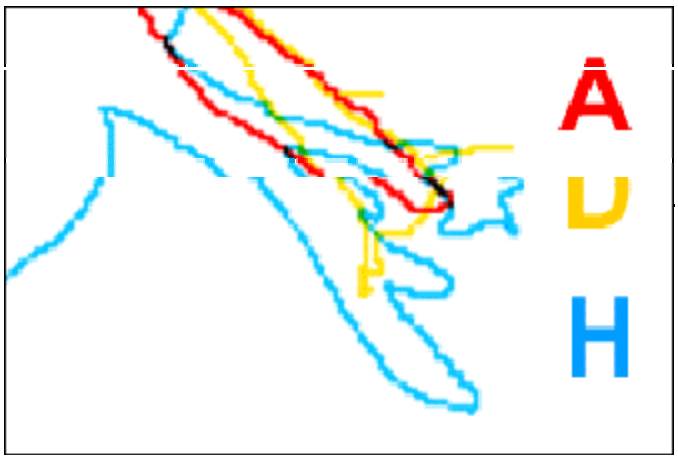

Figure 11.4 Outlines of the Guided Neurite of Figure 11.3 Frames A, D, and H. Until the laser was introduced, no significant forward growth was detectable. During optical guidance, however, distinct extension is visible. Note the bifurcation observed during guidance and the difference in growth between the guided (lower) and unguided (upper) branches of the neurite for outline H.

11.5.2 Primary Rat Cortical Neurons

The final cell type with which we attempted optical guidance is the primary neonatal rat cortical (pyramidal) neuron. Unlike immortalized cell lines, primary cells are normal, healthy cells taken from a normal organism, rather than being either malignantly transformed in culture or taken from a tumor in an animal. These cells are fully differentiated and functional parts of the organism, they are programmed for eventual apoptosis and are very environmentally-sensitive, and because they can only "be fooled" for so long by the organism-mimicking environment of an incubator and culture medium, their cultures are short-lived. These conditions necessitate the sacrifice of another organism every time a new culture is desired because additionally, primary neurons are not programmed to undergo mitosis any longer.

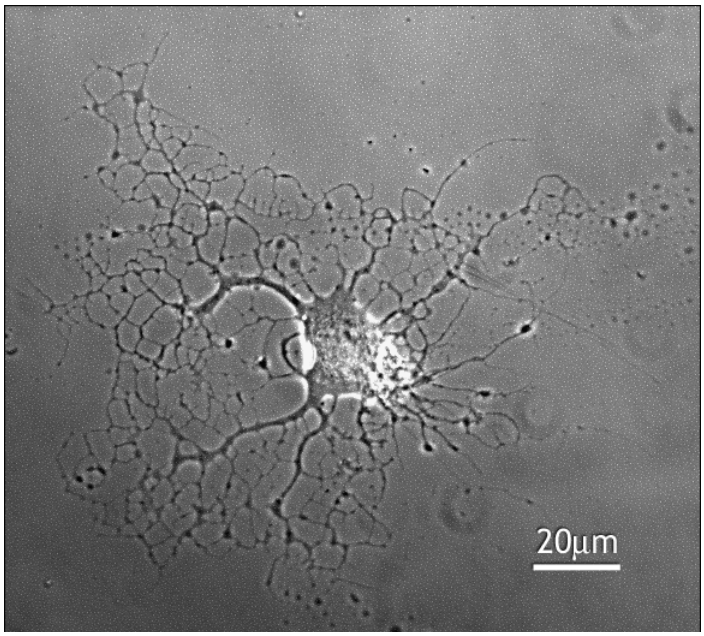

Figure 11.5 Neonatal Rat Cortical Neuron. Note the highly networked structure and lack of polarization. Clearly-defined growth cones are not visible at this point in time.

The guidance of primary neonatal rat cortical neurons was found to be infeasible due to the morphology of the cells. An example of such a cell is shown in Figure 11.5. There is no clearly-defined, single axon at this point in time, and the cell does not appear at all polarized, but rather roughly circularly symmetrical. Additionally, any growth

cones that may exhibit ruffling behavior characteristic of a candidate for guidance are far too small (~1 micron across) to be guided by a laser spot whose minimal diameter is also 1 micron. We also found that these cells were extremely sensitive to changes in environment such that the transition from incubator to microscope caused a deterioration of cellular processes that allowed us only to observe the last faint flickers of growth cone motility before all cellular motion ceased.

Even if the optimal environmental conditions could be engineered for the microscope, the morphology of these cells would still prohibit their optical guidance. There are a few different reasons the cells might have assumed this networked, nonpolarized morphology, and each reason suggests its own potential course of action for a prospective future remedy of the situation. The first possibility is that too much time elapsed between cell preparation and experimentation (at least one full day in all cases) and that earlier cell configurations could have more closely resembled our target shape of an axon protruding from a cell body. This amount of time was allowed to elapse because it was believed necessary for the cells to settle onto the substrate, but in retrospect, this was undoubtedly an overestimate. Another possible contributor to the problematic morphology could have been a result of our laboratory's inexperience in preparing these cells, as the procedure was performed only a total of five times. Finally, although the cell preparation protocol required a double coating of poly-l-lysine and laminin on the substrate, since cells adhering too strongly to their substrate are known generally to be less motile than others [Smalheiser, 1991], it is possible that an overly-strong substrate adherence was responsible for the observed effects.

In summary, there are quite a few reasons the experiments with primary neonatal rat cortical neurons were infeasible, and for that reason we would strongly recommend working with another cell type (either from a different animal, a different region of the

same species, a different classification/function in the same species, or at a different stage of development in the same species) in any future optical guidance experiments.

12. Future Work

Patterns of neuronal growth and development, although they may vary significantly from one organism to another – and from one kind of neuron to another within a given organism – have been investigated and characterized thoroughly in numerous studies, but the majority of the unanswered questions in this realm lie in *why* and *how* these events take place. The answers often involve complex signalling mechanisms and cascades of interactions among proteins and chemical cues, both intracellular and extracellular.

In this context, it seems reasonable to consider experiments from other groups in which increased growth rate and induced turns were observed in neurites, specifically seeking a chain of causality which might be traced back from our observed results to the underlying mechanism. Additionally, of course, there are mechanisms still unexplored which, we conjecture, may be responsible for the effects we see, and those ideas will be presented here as well.

12.1 Taking a Closer Look

With the right equipment and technique, it would be feasible to visualize the transport of membrane material and vesicles to see whether they aggregate near the laser spot. Differential interference contrast (DIC) microscopy, especially with an objective lens of magnification higher than 40X, would allow us better to visualize vesicles while at the same time allowing more laser light through the objective (by virtue of there being no phase rings involved). Additionally, lipophilic fluorescent probes (such as DiI) incorporate themselves into the cell membrane and could be used as membrane tracers for investigating membrane and vesicle transport [Haugland, 2002]. In this way, we

would be able to detect any patterns induced in the membrane by the laser, which might not be clearly visible at all in phase contrast, and we would be able to see whether any tweezing of vesicles were taking place.

12.2 CYTOSKELETAL VISUALIZATION AND ALTERATION

Although the simplest techniques for cytoskeletal visualization require fixing and staining cells (which kills the cells), there do exist ways of visualizing the cytoskeleton in living cells. One way is to transfect cells like NG-108s with a genetic sequence for expressing GFP-actin, which results in all of the cells' actin fluorescing when exposed to UV light. Also, after the administration of nocodazole to a cell sample to depolymerize the microtubules, fluorescently-labelled tubulin can be injected directly into the cells so that upon repolymerization the microtubules will fluoresce and many will be individually visible [Baas, 2000]. This would allow visualizaton of microtubule transport and elongation, and skipping the depolymerization step would allow one to visualize only the growing microtubule ends. In the context of the microtubule biased diffusion discussed above, such an experiment might shed some light on optical guidance.

There is a relatively new fluorescence method which obviates the use of some dyes, which is attractive because the by-products of many fluorescent dyes or labels are cytotoxic and/or undergo photobleaching after a number of seconds and refuse thereafter to fluoresce. This new method uses quantum dots to label proteins via antibodies that attach to the quantum dot on one side and to the protein of interest on the other (although there may be other intermediate antibodies in a chain, as well). Using quantum dots as protein labels is advantageous because there are no chemical by-products or free radicals produced and also because there is no photobleaching effect, since electrons can be driven repeatedly into an excited state without losing efficiency. Since quantum dots

have become an off-the-shelf commodity (e.g., Evident Technologies), their use is becoming widespread, and for this application it is optimal to minimize cellular stimuli other than optical guidance, so quantum dots would make an excellent choice for monitoring cytoskeletal morphology.

Aside from visualizing the cytoskeleton, there exist very solid methods by which the cytoskeleton may be altered to investigate the effects produced. Latrunculin A, for example, will stop the polymerization of actin networks, and an abolition of the optical guidance effect in its presence would lend support to the hypothesis that optically-induced growth is driven by actin polymerization. The addition of vinblastine locks microtubules in a stable state [Tanaka *et al.*, 1995] and this could be added in an attempt to learn more about the role played by microtubule dynamic instability in optically-induced guidance.

12.3 ION CHANNEL VISUALIZATION AND ALTERATION

The best way to visualize ion channels is by visualizing the ion fluxes they initiate, and there are several voltage-sensitive dyes (such as the family of RH dyes) commercially available for purposes such as these [Haugland, 2002]. A combination of voltage-sensitive and calcium-sensitive dyes (such as fura-2) would provide information about whether an ionic species were experiencing cellular influx or efflux concurrently with calcium. There also exist dyes made especially for conjugating to the ion channels themselves, and fluorescence imaging of these would certainly address the issue of whether the ion channels themselves were being drawn into the laser focus. However, it is necessary to note that, due to the extreme sensitivity of all types of ion channels to conformational changes, the conjugation of any probe to an ion channel will always alter

the function of that channel, whether it be to inhibit or to promote the flow of ions [Haugland, 2002].

Another way to determine whether SA calcium channels are a causative force in optical guidance is to add gadolinium ions to the cell medium, as these ions fit directly into the channels to block their mechanism of action [Lee *et al.*, 1999]. The method which is perhaps the most difficult but probably gives the most definitive results is cell line transfection: cells can be transfected either to overexpress (overproduce) or not to express a certain kind of ion channel, and in this way the role of that specific channel can be elucidated (see [Maingret *et al.*, 1999] for description of an example system).

12.4 FUTURE DIRECTIONS

Needless to say, the future of this project lies in determining the mechanism of action of optical neuronal guidance in order that circumstances might be optimized for enhancement of the effect and its ultimate application to *in vivo* systems. I believe that this work can best be carried out in an environment of interdisciplinary collaboration, as experts from the fields of physics, mathematics, biology, chemistry, medicine, and engineering should all be able to contribute a great deal to the project's advancement. It is my sincere hope that the work here presented may prove useful in future endeavors of this kind.

IV. APPENDICES

Appendix A. Data Tables

A.1 General Remarks

Table 1 (Section A.3) represents the first pass over the data and divides the data into appropriate segments for analysis. Only the segments labeled R will be counted as « runs, » or valid data segments for analysis. For data that were disregarded, there are notations as to why this decision was made for certain data sets. These determinations, as well as those of success/failure of optical guidance, are based on the image data acquired, all of which cannot be displayed here in the interest of space.

Table 2 (Section A.4) shows the final determinations for success (Y) and failure (N) of guidance according to the day on which the data were taken. There are also some comments in this table as to the degree to which success or failure of optical guidance was noted. These measures of degree have not been considered for our analysis but are included as a supplement for reference.

These data tables illustrate the process of data analysis and the determination of how data sets are grouped, how success is determined, and how a final decision is made for a binary representation of each data segment. In the following section (A.2), some of the commonly-employed abbreviations are listed and described to give the reader an insight into the shorthand notations in the data tables.

A.2 ABBREVIATIONS FOUND IN TABLE NOTES

nt – neurite

IDOLS – **i**n **d**irection **o**f **l**aser **s**pot

M – manual [guidance]

A – automated [guidance]

GC – **g**rowth **c**one

LOC – **l**aser **o**n **c**ell

xloctn – translocation

GRAB cycle – GRowth-ABatement cycle

retraxn – retraction [of neurite]

ITS – **i**nterval [of time] **t**oo **s**mall [for inclusion in data set]

TCTN – [neurite or growth cone] **t**oo **c**lose **t**o **n**eighbor [for inclusion in data set]

P*nnn* – picture # *nnn* in the run file

atten'd – attenuated

A – attenuated to 40% of total power

AE – data taken by another group member; not all data are available

A.3 DATA TABLE 1

HEADER, RUN, NOT?	DATE	RUN	PIC INTVL (s)	START PIC	LASER START	LASER END	END PIC	LASER STAT THIS INTVL	DATE DISH	DATE SFM	DATE cAMP	TIME EXPT
Head	030530	R03	30						030527 17h00	030528 11h00	---	
R	030530	R03	30	31	37	61		1 spot	1 spot, begins to draw out a nt			
R	030530	R03	30		63	112		3 spot	3 spots, increase nt growth, then nt withdraws, maintaining a focal adhesion as a remnant though			
R	030530	R03	30		111	139		off	laser off, can see persistence of new nt			
R	030530	R03	30		140	186		3 spot	another nt on same cell, same MO w 3 spots, induces another bifurcation!			
R	030530	R03	30		187	204	212	1 spot	fails to guide now, nt is wackily bendy, though			
Head	030624	R02	30						030623 00h30	030623 15h30	---	
N	030624	R02	30	10	42	51		2 spot perp	intervals too small			
N	030624	R02	30		52	57		2 spot perp				
N	030624	R02	30		58	67		2 spot perp				
N	030624	R02	30		68	76		2 spot ||				
N	030624	R02	30		77	79		2 spot perp				
R	030624	R02	30		80	130		2 spot perp same nt dif loc	bifurcation induced and GC guidance, in spite of neighboring cell!			
R	030624	R02	30		131	158		1 spot	got the bifurcation again after it got weak for a little bit			
R	030624	R02	30		159	175	175	off; filopodium flipped away	bifurcation's new nt persistent!			
Head	030705	R01	30						030701 05h00	030702 12h30	---	
R	030705	R01	30	12	32	91		2 spots: 1 per cell 4 conxn	2 nts difft cells both guided and make connxn GOOD!			
N	030705	R01	30		92	94		2 spots: 1 per cell 4 conxn	1 spot on same nt, 1 spot switched nts			
N	030705	R01	30		95	101		1 spot	interval too small			

HEADER, RUN, NOT?	DATE	RUN	PIC INTVL (s)	START PIC	LASER START	LASER END	END PIC	LASER STAT THIS INTVL	DATE DISH	DATE SFM	DATE cAMP	TIME EXPT
N	030705	R01	30		105	132		2 spots: 1 per cell 4 conxn	now they're TCTN and I'd disregard this one			
N	030705	R01	30		133	151	161	2 spots: 1 per cell 4 conxn	same TCTN thingys; changed point bc changed nt			
Head	030707	R02	30						030628 23h30	030629 23h00	---	
R	030707	R02	30	17	43	94		1 spot on GC nonmoving	very small amnt of lmp fluttering but no guidance per se.			
R	030707	R02	30		95	120		off				
R	030707	R02	30		121	131		1 spot 1 side broad lmp	active ruffling elsewhere: failed guidance			
R	030707	R02	30		132	151		2 spots: 1 ea side broad lmp	ruffling at leading edge			
R	030707	R02	30		152	205		2 spots: 1 ea side broad lmp	transition to no ruffling, transition to transient ruffling 3 places			
R	030707	R02	30		206	238		NO CHANGE from 152-205	tries to form a filopodium!! But I didn't move the laser so I lost it and it stopped trying			
R	030707	R02	30		239	256		NO CHANGE from 152-205	ruffling goes back to leading edge			
R	030707	R02	30		237	259		NO CHANGE from 152-205	side w spot starts to ruffle again but I quit right then			
R	030707	R02	30		260	265		off	ruffle at former-laser-spot dies down to nothing			
R	030707	R02	30		265	303	303	off	barely perceptible movement back at leading edge, absence of ruffling.			
Head	030811-12	R01	30						030807 ??h??	030808 13h00	---	
R	030811-12	R01	30	98	111	192		2 spot 2 nts 2 cells	1 induces soma xlocation, 1 does nothing			
R	030811-12	R01	30		193	247	247	off	the soma-xlocated cell xlocates back:Rel RATES? Fast nts lots. Unguided cell rtxts completely.			
Head	030815	R04	30						030814 06h00	still in NCM!!!!!!	---	
N	030815	R04	30	26	32	38		1 spot				
N	030815	R04	30		39	40		off	just briefly off nt			

HEADER, RUN, NOT?	DATE	RUN	PIC INTVL (s)	START PIC	LASER START	LASER END	END PIC	LASER STAT THIS INTVL	DATE DISH	DATE SFM	DATE cAMP	TIME EXPT
R	030815	R04	30		41	92		1 spot	nt gets really thin as it's guided, but it is guided. Could it have been twozen, being so thin??			
R	030815	R04	30		93	97		off				
R	030815	R04	30		98	117		1spot, difft nt	nt retracting			
N	030815	R04	30		118	131		off	no pixx microscope problems			
N / N	030815	R04	30		132	168	191	1 spot	TCTN, DISREGARDING			
Head	030819	R09	30						0308?? ??h?? AE	030813 ??h?? AE	---	
R	030819	R09	30	7	35	52		1spot	nt retracts			
R	030819	R09	30		53	121	121	1spot, difft nt difft cell	soma translocation induced			
Head	030828	R04	30						030824 ??h?? AE	0308?? ??h?? AE	---	
N	030828	R04	30	10	32	36		1 spot on edge of soma ?!	ITS			
R	030828	R04	30		37	90	90	end of GC	apparently guidance & soma xloctn- with a delay btw LOC and GC flourishing of ~ 5 minutes			
Head	030908	R03	30						030904 21h00	CDIM 03090521h	---	
R	030908	R03	30	5	43	56		1 spot	retracts in GRAB cycle, extending in opp drxn to laser spot			
R	030908	R03	30		59	71		1 spot other nt same cell	no perceptible change to the GRAB cycle			
R	030908	R03	30		72	82		2 spot same nt	no response, GC keeps curling up			
N	030908	R03	30		83	89		2 spot same nt	ITS			
R	030908	R03	30		91	161		2 spot other nt same cell	slows GRAB cycle AND induces a turn			
R	030908	R03	30		162	212		1 spot same nt	GRAB cycle pauses and after a while, GC does turn			
R	030908	R03	30		213	285		2 spot no atten same nt	GC turns away can't stop the GRAB cycle			
R	030908	R03	30		286	339		2 spot no atten same nt	definite turn toward laser			
R	030908	R03	30		340	377		1 spot with atten same nt	keeps nt in place but no turn really			

HEADER, RUN, NOT?	DATE	RUN	PIC INTVL (s)	START PIC	LASER START	LASER END	END PIC	LASER STAT THIS INTVL	DATE DISH	DATE SFM	DATE cAMP	TIME EXPT
R	030908	R03	30		378	493	493	off	extends and retracts, in GRAB cycle, in the drxn of departed laser spot; later both nts retrxt			
Head	030915	R01	30						030904 21h00	CDIM+ 030912 ?h	---	030912 ?h start of run
R	030915	R01	30	13	25	40		2 spots 1 on 1 off	lasered nt retracts, other nt on cell grows			
R	030915	R01	30		41	76		other nt same cell	NG but when laser off, soma advances in drxn ot where laser was.			
R	030915	R01	30		77	124	124	off	soma advances in drxn of erstwhile laser spot w huge broad lmp.			
Head	030915	R02	30						030904 21h00	CDIM+ 030912 ?h	---	030912 ?h start of run
R	030915	R02	30	30	33	81		2 spot	looks like it might be guiding at first, bifurc, but then retracts & I quit with laser			
R	030915	R02	30		82	226		off	cell looks pretty crappy, but nts from other cells are holding steady (but not flourishing either)			
R	030915	R02	30		227	266		2 spot	small extension in drxn of laser (mostly forward) soma xloctn NOT IDOLS			
R	030915	R02	30		267	296		2 spot same nt	small amnt of extension in drxn of laser (which is straight ahead mostly) little soma xloctn IDOLS			
R	030915	R02	30		298	323		1 spot same nt	extension and thickening of nt, little soma xloctn IDOLS			
R	030915	R02	30		324	367		2 spots same nt	larger extension of nt, more soma xloctn IDOLS			
R	030915	R02	30		368	389		2 spots same nt	holds position but doesn't grow, possibly a little slower soma xloctn IDOLS			
R	030915	R02	30		390	426	426	off	nt completely shrivels up, and so does the cell's other current nt, no soma xloctn			
Head	030915	R04	30						030904 21h00	CDIM+ 030912 ?h	---	030912 ?h start of run
R	030915	R04	30	5	32	60	295	3 spots 200/200/100	guidance! Nice GC - at PIC 53 TCTN manifests OBVIOUSLY and nt retracts			
Head	031118	R01	30						031117 ??h??	1/2 STVMA 1/2 NCM	1/2 STVMA 1/2 NCM	
R	031118	R01	30	25	35	56		1 spot	no discernible growth			
R	031118	R01	30		57	308	309	1 spot chg-spline	nt extends: first automated guidance			
Head	031118	R02	30						031117 ??h??	1/2 STVMA 1/2 NCM	1/2 STVMA 1/2 NCM	
R	031118	R02	30	2	19	154	155	1 spot	ignores laser (grows straight ahead) then shrivels (held back by laser?) unguided nt thrives			

HEADER, RUN, NOT?	DATE	RUN	PIC INTVL (s)	START PIC	LASER START	LASER END	END PIC	LASER STAT THIS INTVL	DATE DISH	DATE SFM	DATE cAMP	TIME EXPT
Head	031118	R03	30									
N	031118	R03	30	5	30	38		1 spot	filopodium flips out of the path and ITS			
R	031118	R03	30		39	370		1 spot chg spline	ignores, then retracts all the way to soma; no other nts in frame survive either, though			
N	031118	R03	30		371	468	664	1 spot	laser not on cell (left automated); then flipper out of place (red pic) for remainder			
Head	031119	R04	30						031117 ??h??	1/2 STVMA 1/2 NCM	1/2 STVMA 1/2 NCM	
R	031119	R04	30	6	29	38		1 spot	spline at an angle that doesn't work - no growth observed but GC (a "knee") is active			
N	031119	R04	30		41	46		1 spot chgd spline	ITS			
R	031119	R04	30		50	89		more spline changes	definite growth w odd angled spline			
N	031119	R04	30		91	93		spline change	ITS			
R	031119	R04	60		94	515		1 spot	chg to 60 s intervals and leave for night. Growth done by P125 latest. P516 breaks off retraxn			
N	031119	R04	60		516	664	664	1 spot	nt breaks off from "stapled" lasered part, which stays put, and retracts fully.			
Head	031124	R01	30						031122 22h00	031123 20h30	031123 20h30	
N	031124	R01	30	28	88	93		changing spline lots				
N	031124	R01	30		94	106		last spline chg now 2 spots	this run is good demo of how difftd cells sometimes still act like undifft ones motility			
R	031124	R01	30		107	177		another spline chg 2 spot	started to grow along spline then TCTN? nt ignores laser & other cell grows straight			
N	031124	R01	30		178	195	195	off				
Head	031124	R02	30						031122 22h00	031123 20h30	031123 20h30	
N	031124	R02	30	4	4	54		off	good demo of cell u-turning wo laser b4 laser			
R	031124	R02	30		55	120		1 spot	guidance! Pulls out of turn - but then seems to grow straight, but the straight after guidance			
R	031124	R02	30		121	372	372	2 spot	230+1splineptwonky 249+conxnw2ndcell & celldebrisunreasonable 315+nolaserimg			
Head	031208	R02	30						031126 23h00	031128 18h00	031128 18h00	

HEADER, RUN, NOT?	DATE	RUN	PIC INTVL (s)	START PIC	LASER START	LASER END	END PIC	LASER STAT THIS INTVL	DATE DISH	DATE SFM	DATE cAMP	TIME EXPT
R	031208	R02	30	6	19	29		1 spot	active ruffling no growth			
R	031208	R02	30		34	56		chg spline and to 2 spots	active ruffling no growth			
R	031208	R02	30		57	77		1 spot	active ruffling little advance spot doesn't stay on egde (is more inside) argh			
R	031208	R02	30		78	97		2 spot	more ruffling, still no growth			
R	031208	R02	30		99	123		1 spot	starts looking less happy, lumping up and now filopodia instead of lmpodia			
R	031208	R02	30		124	160		2 spot	just sits there			
R	031208	R02	30		161	184		chg spline	just sits there			
N	031208	R02	30		185	204	204	off	shrinks back more. Of 5 nts in pic, 1 grows & 4 (incl this) don't			
Head	031208	R05	30									
N	031208	R05	30	4	5	14		1 spot	ITS changing splines and stuff around possible slight extension			
R	031208	R05	30		15	44		1 spot	slight growth			
R	031208	R05	30		45	84		2 spot	nothing			
R	031208	R05	30		85	124		1 spot	ignores, bifurcation begins			
R	031208	R05	30		125	164		2 spot	slight growth, but other branch gets stronger			
R	031208	R05	30		165	204		1 spot	no growth, bif'd branch still there			
N	031208	R05	30		208	210		off				
R	031208	R05	30		211	238		2 spot other nt same cell	seems to undergo 2 ext/ret cycles, slight ext if any but spline-side of GC is flourishing			
N	031208	R05	30		240	247		chgd spline still 2 spot	ITS			
N	031208	R05	30		249	255		chgd spline still 2 spot	ITS now spline follows ALL nt curves			
R	031208	R05	30		256	268		chgd dwells still 2 spot	deftly straightens out in drxn of spot if not extending			
N	031208	R05	30		269	277		2nd spot on 2nd cell nt	ITS 2nd spot ctr of gC to stop growth			
R	031208	R05	30		278	317		chgd dwells still 2 spot	A keeps looking like it'sg uiding but collapses. M is pretty much staying put. P311: M 2 edge 2 guid			

HEADER, RUN, NOT?	DATE	RUN	PIC INTVL (s)	START PIC	LASER START	LASER END	END PIC	LASER STAT THIS INTVL	DATE DISH	DATE SFM	DATE cAMP	TIME EXPT
R	031208	R05	30		318	351		chgd dwells still 2 spot	M nt guides, A nt keeps collapsing.			
R	031208	R05	30		352	391		chgd dwells still 2 spot	M nt guides, A nt bifurcates and keeps collapsing.			
R	031208	R05	30		392	464		chgd dwells still 2 spot	M stays put (curvy) starts to straighten, A trifurcates, grows, collapses twice			
N	031208	R05	30		465	480		chgd dwells still 2 spot	both staying put, tired			
N	031208	R05	30		481	515	516	chgd spline	both staying put, tired			
Head	040109	R05	30						040107 01h30	040108 03h00	---	
R	040109	R05	30	11	26	43		2 spot	ignores (grows)			
R	040109	R05	30		44	56		chgd spline still 2 spot	GC grows and expands			
R	040109	R05	30		60	72		1 spot	grows forward (ignores)			
R	040109	R05	30		73	90		chgd spline still 1 spot	very slight turn about pic 75-80			
R	040109	R05	30		91	131		2 spot	TCTN? Growing toward laser side but not where laser spot is			
R	040109	R05	30		132	163		1 spot	trifurcates, one is along spline. Pointing more on the laserly side now as well			
N	040109	R05	30		164	172			ITS			
N	040109	R05	30		180	193		lots of spline chgs	spline now goes in other drxn. Trifurcation loses the erstwhile-guided leg. Disregarding			
N	040109	R05	30		194	221		off	disregarding NB in here is a good demo of how apoptosing cell communicates somehow			
N	040109	R05	30		222	238		2 spot again	by pic 230, the first cell starts apoptosing. From 30 mins before this, we disregard (170).			
N	040109	R05	30		239	272		chg spline	disregarding			
N	040109	R05	30		273	288	595	1 spot	everything's DYING let's DISREGARD			
Head	040110	R04	30						040107 01h30	040108 03h00	---	
N	040110	R04	30	2	13	60		off				
N	040110	R04	30		61	91		1 spot	a little growth. At pic76, neighboring cell apoptoses. Disregard 30 min previous, which is all we have here.			
N	040110	R04	30		92	128		2 spot				

HEADER, RUN, NOT?	DATE	RUN	PIC INTVL (s)	START PIC	LASER START	LASER END	END PIC	LASER STAT THIS INTVL	DATE DISH	DATE SFM	DATE cAMP	TIME EXPT
N	040110	R04	30		129	154		s1 spot				
N	040110	R04	30		155	189		2 spot	good demo of how a starved but undifferentiated neuron and neurite look			
N	040110	R04	30		190	218		1 spot	starting slowly to retract			
N	040110	R04	30		219	261	263	2 spot	shrinky. Shrinky.			
Head	040111	R03	30						040107 01h30	040108 03h00	---	
N	040111	R03	30	2	14	18		1 spot	ITS			
N	040111	R03	30		19	23		changing spline	ITS			
R	040111	R03	30		24	43		chg spline still 1 spot	some activity starts, small growth			
N	040111	R03	30		44	53		2 spot	ITS			
R	040111	R03	30		54	115		chg spline still 2 spot	some growth along the newly-changed spline			
R	040111	R03	30		116	174		1 spot	2 ext-retrs of filopodia and a little growth too			
R	040111	R03	30		175	248		2 spot	more growth			
R	040111	R03	30		249	292		1 spot	a bifurcation turns into an ignore			
R	040111	R03	30		293	359		2 spot	laser isn't at the leading edge, so we're doomed. Hangs onto the small arm of bifurcation though			
R	040111	R03	30		360	413	428	1 spot	leading edge continues to go slowly, no more bifurc handle.			
Head	040112	R01							SAME	CELLS!!!	Ummm,,,	NOT!!!
Head	040114	R02	30						040109 09h00	--- (only NCM-A)	040110 21h00	
R	040114	R02	30	6	33	101		2 spot	spline's in the wrong bloody place!! >:-(of course the cell can't guide this way, if the laser isn't even on the dang gc!			
N	040114	R02	30		102	113		off and chg spline	throughout this run: no other nts in pic really survive, so in comparison this one's thriving!			
R	040114	R02	30		114	226		2 spot	ignored for a while. 180ish caught a filo and got guidance - needed to move spline to catch up			
R	040114	R02	30		227	272		chg spline still 2 spot	lots of ruffling, no real growth			

HEADER, RUN, NOT?	DATE	RUN	PIC INTVL (s)	START PIC	LASER START	LASER END	END PIC	LASER STAT THIS INTVL	DATE DISH	DATE SFM	DATE cAMP	TIME EXPT
R	040114	R02	30		273	304	331	1 spot	yet more ruffling, lots of floaty crap,			
Head	040115	R03	30						040109 09h00	--- (only NCM-A)	040110 21h00	
R	040115	R03	30	4	79	96		2 spot	extends slightly, folds back, no net growth			
R	040115	R03	30		98	123		chg spline	small growth			
R	040115	R03	30		124	174		chg spline	ignored; laser held a bif branch but main one went straight forward.			
N	040115	R03	30		175	215		off	immediately starts to grow in nonlaserly drxn			
R	040115	R03	30		216	254		1 spot	extends straight			
N	040115	R03	30		255	293		off	no growth			
R	040115	R03	30		294	313		2	slight extension			
R	040115	R03	30		314	411		chg spline	ruffling thru 380ish, then good growth when GC flips into spline			
R	040115	R03	30		412	609		no flipper - no laser img	slow, steady growth throughout long interval			
R	040115	R03	30		610	663	663	chg spline	big spurt along spline but then ignores (grows straight)			
Head	040116	R02	30						040109 09h00	--- (only NCM-A)	040110 21h00	
R	040116	R02	30	5	65	219		2 spot	no growth. Other nts other cells in area growing.			
N	040116	R02	30		220	415	415	off	grows in opposite drxn to spline (would be a GIANT ignore if laser were on)			
Head	040118	R02	30	no counting any of these b/c it's these cells' 4TH DAY STRAIGHT being on microscope.					040109 09h00	--- (only NCM-A)	040110 21h00	
N	040118	R02	30	2	85	93		2 spot	ITS			
N	040118	R02	30		95	123		chg spline	little advancement at first, then just ruffling			
N	040118	R02	30		124	154		time septn, no state septn	bifurcation begins, ruffles and grows. Guided branch is quiescent.			
N	040118	R02	30		155	184		time septn, no state septn	unguided bif branch quiescent, as well as guided branch			
N	040118	R02	30		185	226		chg dwelltime still 2 spot	ruffling begins on guided nt again at Pic 192!! Then growth			

HEADER, RUN, NOT?	DATE	RUN	PIC INTVL (s)	START PIC	LASER START	LASER END	END PIC	LASER STAT THIS INTVL	DATE DISH	DATE SFM	DATE cAMP	TIME EXPT
N	040118	R02	30		227	281		time septn, no state septn	guided gc quiescent again. Pic 248, a trifurcation branch begins and grows. Ruffles			
N	040118	R02	30		282	284		time septn, no state septn	3rd branch quiescent, guided branch starts again			
N	040118	R02	30		285	350		chg dwelltime still 2 spot	ruffles, growth near spline, growth along spline, and shrinkback, then quiescence			
N	040118	R02	30		351	384		time septn, no state septn	anotherfurcation starts, the topmost (near spline) branch grows			
N	040118	R02	30		388	473		chg spline and dwelltimes	chg spline s.t. growing branch is guided branch, and it stops growing.			
N	040118	R02	30		474	487		time septn, no state septn	changed placement of 2nd laser spot and right then it started ruffling again briefly			
N	040118	R02	30		488	543		chg dwelltime still 2 spot	P500 quiescent again. No growth here.			
N	040118	R02	30		544	637	664	chg dwelltime still 2 spot	no growth; nt skinnies up			
Head	040119	R02		STILL the same dish from 1-14 -- disregarding all!					040109 09h00	--- (only NCM-A)	040110 21h00	
Head	040121	R01	30	aarchival neurite (prosposterous)					040115 19h30	040119 0h00	040119 0h00	
R	040121	R01	30	5	52	138		2 spot	definiteive guidance, then dead cell tumbleweeds on the nt, then it stops growing			
N	040121	R01	30		139	183		off	nt straightens out a little but GC doesn't move			
N	040121	R01	30		184	249	287	2 spot	concentration of cell debris doesn't allow for good edge recognition - DISREGARD THIS PART			
Head	040124	R02	30	difft dish of cells from above					040115 19h30	040119 0h00	040119 0h00	
N	040124	R02	30	15	47	51		2 spot	ITS			
Y	040124	R02	30		52	112		chg spline	pic 92 begins retraction no healthy nts anywhere in the picture			
N	040124	R02	30		113	217		off	some minor ruffling but no growth here either			
Y	040124	R02	30		218	288	293	2 spot	pic 267 begins retraction still no healthy nts in picture			
Head	040126	R01		All cells dying - DISREGARDING COMPLETELY argh - they are the same cells as 040124								
Head	040213	R01	30	Spot didn't move due to incorrect software settings (max advance = 1 micron)								
Head	040218	R03	30	hardware problem, laser leaking into cell pic, can't do edge detection, must disregard								

HEADER, RUN, NOT?	DATE	RUN	PIC INTVL (s)	START PIC	LASER START	LASER END	END PIC	LASER STAT THIS INTVL	DATE DISH	DATE SFM	DATE cAMP	TIME EXPT
Head	040227	R05		HUGE growth along spline, but TCTN: another nt touches guided nt so must disregard. ARGH								
Head	040402	R03	30	no detection images saved! Lots of stationary cell debris or bacteria					040323 16h00	040331 17h00	040331 17h00	
R	040402	R03	30	2	45	109		2 spot	nt stops growing and retracts			
N	040402	R03	30		110	138		off	another cell another nt is beginning			
N	040402	R03	30		139	144		2 spot	ITS			
R	040402	R03	30		146	168		chhg spline still 2 spot	grows in wrong drxn			
R	040402	R03	30		169	188		chg spline	looks like a branch might be trying to grow along spline			
N	040402	R03	30		189	202	249	auto guidance failure	automated guidance failure: spline points floating around and laser spot lands off of cell			
Head	040402	R05	30						040323 16h00	040331 17h00	040331 17h00	
N	040402	R05	30	15	40	52		2 spot	starts not at leading edge: disregard			
N	040402	R05	30		53	69		chg spline	tons of spline-changing, lots of ITSs			
R	040402	R05	30		70	98		chg spline	GC collapses into filopodia, no growth			
N	040402	R05	30		99	147		off				
R	040402	R05	30		148	184		2 spot	tackling another cell another nt, the one which retracted earlier DEF growth IDOLS			
R	040402	R05	30		185	202		2 spot chg dwelltime	extends, then retracts bifurcates & reaches in other branch drxn			
N	040402	R05	30		203	231		2 spot chg dwelltime	nt being run over by a motile cell, hard to tell whether growth, little if any			
N	040402	R05	30		232	246	423	2 spot chg dwelltime	obviously getting swooshed away; must disregard			
Head	040402	R07	30						040323 16h00	040331 17h00	040331 17h00	
R	040402	R07	30	5	41	89		2 spot	definite growth IDOLS. Picks guided branch of bifurcation and other retracts			
N	040402	R07	30		90	114	127	2 spot	spline doing funky things, laser on cell only inconsistently, autoguid misses edge of GC, DIS			
Head	031027	R17	15	note in lab book: "abnormal program termination" DISREGARDING								
Head	031027	R18	30	not lots of notes in lab book, but enough to follow what's going on.					unknown	yes	yes	

HEADER, RUN, NOT?	DATE	RUN	PIC INTVL (s)	START PIC	LASER START	LASER END	END PIC	LASER STAT THIS INTVL	DATE DISH	DATE SFM	DATE cAMP	TIME EXPT
N	031027	R18	30	4	9	25		2 spot	on small nt (a). Nt thickens but no discernible growth.			
N	031027	R18	30		40	112		off	difft field of view.			
Y	031027	R18	30		113	130		1 spot	looks like an induced turn			
N	031027	R18	30		131	135		2 spot	ITS			
Y	031027	R18	30		136	172		2 spot 2 cells 2 nts	nt#1 growing more straight, then turns, straightens, pauses nt#2 thickens, grows, thins			
Y	031027	R18	30		173	191		1 spot	nt thins, reaches out a filo. Unlasered nt(#2) thins more			
N	031027	R18	30		192	198	220	2 spot 2 cells 2 nts same	ITS			
Head	031029	R03	30						same cells 031027	same cells 031027	same cells 031027	
N	031029	R03	30	2	112	126		2 spot	trying to guide w multiple spots but with filter in there. Lots of changes anyway, would be itss.			
R	031029	R03	30		127	147		3 spot 2 cells 2 nts	growth on both, though less on one that will soon retract			
R	031029	R03	30		149	167		1 spot	bifurcates and other branch grows, guided branch starts to fade			
R	031029	R03	30		168	187		3 spot 50-50-25 2? Loc	extension on guided bif branch, but other branch is still growing stronger			
R	031029	R03	30		188	208		3 spot 200-200-100 2 loc	guided branch stays same, unguided branch grows lots			
R	031029	R03	30		209	228		3 spot 50-50-25 1 loc	guided retracts, unguided grows more			
R	031029	R03	30		229	248		3 spot 200-200-100 1 loc	guided branch stays same, unguided branch retracts			
N	031029	R03	30		249	258		3 spot 300-300-150 1 loc	ITS			
N	031029	R03	30		259	315		off	erstwhile-guided branch disappears, erstwhile-unguided branch grows again but not as quickly			
R	031029	R03	30		316	335		3 spot 399-399-199 1 loc	unguided->guided and straightens, staying same length. 2nd spot starts on an elbow.			
R	031029	R03	30		341	352		3 spot 20-20-10 1 loc	guided retracts and starts to grow in opposite drxn - ignore			
N	031029	R03	30		353	373		chg spline	chg spline drxn to match growth drxn can't tell anything nd			
R	031029	R03	30		374	393		1 spot	guided retracts			

HEADER, RUN, NOT?	DATE	RUN	PIC INTVL (s)	START PIC	LASER START	LASER END	END PIC	LASER STAT THIS INTVL	DATE DISH	DATE SFM	DATE cAMP	TIME EXPT
R	031029	R03	30		394	425		ON 30s, OFF 30s ALTG PIX	stays more or less the same			
R	031029	R03	30		426	445		3 spot 50-50-25 1 loc	retraction			
N	031029	R03	30		446	542	542	off	starts to grow back up again.			
Head	031104	R06	30	TCTN the whole time DISREGARDING ALL								

A.4 DATA TABLE 2

DATE	RUN	ST PIC	LAST	LAST END	END PIC	TIME (min)	CYCLE PD (ms)	DUTY CYC (%)	GUID?	Growth Comnts.	GENERAL COMMENTS
030530	R03	31	37	61		12	80	100	Y		1 spot, begins to draw out a nt
030530	R03		63	112		24.5	160	25	Y	SUPER	3 spots, increase nt growth, then nt withdraws, maintaining a focal adhesion as a remnant though
030530	R03		140	186		23	240	33	Y		another nt on same cell, same MO w 3 spots, induces another bifurcation!
030530	R03		187	204	212	8.5	80	100	N		fails to guide now, nt is wackily bendy, though
030624	R02		80	130		25	320	50	Y	SUPER	bifurcation induced and GC guidance, in spite of neighboring cell!
030624	R02		131	158		13.5	160	100	Y	SLIGHTLY	got the bifurcation again after it got weak for a little bit
030705	R01	12	32	91		29.5	200	50	Y	SUPER	2 nts difft cells both guided and make connxn GOOD!
030908	R03	5	43	56		6.5	A	100	Y		retracts in GRAB cycle, extending in opp drxn to laser spot
030908	R03		59	71		6	A	100	N		no perceptible change to the GRAB cycle
030908	R03		91	161		35	280	29	N	grab as normal	slows GRAB cycle AND induces a turn
030908	R03		162	212		25	A	100	Y		GRAB cycle pauses and after a while, GC does turn
030908	R03		213	285		36	280	29	N	finishes grab cycle	GC turns away can't stop the GRAB cycle
030908	R03		286	339		26.5	190	42	Y		definite turn toward laser
030908	R03		340	377		18.5	A	100	Y	holds where it would've retrxtd	keeps nt in place but no turn really
030915	R01	13	25	40		7.5	160	50	N	RETRAXN	lasered nt retracts, other nt on cell grows

DATE	RUN	ST PIC	LAS ST	LAS END	END PIC	TIME (min)	CYCLE PD (ms)	DUTY CYC (%)	GUID?	Growth Comnts.	GENERAL COMMENTS
030915	R01		41	76		17.5	160	50	Y	SOMA XLOCATION	NG but when laser off, soma advances in drxn ot where laser was.
030915	R02	30	33	81		24	160	50	N		looks like it might be guiding at first, bifurc, but then retracts & I quit with laser
030915	R02		227	266		19.5	160	50	Y		small extension in drxn of laser (mostly forward) soma xloctn NOT IDOLS
030915	R02		267	296		14.5	40	50	Y	SOMA XLOCATION	small amnt of extension in drxn of laser (which is straight ahead mostly) little soma xloctn IDOLS
030915	R02		298	323		12.5	A	100	Y	axon thickens and advances	extension and thickening of nt, little soma xloctn IDOLS
030915	R02		324	367		21.5	400	50	Y	SUPER	larger extension of nt, more soma xloctn IDOLS
030915	R02		368	389		10.5	40	50	Y		holds position but doesn't grow, possibly a little slower soma xloctn IDOLS
030915	R04	5	32	60	295	14	480	42	Y	example of rxn to tctn	guidance! Nice GC - at PIC 53 TCTN manifests OBVIOUSLY and nt retracts
031027	R18		113	130		8.5	A	100	Y	turn	looks like an induced turn
031027	R18		136	172		18	250	40	Y	one thickens	nt#1 growing more straight, then turns, straightens, pauses nt#2 thickens, grows, thins
031027	R18		136	172		18	250	40	Y	one extends	nt#1 growing more straight, then turns, straightens, pauses nt#2 thickens, grows, thins
031027	R18		173	191		9	A	100	N		nt thins, reaches out a filo. Unlasered nt(#2) thins more
031029	R03		127	147		10	250	40	Y	SLIGHTLY	growth on both, though less on one that will soon retract

DATE	RUN	ST PIC	LAST	LAST END	END PIC	TIME (min)	CYCLE PD (ms)	DUTY CYC (%)	GUID?	Growth Comnts.	GENERAL COMMENTS
031029	R03		149	167		9	A	100	N	RETRAXN	bifurcates and other branch grows, guided branch starts to fade
031029	R03		168	187		9.5	125	40	Y	SLIGHTLY	extension on guided bif branch, but other branch is still growing stronger
031029	R03		188	208		10	500	40	N		guided branch stays same, unguided branch grows lots
031029	R03		209	228		9.5	125	40	N		guided retracts, unguided grows more
031029	R03		229	248		9.5	500	40	N		guided branch stays same, unguided branch retracts
031029	R03		316	335		9.5	997	40	Y		unguided->guided and straightens, staying same length. 2nd spot starts on an elbow.
031118	R01	25	35	56		10.5	F	100	N	phps time delay?	no discernible growth
031118	R01		57	308	309	125.5	F	100	Y	1st automated guidance	nt extends: first automated guidance
031119	R04		50	89		19.5	F	100	Y	SUPER	definite growth w odd angled spline
031119	R04		94	515		210.5	F	100	Y	camel swallowing - leaves pieces	chg to 60 s intervals and leave for night. Growth done by P125 latest. P516 breaks off retraxn
031124	R02		55	120		32.5	200	100	Y	SUPER	guidance! Pulls out of turn - but then seems to grow straight, but the straight after guidance
031124	R02		121	372	372	125.5	40	50	N	really does stop guiding	230+1splineptwonky 249+conxnw2ndcell & celldebrisunreasonable 315+nolaserimg
031208	R05		211	238		13.5	100	40	Y		seems to undergo 2 ext/ret cycles, slight ext if any but spline-side of GC is flourishing
031208	R05		256	268		6	998	40	N		deftly straightens out in drxn of spot if not extending

DATE	RUN	ST PIC	LAS ST	LAS END	END PIC	TIME (min)	CYCLE PD (ms)	DUTY CYC (%)	GUID?	Growth Comnts.	GENERAL COMMENTS
031208	R05		318	351		16.5	998	40	Y		M nt guides, A nt keeps collapsing.
031208	R05		318	351		16.5	998	40	N		M nt guides, A nt keeps collapsing.
031208	R05		352	391		19.5	100	40	Y		M nt guides, A nt bifurcates and keeps collapsing.
031208	R05		352	391		19.5	100	40	N		M nt guides, A nt bifurcates and keeps collapsing.
031208	R05		392	464		36	998	40	Y		M stays put (curvy) starts to straighten, A trifurcates, grows, collapses twice
031208	R05		392	464		36	998	40	Y		M stays put (curvy) starts to straighten, A trifurcates, grows, collapses twice
040109	R05	11	26	43		8.5	200	40	Y	pretty sure	ignores (grows)
040109	R05		44	56		6	200	40	N		GC grows and expands
040109	R05		60	72		6	A	100	N		grows forward (ignores)
040109	R05		91	131		20	200	40	Y		TCTN? Growing toward laser side but not where laser spot is
040109	R05		132	163		15.5	A	100	Y		trifurcates, one is along spline. Pointing more on the laserly side now as well
040109	R05		73	90		8.5	A	100	Y		very slight turn about pic 75-80
040111	R03		24	43		9.5	A	100	Y	SLIGHTLY	some activity starts, small growth
040111	R03		54	115		30.5	200	40	Y	SUPER	some growth along the newly-changed spline
040111	R03		116	174		29	A	100	Y	SLIGHTLY	2 ext-retrs of filopodia and a little growth too
040111	R03		175	248		36.5	200	40	Y	SUPER	more growth
040111	R03		249	292		21.5	A	100	N		a bifurcation turns into an ignore

DATE	RUN	ST PIC	LAS ST	LAS END	END PIC	TIME (min)	CYCLE PD (ms)	DUTY CYC (%)	GUID?	Growth Comnts.	GENERAL COMMENTS
040114	R02	6	33	101		34	120	83	Y	SUPER	spline's in the wrong bloody place!! >:-(of course the cell can't guide this way, if the laser isn't even on the dang gc!
040114	R02		114	226		56	120	83	Y	SUPER	ignored for a while. 180ish caught a filo and got guidance - needed to move spline to catch up
040114	R02		227	272		22.5	120	83	Y	SLIGHTLY	lots of ruffling, no real growth
040114	R02		273	304	331	15.5	100	100	Y	SLIGHTLY	yet more ruffling, lots of floaty crap,
040115	R03	4	79	96		8.5	110	91	Y	SLIGHTLY	extends slightly, folds back, no net growth
040115	R03		98	123		12.5	110	91	N		small growth
040115	R03		124	174		25	110	91	Y	SLIGHTLY	ignored; laser held a bif branch but main one went straight forward.
040115	R03		216	254		19	F	100	N		extends straight
040115	R03		294	313		9.5	110	91	Y	SLIGHTLY	slight extension
040115	R03		314	411		48.5	110	91	Y	SUPER	ruffling thru 380ish, then good growth when GC flips into spline
040115	R03		412	609		98.5	110	91	Y	SLIGHTLY	slow, steady growth throughout long interval
040115	R03		610	663	663	26.5	110	91	Y	SUPER	big spurt along spline but then ignores (grows straight)
040116	R02	5	65	219		77	120	83	Y	grows early but gets nailed down	no growth. Other nts other cells in area growing.
040121	R01	5	52	138		43	220	91	Y	SUPER	definiteive guidance, then dead cell tumbleweeds on the nt, then it stops growing

DATE	RUN	ST PIC	LAS ST	LAS END	END PIC	TIME (min)	CYCLE PD (ms)	DUTY CYC (%)	GUID?	Growth Comnts.	GENERAL COMMENTS
040402	R05		148	184		18	1200	83	Y	SUPER	tackling another cell another nt, the one which retracted earlier DEF growth IDOLS
040402	R05		185	202		8.5	1400	71	Y		extends, then retracts bifurcates & reaches in other branch drxn
040402	R07	5	41	89		24	1400	71	Y	SUPER	definite growth IDOLS. Picks guided branch of bifurcation and other retracts

Appendix B. Neuron Program User Manual

The Neuron program allows for the automation of neuronal guidance, which represents an enormous step forward in our data collection technique. Not only is automation a great convenience, freeing much of the experimenter's time for other laboratory tasks, but it also serves to eliminate user bias in the placement of the laser spot at the leading edge of the cell, making collected data more reliable.

There are two distinct purposes with which the user (hereafter referred to as "you") will run the program: for taking data and for reviewing data. Some of the program's functions will be more useful for one of these tasks than the other, but all program functions are available regardless of your purpose in running the program (i.e., there are no separate "run" and "review" modes).

Only the menus, functions, et cetera which are specific to the program will be discussed in detail. A general knowledge of computer use and of the Windows family of operating systems is assumed.

B.1. TOOLBAR

Figure B.1 shows the layout of the menu bar and toolbar, both of which always reside at the top of the main Neuron program window. All of the features accessible through the toolbar buttons are also accessible through the menu items, but their presence saves time and effort in data acquisition. The first nine buttons on the toolbar from left to right (New, Open, Save, Cut, Copy, Paste, Print, Help, Context-Help) are standard Windows fare; only the Open button, which opens a saved run, ever approaches usefulness. We shall begin, therefore, with the tenth button and move onward from there.

The tenth button from the left is the Zoom In button, which zooms in by a factor of two when clicked on once. It companion button, the Zoom Out button, does the opposite. Sometimes it is very useful to zoom in by a factor of two or four in order to visualize details on the scale of a micron or less.

Figure B.1 The Neuron Program Menu Bar and Toolbar. Each feature unique to the Neuron program is detailed in the following tutorial.

The Select Region button (blue square) allows you to click and drag the mouse over a portion of the viewing area and thereby select a sub-region of the acquired image. An image must be displayed in order for this button to work. The Select Region function is necessary in order properly to optimize contrast, when taking images, and to save a region of interest in successive images to disk, when analyzing data. To do each of these things, select the region first using this tool and then select the action you wish to perform on the selected region immediately thereafter. Single-left-clicking anywhere on the image clears any selection that has been made.

The Acquisition Parameters button (camera) calls up the similarly-named dialog box. The Guiding Parameters button (truck) does the same, correspondingly. These dialog boxes are described in detail in Section 3.3 below.

B.2. FILE MENU

The File Menu is mostly standard Windows fare: the New option creates a new run, the Open option opens a saved run, and so on. There are, however, a couple of notable exceptions especially made for our purposes.

B.2.1 Save As BMP... Menu Choice and Picture Export Parameters Dialog Box

You should only have to use the file menu for its "Save as BMP..." function. Choosing this option will cause the dialog box in Figure B.2 to pop up, and its options are as follows. The region, if you have already defined one with the "Select Region" function, will have its values in the first four text boxes here. If a region has not been previously selected, there will be zeros in these boxes and they will have to be changed manually (unless you are saving the entire image area, which is quite space-consuming). The Do Everything option sets the range of pictures to be saved to the entire set of images in the current run. There is also a Make AVI Movie option, which works only inconsistently as of the time of this writing.

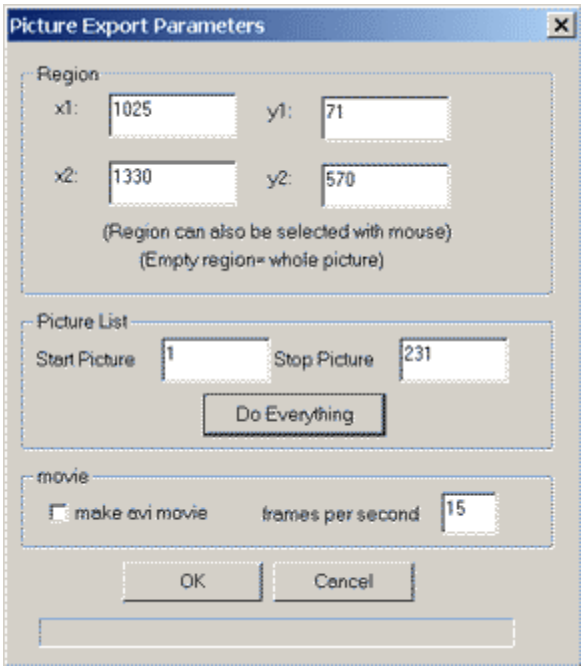

Figure B.2 Picture Export Parameters Dialog Box. This is best implemented when a region of interest has already been selected, as the coordinates of the region are automatically entered into the appropriate text boxes.

B.2.2 Save Laser Path

This selection actually saves much more than just the laser path, but all of the relevant poperties for each image in a run. They are saved in a spreadsheet format and can be accessed through a program like Microsoft Excel. Each data point has its own row, in which the (x,y) positions (in microns) of each laser spot and each spline point are displayed. There are also listings of a data point's time stamp, a binary record of whether the laser was turned on, and calculated numerical values for growth cone advancement as discussed in Section 9.3. There is only a standard dialog box for specifying the location of the file before it is written, and no other options are available.

B.3. CONFIGURATION MENU

B.3.1 General Properties

This menu item brings up a dialog box through which you may set values for global parameters that affect each run. It is not recommended that you change any of these settings during the acquisition of a run.

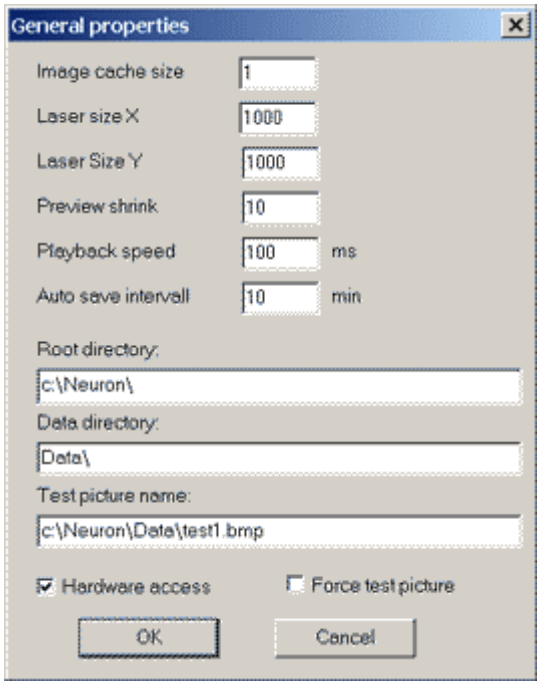

Figure B.3 General Properties Dialog Box. These global parameters are read into the program at startup and are recorded in the Params.dat file.

B.3.1.1 Image Cache Size

This is the number of acquired data points (including all images taken and rendered) that the program will keep in memory (RAM). If the number of data points

viewed in succession exceeds this number, then the program will delete the oldest data point from memory before adding the newest data point. This number, therefore, should not exceed the number of megabytes of available RAM divided by the typical number of megabytes per data point, or the program will have to start accessing a pagefile from the hard disk and it will be much slower going through data points. The amount of available RAM can be found, in the Windows 2000 Operating System, by running the system program "Task Manager." During acquisition, the image cache size parameter becomes less relevant.

B.3.1.2 Laser Size X, Laser Size Y

These are the dimensions of the laser spot in nanometers. For our purposes, the laser spot is about a micron in diameter.

B.3.1.3 Preview Shrink

The Preview Image is a relic of previous program versions and is no longer used. This value specified here was the factor by which the cell image was shrunk in order to make the preview image. The preview image was made by "binning" the pixels of the cell image and converting to 8 bit, with no smoothing or anti-aliasing algorithms, and thus these images were small, grainy, and difficult to read.

B.3.1.4 Root Directory

This parameter tells the program where the Neuron program is located in the hard disk's main directory structure. It is the point from which it begins to search for auxiliary

files that it needs to access, and if this parameter is incorrect, the program will not load properly.

B.3.1.5 Data Directory

This is the location of the Data folder on the hard disk, which tells the computer where to begin writing data during acquisition. If this parameter is incorrect, your data will be saved in some indecipherable place or not at all.

B.3.1.6 Test Picture Name

This is the directory path leading to the image you'd like the program to display upon acquisition if you've checked the "Force Test Picture" box (§ 3.1.8, just below).

B.3.1.7 Hardware Access

Having this box checked is necessary for data acquisition. If it is not checked and you try to acquire data, you will notice that the test picture pops up when you start acquiring data. The function of this checkbox is one of convenience for people (like programmers) running the program from remote computers not connected to the requisite hardware: if you try to run the program on a machine not hooked up to the experiment, you get a slew of hardware errors and the program won't let you proceed. Having this checkbox unchecked helps in this situation.

Additionally, if you start the Neuron program running while there is already an instantiation of it running, then the program will automatically turn this option off (checkbox unchecked) so that there are not two programs trying to access the hardware at

the same time, leading to multiple interrupt requests to the same hardware device crashing into each other.

If this checkbox is unchecked and you wish it to be checked, you must check the box, close the program (to save the parameter to disk), and restart the program. The program only reads the status of this checkbox when it first opens, and the value cannot be changed without closing and restarting the program. This is a fail-safe put in place in order to avoid the hardware IRQ problem described above.

B.3.1.8 Force Test Picture

Check this box if you wish not to take data, but rather to load the image specified in "Test Picture Name" (§ 3.1.6) into memory instead of acquiring a new image with the hardware. The hardware access box can be checked at the same time this box is checked: if it is, this function ensures that no new data will be taken even though hardware access is technically possible.

The difference between enabling/disabling hardware access through this checkbox and doing it through the "Hardware Access" box (§ 3.1.7) is that when the value of this checkbox is changed, the program does not need to be restarted for the new value to take effect. Instead, it will take effect as soon as you close the dialog box.

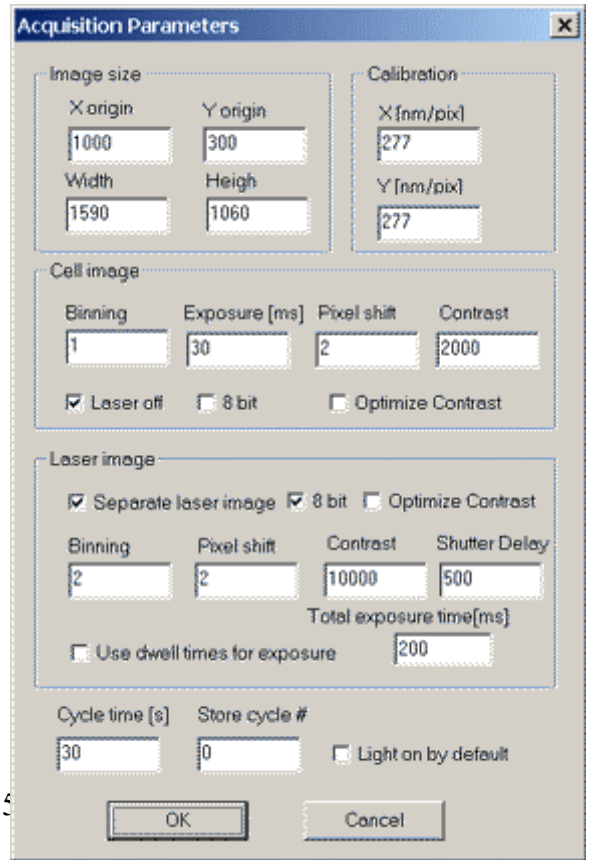

Figure B.4 Acquisition Parameters Dialog Box. It is appropriate to change these parameters while acquiring data to optimize image quality.

B.3.2 Acquisition Parameters

The Acquisition Parameters dialog box is featured in Figure B.4. The parameters here determine how the images will be gathered and what their resultant quality will be. This is one of the dialog boxes most often called upon because many of these values need fine-tuning with every new experiment.

B.3.2.1 Image Size

The four input boxes for image size are in units of pixels and they count X from left to right and Y from top to bottom. They specify which pixels on the CCD camera chip, which is 1024 x 2048 pixels, will have the data read from them and displayed as the images that are acquired. These parameters, therefore, only need to be replaced when the CCD camera moves (or any imaging hardware moves relative to it). The area designated here should be the area which is best in focus on the CCD chip when the imaging hardware is being physically configured. The current values for image size give the largest possible image which will fit on our particular monitor without bringing up X or Y scrollbars, so that the maximum possible area is viewed at a time.

B.3.2.2 Calibration [nm/pix]

Initially, this value is determined experimentally by placing a diffraction grating of known line spacing on the microscope and taking a good average of how many pixels are needed to span this known distance. Then, a value of nanometers per pixel may be specified here, and the program uses this value when it takes pixel distance information from the camera and converts it into micrometer distance information displayed for the user.

B.3.2.3 Cell Image

- Binning: This specifies how large the "bin" is into which data from the CCD camera are grouped in order to make one pixel in the final image. For example, if the Binning is 1, the CCD pixels and the image pixels have a 1:1 correspondence. However, with a binning of 2, the computer adds the signal from each 2 x 2 pixel area on the CCD chip and uses that result as the value for each single pixel in the image it displays. For a binning of 2, the CCD pixels and the image pixels have a 4:1 correspondence, so the resultant image you get will be 4 times smaller than the image you'd get with a binning of 1, and acquisition proceeds along more quickly. For the cell image, it is important not to lose any information collected by the CCD chip, so the binning always should have a value of 1.
- Exposure [ms]: This is the time, in milliseconds, for which the camera shutter (a piece of hardware fully integrated into the camera apparatus) is open to collect light from the sample. When in doubt, set this value lower rather than higher, because too much light saturates the CCD chip's pixels and, over time, may cause damage to them! The length of the exposure time for the cell image should depend upon how much light will be coming through the phase-contrast optics of the microscope to make the image. This value would change if, for example, you were to exchange one microscope light filter for another (refer to Section 2.3.4), allowing a different amount of light (integrated

over all wavelengths to which the camera is sensitive, which ranges from the visible through the NIR) through the microscope optics.

- Pixel Shift: Shifts the grayscale values coming in from the camera to higher values in order that the image be lighter for display and data saving. A reasonable range of values for this parameter is anywhere from 0 (no lightness augmentation) to 3.
- Contrast: This is the factor by which the incoming pixel grayscale values are "spread out" across the spectrum of possible values. This works just like the contrast in an image editing program: use higher values if your growth cone of interest has broad lamellipodia which do not distinguish themselves readily from the background, and use lower values if your image appears to contain little besides black and white pixels. Typical values for this parameter are 500-5000, depending a great deal on imaging conditions and cell characteristics.
- Laser Off: If you are acquiring two separate images for cell and laser, you want this box checked. If it is left unchecked, you will get a laser spot image acquired at the same time as the cell image. This is usually unfavorable mainly because the exposure times needed for the cell image and laser image are very different in most cases.
- 8 Bit: The CCD camera delivers 14 bit images, not 16 bit images, so they cannot be saved as bitmap (BMP) files, but rather must be saved in the Targa (TGA) file format, which is nearly obsolete and difficult to use with other programs. If this box is checked, the 14 bit images will be scaled down to 8 bit images which, although it results in loss of

data, would allow you to save the acquired images in bitmap format. This value is typically set to unchecked to prevent loss of data.

- Optimize Contrast: This checkbox allows contrast to be optimized. Again, this results in some data loss (though much more minor than that of going from 14 bit TGA to 8 bit BMP format), but is very helpful in improving image clarity.

B.3.2.4 Laser Image

- Separate Laser Image: Check this box if you would like to have a separate laser image acquired with each data point: the typical value is *checked*. Uncheck this box if you prefer to acquire the cell and laser images concurrently (see Section 3.2.3: "Laser Off" checkbox, above), or if you wish not to have any laser image saved at all.
- 8 Bit: The function of this option is the same as in Section 3.2.3 above. For the laser image, however, this box should always be checked because detail in the laser image is not at all important: we only need to record where the laser spot is positioned. Of course, if there is a time in which investigating and recording the exact laser profile is important, then this box should be left unchecked. Checking this box saves lots of space on the hard disk.
- Optimize Contrast: This has the same function as described in Section 3.2.3 above, and for our purposes should always be checked in order to maximize the laser spot's standing out against the background.
- Binning: This has the same function, again, as in Section 3.2.3. However, for the laser image, setting the binning to 2 is preferable, for

the same reasons as given in the discussion of 8 bit conversion above. Having a binning value of 2 for the laser image also results in faster acquisition of this image and, since the values of 4 pixels are summed to produce every single image pixel, results in brighter images and/or shorter required exposure times.

- Pixel Shift: Exactly the same as described above in Section 3.2.3. The typical value for this parameter is 3.
- Contrast: This is the laer image parameter which most often requires adjustment. Depending on how many laser spots there are in the laser image and for what amount of time they are imaged, this value usually ranges anywhere from 300-3000.

B.3.2.5 Additional Parameters

- Cycle Time [s]: This sets the interval of time between the acquisition of data points, so that the pictures are spaced as close as possible to this many seconds apart. If, for some reason, the program cannot acquire data at the specified time (for example, when an open and/or unconfirmed dialog or alert box prevents the program from proceeding), then it will acquire a new data point as soon as possible after the specified time and then acquire the *next* data point an exact multiple of intervals from the last data point that was acquired on time. *For example:* Say the interval specified for this parameter is 30 seconds: Program takes Picture #51 - User opens a dialog box and doesn't close it properly - The time for Picture #52 comes and goes

because the computer can't acquire a data point - The user then gets with it and closes the dialog box a few seconds after Picture #52 was supposed to be taken - The program now acquires Picture #52 a little bit late - The program then acquires Picture #53 exactly 60 seconds after it took Picture #51. Result: Picture #53 is on time with respect to Picture #51, and Picture #52 is the only one out of place. The reason this plan was implemented is that you often want to make movies of the image sequences acquired by the program, and you want to have the most consistently-spaced set of images possible so that your movie doesn't lose its scale to real time.

- Store Cycle #: If set to a number *n* other than zero, this parameter will have the program save only every n^{th} data point it acquires. To date, this function has not been used.

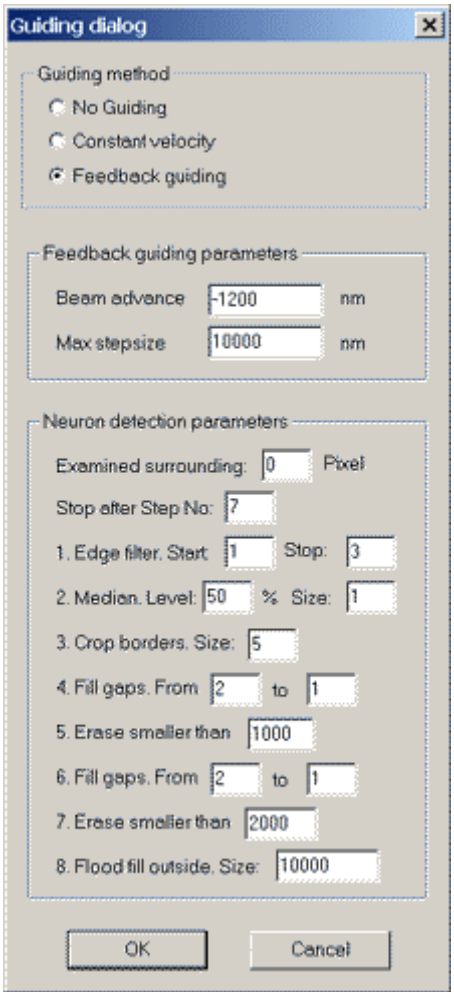

Figure B.5 Guidance Dialog Box. Herein lie the settings which make edge detection possible (and often highly accurate).

B.3.3 Guiding

The use of this dialog box is perhaps not as

straightforward as that of the ones earlier referenced because these parameters affect the inner workings of the edge detection process. The delicacy of tuning these values comes from the heavy dependence of the edge detection's results on the initial histogram of grayscale values in the region selected for running this algorithm. Figure B.5 shows the plethora of options available.

The end result of the edge detection process is a one-bit image (black/white pixels only), where black pixels indicate the region detected to be within the cell and white regions are detected to be outside of the cell. It should end up with as many black structures on a white background as there are growth cones in the selected area, and the black shapes should closely approximate the shape(s) of the growth cone(s). This can be done with excellent accuracy with the available parameters, in part because there are so darn many of them.

B.3.3.1 Guiding Method

The option for no guidance just turns off the automatic placement of the laser spot: the edge detection algorithm will still function and give detection images, but any displacement of the laser spot must be done by hand. This setting, therefore, is for manual guidance.

When first this program was implemented, we sought to have both a simple and a complex manner in which optical guidance could be achieved. The simple way was to set the laser spot going in a given direction at a given rate of speed, but this method had the drawback, of course, that it could not take into account the position of the leading edge of the cell. This feature has since been disabled, but its menu option remains.

Feedback Guiding refers to the combination of edge detection and adjustment of the laser spot's position during every iteration of acquiring a data point. When this choice is active, the Feedback Guiding Parameters below come into play.

B.3.3.2 Feedback Guiding Parameters

Beam Advance is a very handy parameter to have around, as it often needs to be adjusted based on the morphology of the growth cone being guided. The value here, in nanometers, signifies an advancement (or negative advancement) in microns of the laser spot along the contour of the spline. The reason that different laser spot advancement values are helpful is that the edge detection algorithm produces slightly different results when acting upon phase-dark objects (like filopodia) than on phase-lighter objects (like broad lamellipodia). It is more often the case that the value is negative, signifying laser placement further into the cell, than positive, signifying laser placement toward the outside of the cell.

Max Stepsize is the maximum distance, in nanometers, allowed between successive adjustments of the laser spot position. If, for example, there were a temporary problem with imaging such that the detected edge was shifted far away from the cell, the laser would be kept from jumping off the cell if the distance were too great from its original position. If this were the case and the distance the laser spot would have to move (either forward or backward) to catch up with the detected edge were greater than the value specified here, the laser spot would simply not move at all for that time period. This, of course, would be the best outcome for the case of imaging disruption for a limited interval.

B.3.3.2 Neuron Detection Parameters

- Examined Surrounding *N* Pixels: When *N* is set to a value other than zero, the program will automatically select the region of interest for you. That is to say, instead of your having to select an area in which edge detection will take place, the program determines this area by forming a rectangle with the laser spot at the center and with sides of length 2*N*. When this option is set to zero, the function is turned off and the region for edge detection is selected by the user. This is the preferred setting because the ideal edge detection area is very rarely, if ever, symmetrical about the position of the laser spot. Additionally, having this feature active means that the edge detection area would change as the laser spot moved in its guidance of the growth cone, inviting both imaging and edge detection problems through constantly shifting the histogram of grayscale values for the selected area.
- Stop After Step Number: The step (numbered 1 through 8 in the list below) in the algorithm after which the program will stop calculating and display what it has obtained.
- (1) Edge Filter: Start, Stop: The program uses a standard edge detection method explained in Part II, Section 4.3.1 above. If the start and stop values are the same, the program uses that value for the size of the matrix it uses in its calculations. If the numbers in these boxes are different, though, the program will do a calculation for each one and then average the results for each pixel.
- (2) Median Level and Size: The median level is the parameter by which the program determines whether each pixel constitutes part of an edge.

Higher values will exclude more pixels, whereas lower values will be able to pick up weaker signals from the camera. Very often, the median level is above 90. The size parameter was originally present to prevent single-pixel failures in detection due to camera malfunction, and it works by binning together a number of pixels (in an *s* x *s* matrix, where *s* is the value) and taking their average grayscale value as the value of each of the pixels in the matrix. It has not been necessary to manipulate the size parameter in order to obtain clear images, so it can be left at 1.

- (3) Crop Borders Size: From the outer border of the region selected for edge detection, this number of pixels will be counted inward toward the center and then all pixels between these and the outer border will be counted as "in" the cell. Since the growth cone usually comes in from one side of the selected area, the detected cell will intersect with this thick band and not be left "floating" in the middle of the image or be eliminated in steps (4) or (6). A typical value for this parameter is 5.
- (4) Fill Gaps From *N* to *N'*: The program takes the higher of these two values first (or the single value, if they are the same) and uses it for the following procedure. For each black pixel, for each of four axes (up/down, left/right, and the two diagonal axes) the program counts N pixels outward along the axis in both directions such that two pixels are selected on either side of the central pixel. If both of these side pixels are white, then the central pixel is changed from black to white. If *N* and *N'* are not equal, the program then carries out the same the same procedure with *(N-1)*, *(N-2)*, etc. until it arrives at the smaller of the two values for its last iteration. Note that this is indeed done iteratively – not as an average

as in step (1) – and that the resultant image from iteration *i* is the one to which iteration *(i+1)* is then applied. This procedure helps to eliminate stray black pixels which are not part of the cell.

- (5) Erase Smaller Than: For every contiguous island of black pixels that remains, if the number of pixels belonging to that island is less than *N*, the entire island is erased (changed from black to white). This eliminates detection of cell debris and exocytosed particles.
- (6) Fill Gaps From *P* to *P'*: This is the same procedure as step (4) done once again, but is not identical to step (4) because different values may be selected here.
- (7) Erase Smaller Than: This is the same procedure used in step (5), but again a different value may be used (usually a larger value).
- (8) Flood Fill Outside Size: The value here determines in what size chunks the program goes through and flood fills the outside of the detected cell with white pixels.

B.3.4 Reference Image

While acquiring data, it is possible to superpose detection image number *N* (first value) with the current display in an attempt to get a direct comparison of the growth cone positions and estimate whether the cell is growing in the intended direction. Additionally, you can have the program superpose an image *M* iterations ago (second value) with the current image to preserve

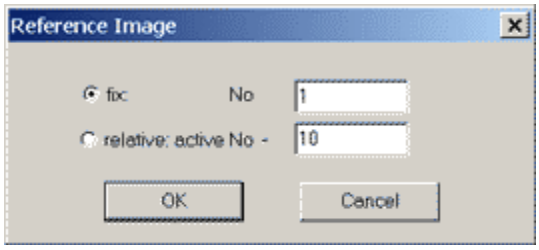

Figure B.6 Reference Image Dialog Box. Choose which detection images to superpose with the one currently being acquired.

the time interval between the two images being compared. In the superposition, the white areas of the earlier image are made to look green to set them off from the current images. It turns out that, with the superposition of cell, laser, detection, spline, and reference images, it is very difficult to see what is intended by this feature. Also, a static image-to-image comparison is not as valuable an analysis tool as is a look at a sequence of the past several images in rapid succession. This can be achieved by invoking the "Save As BMP..." command (see Section 2.1 of this Appendix) for the relevant area and viewing the bitmaps in rapid succession with a freeware picture viewer.

B.3.5 Data Extraction Parameters

These parameters are no longer in use, as there were devised more consistent methods of analyzing the data than those here, which rely on a lack of fluctuations in the cell and detection images (not to mention a lack of cell motility and subsequent soma encroachment into the region of interest) for their consistency. Briefly, these parameters come into play when calling the "Save Laser Path" function (see Section 2.2 in this Appendix): the options whose boxes are checked are saved to the spreadsheet in additional columns. Cell Area refers to the total area (in square microns) of growth cone in the detection image through a summation of all the black pixels. The Axon Area refers to the Cell Area found only in the region between the leading edge and the first (innermost) spline point (which usually resides at the base of the axon).

The parameter Grown Distance is always recorded in the spreadsheet but has been replaced by a function which determines cell growth numerically through how far along the spline it has grown (as opposed to measuring endpoint-to-endpoint in a straight line).

B.3.6 Beamstop Template

The default parameters with which new laser spots are defined can be altered with this dialog.

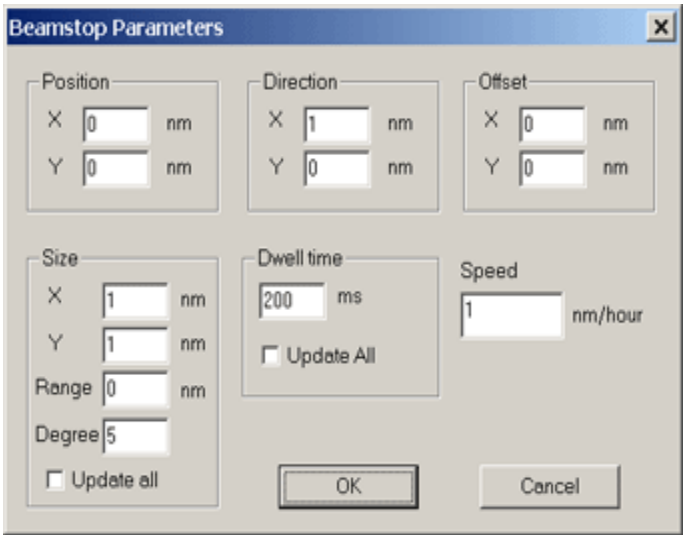

Figure B.7 Beamstop Template. Choose the default values for newly-initiated laser spots here.

- Position: Since the user clicks in the image window to create a laser spot, the values for Position in X and Y are more for a readout of a spot's position than an input space for plugging in values.
- Direction and Speed: These were parameters once used in the Constant Velocity Guiding activities of yore (see Section 3.3.1 in this Appendix), which are no longer performed. In fact, we have gotten rid of the vector which defines this direction for each laser spot, so these fields, which define its direciton and speed (magnitude), are now completely obsolete.
- Offset: Defining these values is the last step in calibrating the actual laser spot position to the intended spot position (refer to Section 4.1 in Part II). They must be altered slightly for laser spot positions in different areas of the image, but their optimal settings for different areas will not change unless the microscope, camera, or laser hardware were moved.

- Size: The galvanometers can be made to wiggle back and forth across a very small angle such that they can easily raster lines (for one galvo) or areas (with both X and Y galvos) in the plane of the cells. Because of the strange and nonliear correspondence of galvo voltage to laser position across various regions of the image in which the laser is placed, however, what is a size of 3 microns in one quadrant may be a size of two microns in the next, so proceed with caution here.
- Range and Degree refer to a polynomial fit to the leading edge of the growth cone, over which the galvos can scan back and forth. At one point, we had an idea to raster a curve at the leading edge with the lasers, and this is what made it possible. Range is the distance in nanometers across which the curve would stretch, and degree is the degree of the polynomial used for the curve fit.
- Dwell Time refers to how long the laser dwells at a certain stopping point before going off to the next one. For cases in which there is only one laser spot, or cases in which the sum of the dwell times of all laser spots is less than the total laser exposure time specified in the Acquisition Parameters dialog, the sum of the dwell times of all laser spots conveys its value to the laser image exposure time. If the Update All checkbox is checked, then when OK is clicked for the dialog box, all laser spots acquire this value for their Dwell Times.

B.3.7 Beam Guiding Parameters

B.3.7.1 Parameters in First Column

- Scan Speed: This is the speed with which the laser should move back and forth along the curve fit to the leading edge of the cell. It is not terribly relevant now.
- Hop Time: In order to give the galvos a rest, set this number to something other than zero, as this parameter determines the interval for laser spot jumps from one beam stop to the next. Ideally for the experiment, though, this is as low as possible. If the galvos are moving but not making crisp clicking sounds when hopping back and forth, come back to this option and ensure that its value is set to zero.
- Sampling Frequency: This is the rate at which the computer makes a conversion of internally-generated digital values to analog values it can send to the galvos. This value, therefore, determines how often the level of signal to the galvos is refreshed, and consequently it defines the time quantum for the experiment. This number can be set as high as 12 MHz.
- Off Voltage DAC0 and Off Voltage DAC2: These are pre-defined voltages which are sent to the galvos so that they point the laser away from the experiment and into a beam trap. These voltages come into play when the laser must be directed away from the sample during the acquisition of the cell image.
- Wobble X Frequency and Wobble Y Frequency: In the Beamstop Template dialog box, where the size of the spot in X and Y is defined, these wobble values define at what frequency the laser rasters its line(s). Sinus Sweep does not have anything to do with the nasal cavity, but rather

is meant to denote a sinusoidal wave, with which one can choose to scan in this case instead of going linear (which makes intensity build up at the ends but taper off toward the center of the scanned length).

B.3.7.2 Anti-Hysteresis

All of these parameters were useful only back in one of the first incarnations of this program, at which time the galvanometers we had were open-loop galvos. These open-loop galvos had a hysteresis effect which ruined their precision in laser spot placement: the position of the n^{th} point affected the position of the $(n+1)^{th}$ point, so every time you went to a certain voltage combination in the hopes of getting your laser spot to the same place every time, it would end up in slightly different places based on where it had been before.

The method we used to combat this problem was getting the galvos to "hop" to a fixed set of voltages for a short time in between "hopping" to the designated laser positions. This way, the placement of every laser spot position was preceded by the SAME fixed laser spot position, and the hysteresis effect was thus minimized.

Now that we have closed-loop galvanometers in the system, however, these options have become obsolete because the galvos themselves come with complex controller boards and insane amounts of calibration to ensure a complete lack of hysteresis.

B.4. TOOLS MENU

Here resides the greatest number of data acquisition tools to be found in the program.

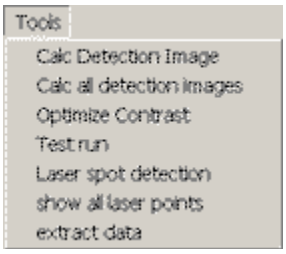

Figure B.8 Tools Menu. Select features for acquisition and analysis.

B.4.1 Calculate Detection Image and Calculate All Detection Images

During acquisition, once you have selected the region in which you would like the program to edge detect, select Calculate Detection Image to start edge detection. If there is a laser focus in the region you have selected, then for subsequent data point acquisitions the edge detection will be run automatically.

When not acquiring data, this function still works perfectly well, and can be used repeatedly during a Test Run (see Section 4.3) to get a feel for exactly how changing different parameters in the Guiding dialog box affects the resultant edge detection image. The Calculate All Detection Images was put in place mainly for times when you are reviewing data for which edge detection images have not yet been created. When this option is selected, the program goes through each cell image in the stack and creates an edge detection image for it.

B.4.2 Optimize Contrast

This is the first function you will want to use when you begin acquiring data in a new run, as at this point in time, no scheme of contrast optimization will yet have been defined for the incoming cell images and it is likely that cell features will be difficult to see. There are two ways to invoke this feature: using the whole cell image acquired,

which requires only calling the function, or basing the determination of contrast optimization parameters on only a subset of the pixels available. This latter method is recommended both because of the better results it can produce and because of the time saved in the program's not having to take into account the grayscale values of each pixel in the image. Regardless of whether the whole image or a part of it is employed in the determination of the constrast optimization parameters, the optimization scheme is always subsequently applied to all of the pixels in the image.

For best results, before invoking this feature, select a region of interest with the Select Region function (see Section B.1); there are some strategies of note for this preliminary step. If there is any floating cell debris, other objects, or areas of the image whose pixels are mainly very bright or mainly very dark, exclude these objects and areas from your region of interest. It is in your best interest to select an area around the growth cone you would like to view, perhaps including the growth cone, axon, and cell body. If the span of the histogram of the pixels you select is too narrow, however, too large a multiple will be given to the grayscale values and you may lose a great amount of detail in the images. On occasion, the entire field of view (with default values, approximately 300 x 440 microns) will present an appropriate region for contrast optimization, and only experimentation with optimizing contrast based on different image regions will give you a "feel" for the optimal area to choose. After having chosen your area, run the contrast optimization algorithm.

If you have selected a region from which to determine the parameters, for subsequent images acquired, the program will continue to use the pixel grayscale values coming from this region of the CCD chip for determination of the right contrast for every incoming image. This means that if the grayscale histogram of the selected region

changes drastically, as happens on occasion when a piece of debris floats by, the contrast optimization parameters will change drastically as well.

It is possible to invoke more than one contrast optimization for the same image, but if this is done, the histogram for the optimized image, not the original image, will be used for the determination of the new optimization parameters, and the results may not appear very different from what you had before. In this case, acquiring another image from the camera loads another original image into memory, from which the new optimization scheme can derive its histogram values and produce the desired image.

B.4.3 Test Run

This is one of the newer features implemented in the program, and its main purpose is to test the program's funtionality on a computer which is not attached to the experiment's hardware. This can be done with the Force Test Picture feature (see Seciton B.3.1.8), but this feature is limited to loading one particular image repeatedly and cannot aid in the development of new features which directly involve the analysis of newly-acquired images. With the Test Run feature, you can open any existing run and go through the motions of acquiring successive images which, instead of being read from the experimental setup, are read from the image files already present on disk. This also allows you to "re-enact" a run if you wish.

WARNING: when using this feature, be absolutely sure that the Record button on the toolbar is OFF to avoid the danger of overwriting your existing files (see Section B.9.3 on known bugs).

B.4.4 Laser Spot Detection

As of the time of this writing, the Laser Spot Detection algorithm is not yet complete. It is planned that this feature will involve analysis of the laser image to pinpoint the location of the laser spot(s) on the field of view and then using this information to update the laser position Offset values (see Section B.3.6) without user intervention.

B.4.5 Show All Laser Points

Selecting this option displays the positions of the laser foci in all data points with the corresponding data point number shown above the point in a small font. This option allows you to visualize trends in the laser's progress (and thus, in the case of automated guiding, the cell's progress) for all data points at once. It is especially useful for reviewing data that were acquired in the era before automated guiding was implemented.

B.4.6 Extract Data

A few options for data extraction via the Save Laser Path function (see Section B.2.2) can be set here. As of this writing, calculation of the data values shown here is no longer useful because other methods have since been employed for the purposes of analysis.

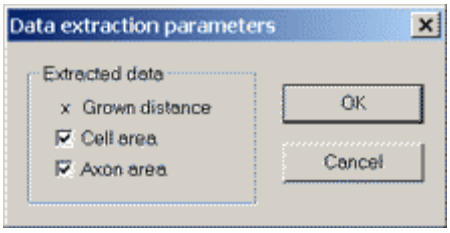

Figure B.9 Data Extraction Parameters Dialog Box. Choose which items are to be saved to spreadsheet format with the Save Laser Path function.

B.5. VIEW MENU

Select with this menu those images which you would like superposed for display on the monitor. Choosing options here will not affect any data saved to disk, but will affect only what is presented to you. Each of the options here, when selected, toggles the display of that option's referent on or off. There are buttons on the toolbar for the cell, laser, detection, and spline images because during acquisition it is necessary to toggle these images on and off fairly frequently. This menu only appears when a data set is open, during either acquisition or review.

Figure B.10 View Menu. Toggle on/off that which you want displayed.

B.6. RIGHT-CLICK MENU

This is the menu which appears when you right-click on the main image window. Although it will appear both during acquisition and data review, it is only to be used during data collection. Using these features (with the exception of the Zoom functions) during data review may have the undesirable effect of overwriting data and can lead to data loss.

Figure B.11 Right-Click Menu. Includes features essential to data collection.

B.6.1 Zoom In and Zoom Out

These are the same features available in the menu bar items and the toolbar buttons.

B.6.2 New Laser Focus and Delete Laser Focus

Selecting New Laser Focus and then left-clicking anywhere on the Main Image Window places a new laser focus (also called "beam stop," as in a stop on a journey) at that location. Note that the term "laser focus," which refers to the location the user has specified for the laser, is different from the term "laser spot," which refers to the actual place at which the laser shows up as it passes through the sample.

There must be at least one laser focus specified in order for the laser to be directed through the sample when the Laser On toolbar button is active. A large number of concurrent laser foci are possible, but it is recommended not to exceed five with the laser hopping among them. Having five laser spots concurrently is very useful for calibrating the laser spot to the laser focus (see Section 9.1.2).

To delete a laser focus, first select the Delete Laser Focus function and then the next laser focus you click on (or near) in the Main Image Window will be eliminated. Note that this is to take place "backwards" with respect to usual Windows functions, whereby an object is first selected and then the operation to be performed on the object is chosen thereafter.

B.6.3 Add Spline and Delete Spline

After the Add Spline function is selected, you are to click on the Main Image Window near an existing laser focus (if there are no laser foci, this function will not work). A spline curve (here, a straight line) between two points – one at the existing laser focus and one at the point that was just clicked on – will appear. Then, the laser focus can be "slid" back and forth along the curve, and the spline points, designated by green crosshairs, can be moved independently of each other.

The point called the first spline point is the one which originally appears at the position of the laser focus. It is graphically different from the other spline points in that its crosshairs have red tips. One counts the spline points starting from this first point – which is usually placed inside the neurite or even the cell body – out to the last spline point, which will lie outside the neurite in the direction of proposed growth.

Several spline points should be added right away so that there are enough to get the spline curve to conform to the shape of the neurite you wish to guide.

The penultimate spline point will usually lie within the growth cone, toward the edge at which the laser spot is aimed, and this is the case because that position is the point at which the spline must start to change direction from the neurite's present orientation to its proposed orientation.

The position of spline points can be altered at any time; however, once this is done, since human intervention has influenced the proposed direction of growth, the "clock is reset" for timing how long automated guidance has taken place at a stretch.

Deleting spline points works just the same way as deleting laser foci, and this function is not often needed.

B.6.4 Select Region

This is the same function described in Section B.1.

B.6.5 Add Comment

Beware of this function, and note that it is always preferable to write comments directly in the experiment lab notebook when acquiring data instead of adding a comment here. Calling this function brings up a Comment Window, in which you may type as

much text as you desire. The reason for caution, however, is that when the Comment Window is open, the program will wait for the window to close before acquiring any more data, so data acquisition is halted until your comment is finished. Since there is very often only a short time interval between the end of one data point acquisition and the start of the next, it is generally not a good idea to use this feature.

B.6.6 Elements Visible...

This option brings up a dialog box which duplicates the function both of the View menu item and the four toggle buttons on the toolbar for display and removal of data point components.

B.6.7 Measure Distance

Choose this function, click on two successive points in the Main Image Window, and the distance between those two points will be calculated.

B.6.8 Anchor Spline Point

This is a new feature whose functionality has not yet been fully tested, but I shall describe its intended purpose.

In the program's original incarnation, all spline points remained fixed in place (until moved about by the user) with the exception of the first spline point, which would move itself every time the edge detection algorithm was called. The program took the vector made by the line segment just exiting the first point, calculated a perpendicular line, and centered the first spline point along that perpendicular with respect to the detected cell boundaries at that position. This feature always had the disadvantage that, if

the edge detection image somehow got disrupted due to changing image conditions, the first spline point would run amok and assume positions which were not helpful to our analysis.

Next, the program was changed so that every spline point *except for* the first spline point was mobile and was repositioned every time edge detection was called. This way, both the first and last spline points would remain fixed (for a spline point does not change position relative to the detected cell edge if it was not within the cell to begin with), and the remaining points would adapt to the changing shaps and angle of the neurite. Since this scheme seemed to work well for some spline points (such as the penultimate spline point) and not so well for the rest, the third incarnation of spline repositioning was born. At this time, all of the spline points can have automatic repositioning enabled or disabled independently of the others, and the consistency of proper functionality is still being tested.

B.7. ADDITIONAL WINDOWS AND DIALOGS

B.7.1 Control Window

This window had to be made a dialog box so that it would stay on top of the Main Image Window (Section B.4.2), but it is actually the central control window for an open run. There is no title in the window's title bar saying "Control Window," so I have named it by its function while its actual title bar contains something more useful: the

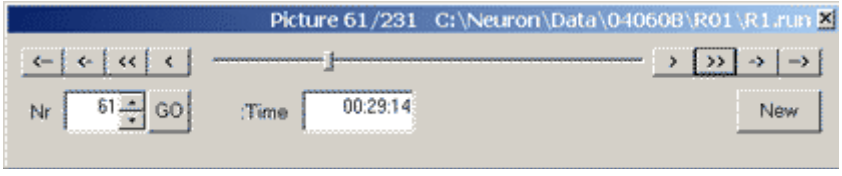

Figure B.12 Main Control Window. Functions both as an input panel and a display, depending on your purposes. Control which data point's images are displayed or show many successively.

directory path in which the run is being stored (or from which it is being recalled).

The most salient thing about this window is its scrollbar, with which you can click and drag the positioner to change the picture number that's being displayed. You can move around in the picture set by clicking on the buttons to the immediate left and right of the scrollbar. This comes in very handy when you're in analysis mode. A summary of the buttons is:

- **<--** Automatically advance backward every 10th picture, e.g., 121, 111, 101, etc. at a speed determined in the General Properties dialog box.
- **<-** Automatically advance backward picture by picture, e.g., 121, 120, 119, etc. at a speed determined in the General properties dialog box.
- **<<** Advance backward by 10 pictures, e.g., if you start at 145, go to 135.
- **<** Advance backward by 1 picture and stop.
- **>** Advance forward by 1 picture and stop.
- **>>** Advance forward by 10 pictures, e.g., if you start at 145, go to 155.
- **->** Automatically advance forward picture by picture, e.g., 121, 122, 123, etc. at a speed determined in the General properties dialog box.
- **-->** Automatically advance forward every 10th picture, e.g., 121, 131, 141, etc. at a speed determined in the General properties dialog box.

The "Nr." box displays the number of the current picture (passively), but its contents can also be edited if you want to select a specific image to view (actively). The "Time" box is meant to be a passive element which displays how many hours, minutes,

and seconds you are into the run for the picture which is currently being displayed. If you are acquiring data, this box tells you for how long the current run has been going.

B.7.2 Main Image Window

This is the window in which finally appears the combination of cell, laser, detection, and spline images you have chosen to display (see Section B.5). It is best viewed when maximized so that minimal scrolling (or none) is required to view all areas of the image.

B.7.3 Comment Window

This window lives behind other windows until being either brought to the fore by the user or populated automatically with an error message from the program. The only two error messages which are entered are for a calculated change in laser focus position which is greater than the value specified in the Guiding Dialog Box (see Section B.3.3) or when the hard disk has run out of space.

B.7.4 Information Box

The Information Box (or Info Box) is a dialog box which appears automatically when a run is opened or a new data point is

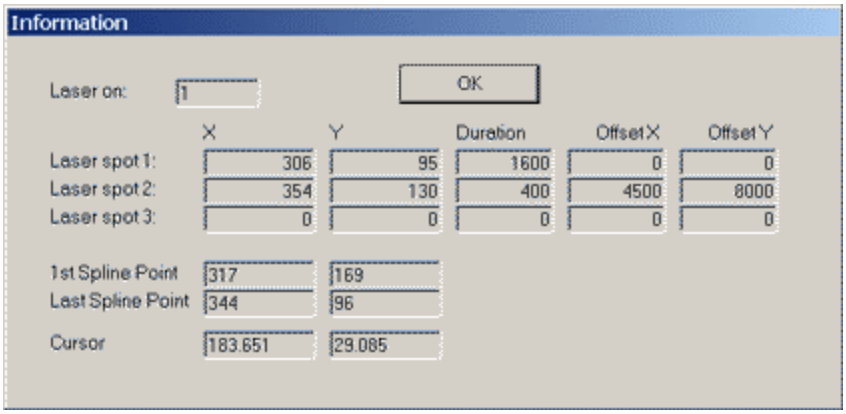

Figure B.13 The Information Box. Most helpful for data review and can largely be ignored during acquisition, this box reminds you of some of the saved parameters which were saved with the data point you are currently viewing.

acquired. It stays on top of the Main Image Window and other windows until "OK" is clicked. This box is most helpful when you are going back over old data sets and are determining where one data segment ends and the next one begins. For example, it obviates having to squint at the monitor to decipher whether the laser has been turned off or whether it is just that the dwell times have changed to such low values that the spots no longer appear as bright as they were. The information contained in this box is some of the same information which is exported to the spreadsheet file with the "Save Laser Path..." command, but the convenience the box provides is the concurrent display of a data point and the parameters which accompany it.

B.8. HELP MENU

This menu option is not currently informative; all of the relevant materials are the ones included here.

B.9. KNOWN BUGS

B.9.1 Lack of Error Message Dialog Boxes

The only two error messages you will see, aside from the occasional complete program crash, are that the hard disk is full and that the intended laser focus displacement was greater than the maximum allowed value. Moreover, these errors do not pop up in dialog boxes to alert you when they happen, but rather they stealthfully appear in the Comment Window, which is usually behind the Main Image Window.

Errors which you must still manually strive actively to prevent include: (a) overwriting existing data sets with ones accidentally altered after the fact and (b) saving the current *.run file to the wrong directory, which opens automatically, and thereby

overwriting the *.run file corresponding to a different data set (which results in loss of data in both data sets).

B.9.2 Inability to Take More than One Data Run at a Time

It is as yet unknown exactly why this is the case, but currently, only one run can be acquired per instantiation of the program. This means that if you wish to take more than one run during a day, when the first run is closed, you must quit and restart the program afresh in order to be able to acquire data again. If you do try to begin another run without closing the program, the entire computer system hangs until the program is halted from the Microsoft "Task Manager" program (which suggests a memory leak of some kind). This will be one of the first program fixes to occur.

B.9.3 Overwriting the "*.run" Files of Older Data Sets

As mentioned briefly above, there exists the danger of overwriting previously-acquired data runs with the currently-acquired one. This is because the program recalls the last directory to which it saved – or in which it opened – a run file, and displays this directory first in the Save As... dialog box which opens when a run is being saved. If you click immediately on "OK" at this point and you are not in the current day's data folder, you will overwrite the run file in the folder displayed and the data for that run will no longer be available for analysis.

Data runs are saved automatically at intervals specified in the General Properties dialog box, and so if you are closing a given run, chances are that you will have to overwrite the existing auto-saved run file. In this instance, you do want to click on "OK" so that the run file with more data is saved over the file which has not saved the last data

points acquired. The dialog box which does appear to confirm an overwrite, however, does not actively alert you when you are in the wrong day's directory.

This can also happen when you are reviewing a data set if the "Record" button on the toolbar is activated, so it is very important to be absolutely sure that this button is OFF before opening a data run for review.

The ideal bug fix for this situation would be for the computer to prohibit ALL overwriting except in those cases in which the current day and run number correspond to those of the file to be overwritten. A special exception would have to be made in the case of a run that extends past midnight on a given day, but extra dialog boxes with warnings about directory name mismatches would help in the management of these files.

B.9.4 Some Data Sets Refuse to Display Every N^{th} Picture

This is another "feature" with which I am endlessly puzzled. For some specific data runs, there is a special problem which could have to do with how a DVD disc was written rather than with any error in the program itself. There is a way around this bug, however, so regardless of its origin I think it appropriate to mention here.

The bug is that, when reviewing data saved to a DVD disc, on occasion there will be data sets for which only a certain number of data point image files will load before the Main Control Window will revert to displaying a data point with number below 10 instead of the next data point in the series. This happens both when loading successive data points and when loading every tenth data point, as described in Section B.7.1.

This bug may have to do with the RAM in the computer, as it has only happened with one computer and it appears that, regardless of which way you load the images, at the point at which it has to load the N^{th} image, it will revert mysteriously back to the early data point, where N may vary from about 7 to 13.

Appendix C. Experiment Dish Schematic Diagrams

The material for these parts is solid lexan, and no diagrams are to scale.

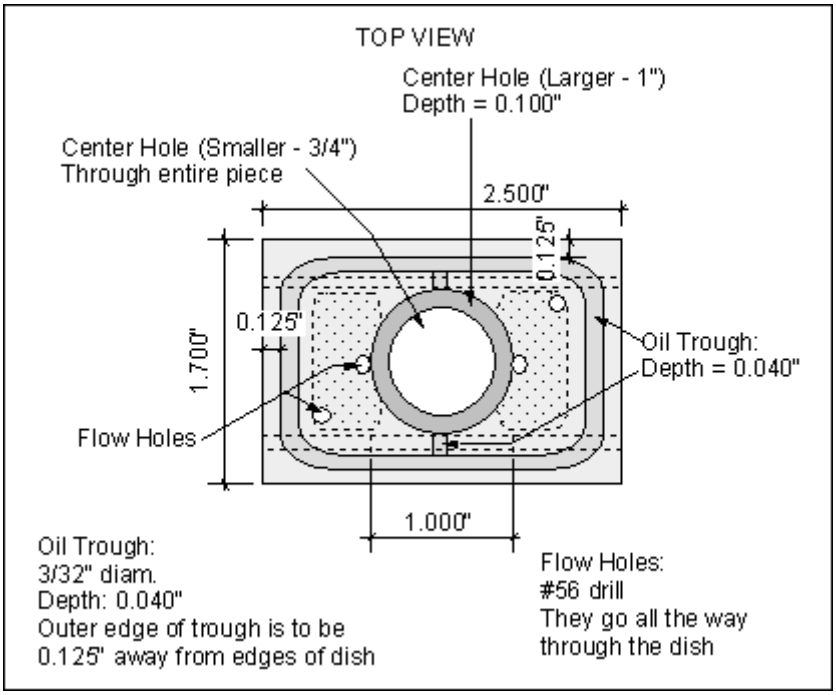

Figure C.1 Experimental Cell Dish, as Viewed from Above

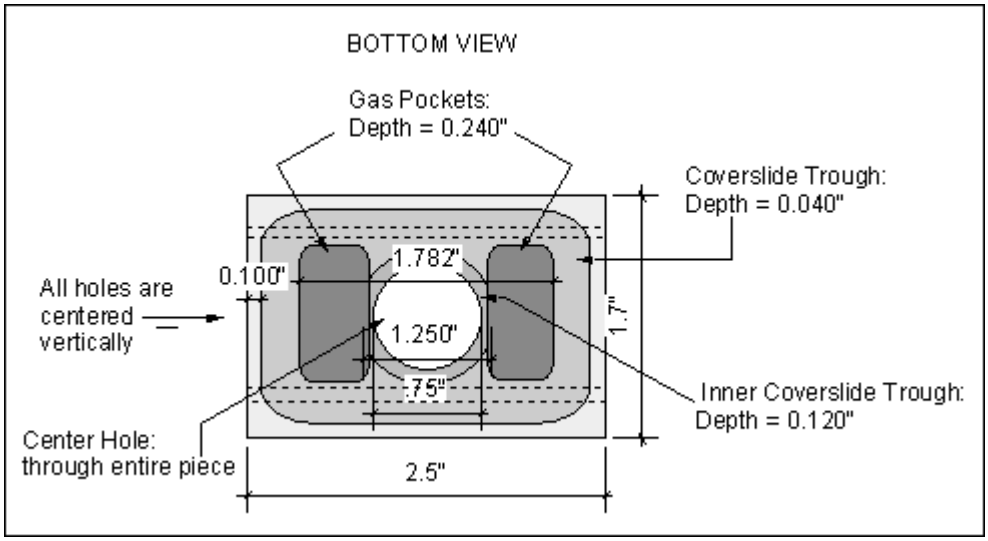

Figure C.2 Experimental Cell Dish, as Viewed from Below

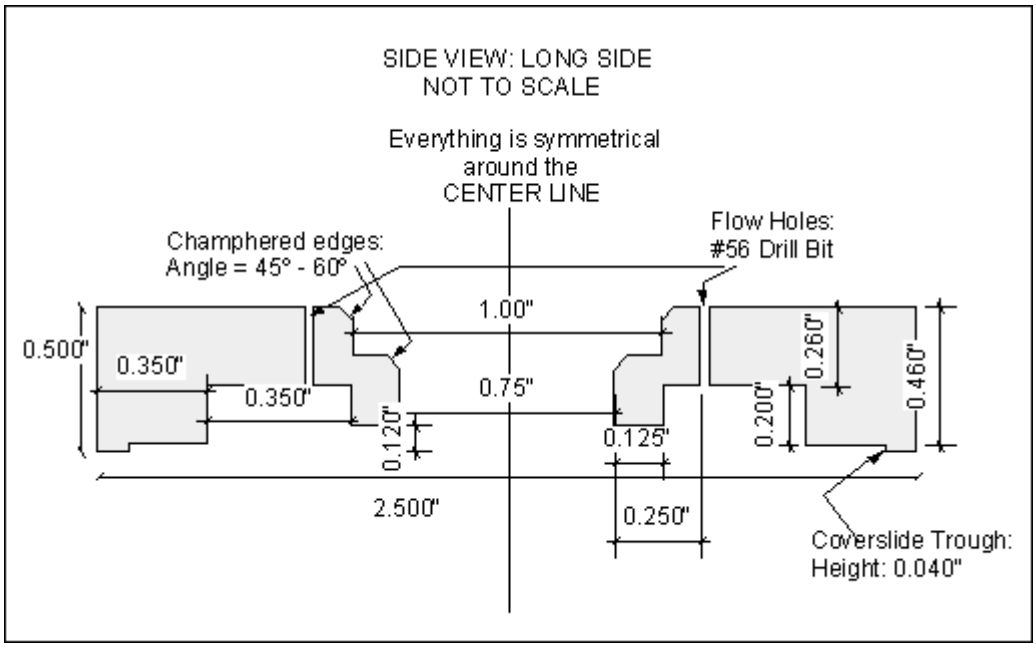

Figure C.3 Experimental Cell Dish, as Viewed from Side, Lengthwise

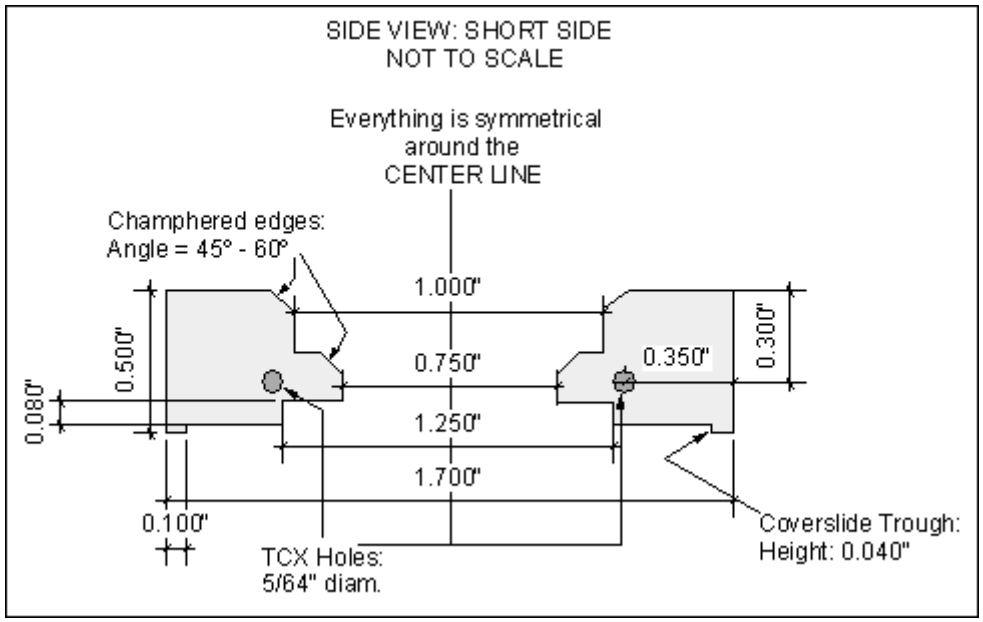

Figure C.4 Experimental Cell Dish, as Viewed from Side, Widthwise

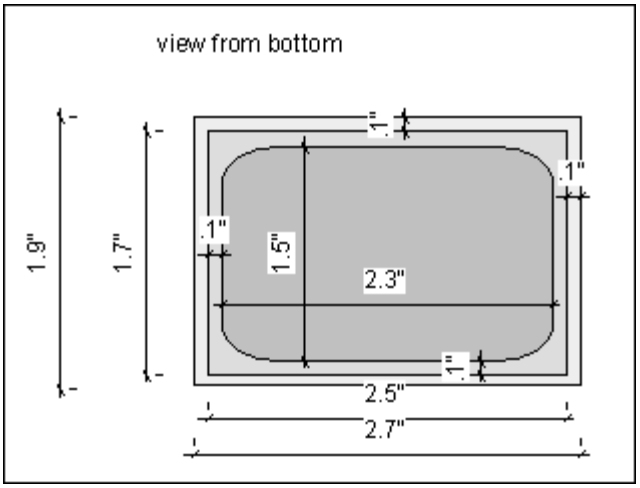

Figure C.5 Experimental Cell Dish Lid, as Viewed from Below

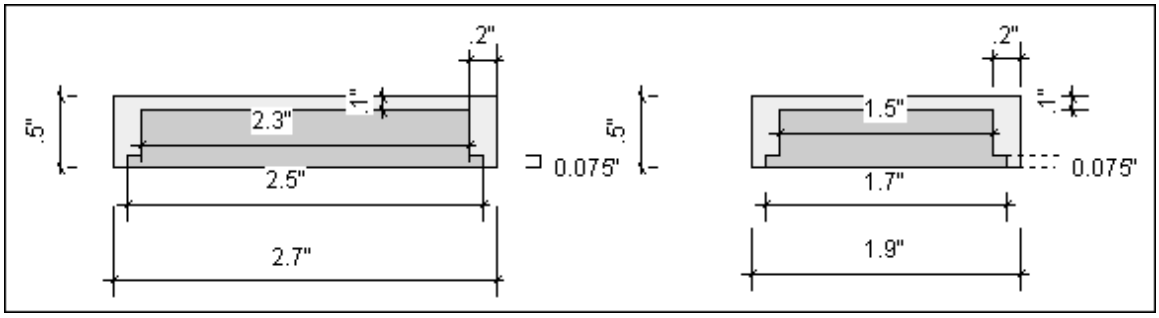

Figure C.6 Experimental Cell Dish Lid, Two Side Views

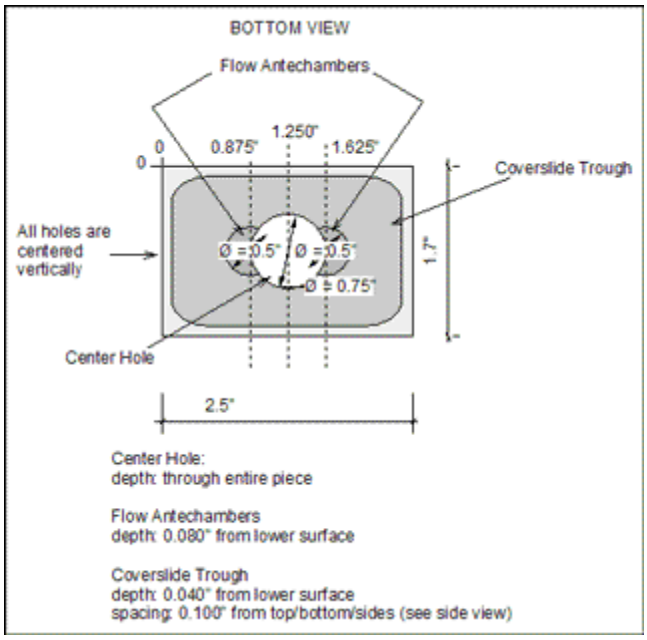

Figure C.7 Preliminary Dish Design, No Longer in Use.

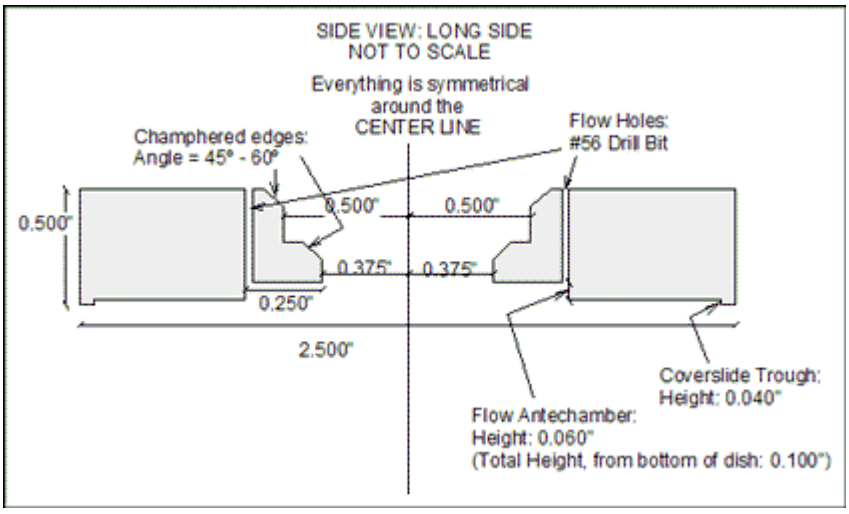

Figure C.8 Prelinimary Dish Design, No Longer in Use.

Appendix D. Buffer and Medium Formulations

D.1. NG-108 GROWTH MEDIUM

Rather a standard medium formulation in cell culture, of which there are multiple versions (with different types of base medium or serum, for example). Base media include Dulbecco's Modification of Eagle's Medium (DMEM) and Ham's F-12 Medium, both of which are available from Mediatech (Herndon, VA) and ATCC (Manassas, VA). Our in-house formulation is as follows, to make **500 ml** of medium:

- **440 ml** base medium (we use DMEM; in past we have used Ham's F-12 medium and 1:1 ratio mixture of DMEM:Ham's F-12 medium)
- **50 ml** Fetal Bovine Serum (FBS)
- **10 ml** of 5,000 IU Penicillin-Streptomycin Solution

These ingredients are combined and then sterile-filtered into an autoclaved glass jar with a bottle-top filter. The medium is aliquotted into 50 ml centrifuge tubes as needed, usually a few centrifuge tubes at a time.

D.2. NG-108 STARVATION MEDIUM

Starvation medium is exactly the same as Growth Medium except in that it contains 1% serum instead of 10% serum. Since this medium is used primarily for cell dishes used in the experiment and not for maintenance of the stock culture, it is typically made 50 ml at a time and then aliquotted into 10 ml portions.

D.3. NG-108 DIFFERENTIATION MEDIUM

Exactly the same as starvation medium, except for the addition of 1 mM N-dibutyryl cyclic AMP. Cyclic AMP is a chemical cue for the differentiation of NG-108 cells, and this medium is placed in cell dishes for that purpose.

D.4. RINGER SOLUTION

125.0 mM NaCl

3.0 mM KCl

10.0 mM CaCl2

5.0 mM Tris

pH = 7.4

(from Spitzer & Lamborghini, 1976)

D.5. MODIFIED AMPHIBIAN RINGER SOLUTION

100 mM NaCl

1.8 mM KCl

2.0 mM CaCl2

1.0 mM MgCl2

either 5.0 mM HEPES-NaOH or 300 mg/liter $NaHCO_3$

pH = 7.6

(From Sive, 2000)

D.6. CMF (CALCIUM- AND MAGNESIUM-FREE) DISSOCIATION BUFFER # 1

115 mM NaCl

2.6 mM KCl

10 mM HEPES

0.4 mM EDTA

pH = 7.6

(From Tabti *et al.*, 1991)

D.7. CMF (CALCIUM- AND MAGNESIUM-FREE) DISSOCIATION BUFFER # 2

88 mM NaCl

1.0 mM KCl

2.4 mM $NaHCO_3$

7.5 mM Tris buffer

pH = 7.6

(From Sive, 2000)

D.8. PRIMARY NEONATAL RAT NEURON CULTURE MEDIUM

Per 50 ml tube:

Neurobasal-A Medium (Gibco)	48.5 ml
B-27 Supplement (50x) (Gibco)	1.0 ml
L-glutamine 200 mM	0.5 ml
Pen/strep 5,000U/ml	1.0 ml

(Formulation generously shared by the Morrisset Lab at the University of Texas at Austin.)

D.9. PRIMARY NEONATAL RAT DISSOCIATION / TRITURATION BUFFER

N-Methyl-D-Glucamine	130 mM
NaCl	10.0 mM
HEPES	10.0 mM
Dextrose	10.0 mM
MgSO4	1.0 mM

(Formulation generously shared by the Morrisset Lab at the University of Texas at Austin.)

Abbreviations and Glossary

ACh - Acetylcholine

Actin - Semiflexible cytoskeletal protein, lends structure and elasticity to cells; polymerized forms can take the shape of either bundles or a crosslinked network

ADP - **A**denosine **di****p**hosphate, a dephosphorylated (lower-energy) version of ATP

Aliquot – (*v.*) To divide a large volume of liquid into many smaller, measured volumes of liquid for later use, and (*n.*) one such smaller volume

AMP - **A**denosine **m**ono**p**hosphate, a doubly dephosphorylated (much-lower-energy) version of ATP

Aplysia - A species of snail commonly used for primary neuronal cultures

Apoptosis - Programmed cell death

-ase - Suffix signifying an enzyme of some sort

ATP - **A**denosine **t**ri**p**hosphate, the primary unit of energy currency in cells

ATPase - Enzyme promoting the hydrolysis of ATP

BDNF - **B**rain-**d**erived **n**eurotrophic **f**actor

C. elegans - *C. elegans*, a transparent worm very useful as a model for *in vivo* studies

CALI - Chromophore-assisted laser inactivation (of proteins)

CaM - Calmodulin

CAM - Cell adhesion molecule

cAMP - Cyclic adenosine monophosphate

Clonal population - Cell population derived from a single progenitor cell

CMF - Saline solution which is **c**alcium- and **m**agnesium-**f**ree

CNS - Central nervous system (*vs.* peripheral nervous system)

Con-A - Concanavalin A

Cytochalasin - A family of proteins that "cap" actin filaments, blocking further polymerization

Cytoskeleton - The polymer network within a cell which acts as a "scaffolding" and gives the cell structure and elasticity; the trio of polymer types of which the cytoskeleton is comprised are actin filaments, microtubules, and intermediate filaments

Dalton (Da, and kilodalton, kDa) - Unit of measure of mass for (usually large) molecules, where 1 Dalton is equal to the mass of one hydrogen atom

Defined medium – Cell or tissue culture medium for which all chemical constituents are exactly defined in identity and concentration; excludes media containing serum

DIC - Differential interference contrast (microscopy)

Differentiation - Process by which stem cells or other pluripotent cell types respond to certain chemical cues by acquiring a specific functionality; in this process, the cells cease to be "immortal" and are ultimately doomed to apoptosis

DMEM - Dulbecco's Modification of Eagle's Medium

DRG - Dorsal root ganglion (= big neuron clump)

Drosophila - *Drosophila melanogaster*, the fruit fly

ECM - **E**xtra**c**ellular **m**atrix

F-12 - Ham's F-12 Medium

F-actin - Filamentous, or polymerized, actin

FALI - Fluorophore-assisted laser inactivation (of proteins)

FBS/FCS - Fetal bovine serum = fetal calf serum

FGF - Fibroblast growth factor

Fibroblast - An undifferentiated tissue precursor cell

G-actin - Globluar, or monomeric, actin

GDP - The dephosphorylated (lower energy) version of GTP

Gene expression - The reflection of a cell's (or organism's) genotype in its phenotype, often stimulated by external factors

GFP - Green fluorescent protein

Glial cell - Cell often found accompanying neurons in organisms; gives structure and scaffolding to neurons (*pl.* glia)

Glioma - Malignantly transformed glial cell

GTP - Guanosine triphosphate, a secondary energy currency in cells

GTPase - Enzyme which promotes hydrolysis of GTP to GDP

Helisoma - A species of snail commonly used for primary cell culture; its name is derived from the spiral shape of its shell

HGF/SF - Hepatocyte growth factor / scatter factor

Hippocampal neurons - Cells taken from the hippocampus (small region of the brain); CNS neurons

Hydrolysis - The splitting of a molecule into two or more smaller parts in a chemical reaction involving the addition of a water molecule

Intermediate filament - A very flexible cytoskeletal protein, too soft to lend any structural support to the cell and believed not to be as involved in cell motility as actin and microtubules

IP_3 - inositol 1,4,5-triphosphate

Laminin - An extracellular matrix (ECM) molecule; promotes cell adhesion

Lymnaea - *Lymnaea stagnalis*, a species of snail commonly used for primary neuron culture

MAG - Myelin-associated glycoprotein

MAP - **M**icrotubule-**a**ssociated **p**rotein

Medium, cell culture - Also called cell medium or culture medium; the nutrient-rich fluid in which cells and tissues are cultured in an incubator; the cells usually attach to a substrate in a culture vessel and then medium is added to the vessel atop the cells

Microfilament - Actin filament

Microtubule (MT) - The least flexible of the cytoskeletal polymers, these are found in the axonal shaft and will occasionally extend outward into the growth cone

Microtubule dynamic instability - A state wherein microtubules are actively polymerizing and depolymerizing from the same end of the filaments (as opposed to treadmilling, polymerizing and depolymerizing from opposite ends of the filaments)

MTA - 5'-deoxy-5'-methylthioadenosine

NCAM - Neural cell adhesion molecule

Neuro2a - An immortalized neuroblastoma cell line

Neuroblastoma - Malignantly transformed neuroblast cell

Neurofilament - Intermediate filament

NgCAM - Neuron-glia cell adhesion molecule

NGF - Nerve growth factor

NG-108 (or NG-108-15) - A mouse neuroblastoma x rat glioma hybrid cell line

NPN - Neuropilin

NT-3 - Neurotrophin 3

-oma - Suffix signifying "malignantly transformed thingy"

Osmolarity - Of a solution, the balance of salts; this is especially important for cell culture medium because in the case of an imbalance, osmotic pressures (positive or negative) will hinder normal cell functions if not damage the cells

PC – Phase-contrast (microscopy)

PC-12 - **P**heo**c**hromocytoma immortalized cell line (derived form rat adrenal gland tumor)

PDZ - PSD-95, Dlg and ZO-1

Phorbol esters – A class of chemical compounds used in cell differentiation

PK[*X*], where *X* is A through G - Protein kinase *X*

PLC-γ - Phospholipase C- **γ**

PLL - Poly-L-Lysine (my abbreviation)

PNS - Peripheral nervous system (*vs.* central nervous system)

Primary cell culture - the culture of mature (differentiated) cells taken directly from an organism

PSD-95 - Postsynaptic density protein of 95 kDa

Robo - Roundabout

Sema - Semaphorin

Sema III - Collapsin-1 / Sema III / D

Serum - A blood-derived mixture of nutrients, often used in cell culture; the exact composition of serum is not precisely defined and medium with serum is called undefined medium

Taxol - A microtubule-stabilizing drug; inhibits MT dynamics

Transfection - The addition of a genetic sequence to the genome of a cell, accomplished by "sneaking" the genetic material in through the cell membrane and nuclear membrane, after which the cell replicates the new sequence along with its own DNA during mitosis

Treadmilling - State of a polymer wherein monomers are being added to one end of a filament and monomers are being lost at the other end of the filament, with the total filament length generally remaining constant

Trituration - Mixing of two fluids or suspensions by repeatedly drawing in and expelling liquid from a (micro)pipette

Undifferentiated cells - Cells which are in an early stage, can reproduce mitotically indefinitely, and which lack specific functionality in an organism; these cells respond to chemical cues in the body, different ones of which can cause the same undifferentiated cell to metamorphose into many different mature cell types; stem cells are undifferentiated, but not all undifferentiated cells are stem cells

Xenopus - *Xenopus laevis*, the African clawed frog, whose embryos are extensively studied and the neurons from whose embryos are often used for primary cell cultures

Bibliography

Aletta, J. M., and Greene, L. A. (1988). Growth cone configuration and advance: a time-lapse study using video-enhanced differential interference contrast microscopy. *Journal of Neuroscience* **8,** 1425-1435.

Ashkin, A. (1970). Acceleration and Trapping of Particles by Radiation Pressure. *Physical Review Letters* **24,** 156-159.

Ashkin, A., and Dziedzic, J. M. (1987). Optical trapping and manipulation of viruses and bacteria. *Science* **235,** 1517-20.

Ashkin, A., Dziedzic, J. M., and Yamane, T. (1987). Optical trapping and manipulation of single cells using infrared laser beams. *Nature* **330,** 769-71.

Atkins, P. W., and DePaula, J. (2002). "Physical chemistry." W. H. Freeman and Company, New York.

Baas, P. W. (1997). Microtubules and axonal growth. *Current Opinion in Cell Biology* **9,** 29-36.

Baas, P. W. (1999). Microtubules and neuronal polarity: lessons from mitosis. *Neuron* **22,** 23-31.

Baas, P. W. (2000). Strategies for studying microtubule transport in the neuron. *Microscopy Research and Technique* **48,** 75-84.

Bar-Ziv, R., Frisch, T., and Moses, E. (1995). Entropic Expulsion in Vesicles. *Physical Review Letters* **75,** 3481-3484.

Bar-Ziv, R., Menes, R., Moses, E., and Safran, S. A. (1995). Local Unbinding of Pinched Membranes. *Physical Review Letters* **75,** 3356-3359.

Bar-Ziv, R., and Moses, E. (1994). Instability and Pearling States Produced in Tubular Membranes by Competition of Curvature and Tension. *Physical Review Letters* **73,** 1392-1395.

Bar-Ziv, R., Moses, E., and Nelson, P. (1998). Dynamic excitations in membranes induced by optical tweezers. *Biophysical Journal* **75,** 294-320.

Bentley, D., and O'Connor, T. P. (1994). Cytoskeletal events in growth cone steering. *Current Opinion in Neurobiology* **4,** 43-8.

Bjorkholm, J. E., Freeman, R. R., Ashkin, A., and Pearson, D. B. (1978). Observation of Focusing of Neutral Atoms by the Dipole Forces of Resonance-Radiation Pressure. *Physical Review Letters* **41,** 1361–1364.

Borgens, R. B., and Bohnert, D. M. (1997). The responses of mammalian spinal axons to an applied DC voltage gradient. *Experimental Neurology* **145,** 376-89.

Bossu, J. L., and Gahwiler, B. H. (1996). Distinct modes of channel gating underlie inactivation of somatic K+ current in rat hippocampal pyramidal cells *in vitro*. *J Physiol* **495,** 383-397.

Bradke, F., and Dotti, C. G. (1998). Membrane traffic in polarized neurons. *Biochimica et Biophysica Acta* **1404,** 245-58.

Bradke, F., and Dotti, C. G. (1999). The role of local actin instability in axon formation. *Science* **283,** 1931-4.

Bray, D., and White, J. G. (1988). Cortical flow in animal cells. *Science* **239,** 883-8.

Britland, S., and McCaig, C. (1996). Embryonic Xenopus neurites integrate and respond to simultaneous electrical and adhesive guidance cues. *Experimental Cell Research* **226,** 31-8.

Buck, K. B., and Zheng, J. Q. (2002). Growth cone turning induced by direct local modification of microtubule dynamics. *Journal of Neuroscience* **22,** 9358-67.

Bush, M. S., Goold, R. G., Moya, F., and Gordon-Weeks, P. R. (1996). An analysis of an axonal gradient of phosphorylated MAP 1B in cultured rat sensory neurons. *European Journal of Neuroscience* **8,** 235-48.

Carlier, M. F., Valentin-Ranc, C., Combeau, C., Fievez, S., and Pantoloni, D. (1994). Actin polymerization: regulation by divalent metal ion and nucleotide binding, ATP hydrolysis and binding of myosin. *Adv Exp Med Biol* **358,** 71-81.

Challacombe, J. F., Snow, D. M., and Letourneau, P. C. (1997). Dynamic microtubule ends are required for growth cone turning to avoid an inhibitory guidance cue. *Journal of Neuroscience* **17,** 3085-95.

Chen, H., Duncan, I. C., Bozorgchami, H., and Lo, S. H. (2002). Tensin1 and a previously undocumented family member, tensin2, positively regulate cell migration. *PNAS USA* **99,** 733-738.

Clark, P., Britland, S., and Connolly, P. (1993). Growth cone guidance and neuron morphology on micropatterned laminin surfaces. *J Cell Sci* **105** (Pt 1), 203-12.

Collins, F., and Lee, M. R. (1984). The spatial control of ganglionic neurite growth by the substrate-associated material from conditioned medium: an experimental model of haptotaxis. *J Neurosci* **4,** 2823-9.

Corey, J. M., Wheeler, B. C., and Brewer, G. J. (1996). Micrometer resolution silane-based patterning of hippocampal neurons: critical variables in photoresist and laser ablation processes for substrate fabrication. *IEEE Trans Biomed Eng* **43,** 944-55.

Dai, J., and Sheetz, M. P. (1995). Axon membrane flows from the growth cone to the cell body. *Cell* **83,** 693-701.

Dai, J., and Sheetz, M. P. (1995). Mechanical properties of neuronal growth cone membranes studied by tether formation with laser optical tweezers. *Biophys J* **68,** 988-96.

Dai, J., and Sheetz, M. P. (1995). Regulation of endocytosis, exocytosis, and shape by membrane tension. *Cold Spring Harb Symp Quant Biol* **60,** 567-71.

den Braber, E. T., de Ruijter, J. E., Smits, H. T. J., Ginsel, L. A., von Recum, A. F., and Jansen, J. A. (1996). Quantitative analysis of cell proliferation and orientation on substrata with uniform parallel surface micro-grooves. *Biomaterials* **17,** 1093-1099.

Dickson, B. J. (2002). Molecular mechanisms of axon guidance.[erratum appears in Science. 2003 Jan 24;299(5606):515]. *Science* **298,** 1959-64.

DiTella, M. C., Feiguin, F., Carri, N., Kosik, K., S,, and Cáceres, A. (1996). MAP-1B/TAU functional redundancy during laminin-enhanced axonal growth. *Journal of Cell Science* **116,** 1175-1186.

Doherty, P., Williams, E., and Walsh, F. S. (1995). A soluble chimeric form of the L1 glycoprotein stimulates neurite outgrowth. *Neuron* **14,** 57-66.

Doi, M., and Edwards, S. F. (1986). "The theory of polymer dynamics." Clarendon Press, Oxford.

Dubey, N., Letourneau, P. C., and Tranquillo, R. T. (1999). Guided neurite elongation and schwann cell invasion into magnetically aligned collagen in simulated peripheral nerve regeneration. *Exp Neurol* **158,** 338-50.

Duncan, A. C., Weisbuch, F., Rouais, F., Lazare, S., and Baquey, C. (2002). Laser microfabricated model surfaces for controlled cell growth. *Biosens Bioelectron* **17,** 413-26.

Duncan, R. L., Kizer, N., Barry, E. L. R., Friedman, P. A., and Hruska, K. A. (2002). Antisense oligodeoxynucleotide inhibition of a swelling-activated cation channel in osteoblast-like osteosarcoma cells. *PNAS USA* **93,** 1864-1869.

Ehrlicher, A., Betz, T., Stuhrmann, B., Koch, D., Milner, V., Raizen, M. G., and Kas, J. (2002). Guiding neuronal growth with light. *PNAS USA* **99,** 16024-8.

Elsner, H. A., Honck, H. H., Willmann, F., Kreienkamp, H. J., and Iglauer, F. (2000). Poor quality of oocytes from Xenopus laevis used in laboratory experiments: prevention by use of antiseptic surgical technique and antibiotic supplementation. *Comp Med* **50,** 206-11.

Esch, T., Lemmon, V., and Banker, G. (1999). Local presentation of substrate molecules directs axon specification by cultured hippocampal neurons. *J Neurosci* **19,** 6417-26.

Forscher, P., and Smith, S. J. (1988). Actions of cytochalasins on the organization of actin filaments and microtubules in a neuronal growth cone. *J Cell Biol* **107,** 1505-16.

Gallo, G. (1998). Involvement of microtubules in the regulation of neuronal growth cone morphologic remodeling. *Journal of Neurobiology* **35,** 121-140.

Gallo, G., Lefcort, F. B., and Letourneau, P. C. (1997). The trkA receptor mediates growth cone turning toward a localized source of nerve growth factor. *J Neurosci* **17,** 5445-54.

Gallo, G., and Letourneau, P. C. (1998). Axon guidance: GTPases help axons reach their targets. *Curr Biol* **8,** R80-2.

Gallo, G., and Letourneau, P. C. (1998). Localized sources of neurotrophins initiate axon collateral sprouting. *J Neurosci* **18,** 5403-14.

Gallo, G., and Letourneau, P. C. (1999). Axon guidance: A balance of signals sets axons on the right track. *Curr Biol* **9,** R490-2.

Gallo, G., and Letourneau, P. C. (1999). Different contributions of microtubule dynamics and transport to the growth of axons and collateral sprouts. *J Neurosci* **19,** 3860-73.

Gallo, G., and Letourneau, P. C. (2000). Neurotrophins and the dynamic regulation of the neuronal cytoskeleton. *J Neurobiol* **44,** 159-73.

Goldberg, D. J., and Burmeister, D. W. (1986). Stages in axon formation: observations of growth cones of Aplysia axons in culture using video-enhanced differential interference contrast microscopy. *Journal of Cell Biology* **104,** 1921-1931.

Gordan, J. D., Attardi, B. J., and Pfaff, D. W. (1998). Mathematical exploration of pulsatility in cultured gonadotropin-releasing hormone neurons. *Neuroendocrinology* **67,** 2-17.

Gordon-Weeks, P. R. (1991). Control of microtubule assembly in growth cones. *J Cell Sci Suppl* **15,** 45-9.

Gordon-Weeks, P. R. (1991). Evidence for microtubule capture by filopodial actin filaments in growth cones. *Neuroreport* **2,** 573-6.

Gordon-Weeks, P. R. (1991). Growth cones: the mechanism of neurite advance. *Bioessays* **13,** 235-9.

Gordon-Weeks, P. R. (1991). Microtubule organization in growth cones. *Biochem Soc Trans* **19,** 1080-5.

Gordon-Weeks, P. R. (2004). Microtubules and growth cone function. *J Neurobiol* **58,** 70-83.

Gordon-Weeks, P. R., and Fischer, I. (2000). MAP1B expression and microtubule stability in growing and regenerating axons. *Microsc Res Tech* **48,** 63-74.

Guck, J., Ananthakrishnan, R., Mahmood, H., Moon, T. J., Cunningham, C. C., and Kas, J. (2001). The optical stretcher: a novel laser tool to micromanipulate cells. *Biophys J* **81,** 767-84.

Guck, J., Ananthakrishnan, R., Moon, T. J., Cunningham, C. C., and Kas, J. (2000). Optical deformability of soft biological dielectrics. *Phys Rev Lett* **84,** 5451-4.

Gundersen, R. W., and Barrett, J. N. (1979). Neuronal chemotaxis: chick dorsal-root axons turn toward high concentrations of nerve growth factor. *Science* **206,** 1079-80.

Hale, G. M., and Querry, M. R. (1973). Optical constants of water in the 200-nm to 200-mm wavelength region. *Applied Optics* **12,** 555-563.

Hammarback, J. A., McCarthy, J. B., Palm, S. L., Furcht, L. T., and Letourneau, P. C. (1988). Growth cone guidance by substrate-bound laminin pathways is correlated with neuron-to-pathway adhesivity. *Dev Biol* **126,** 29-39.

Hamprecht, B. (1977). Structural, electrophysiological, biochemical and pharmacological properties of neuroblastoma-glioma cell hybrids in cell culture. *International Review of Cytology* **49,** 99-170.

Hamprecht, B., Glaser, T., Reiser, G., Bayer, E., and Propst, F. (1985). Culture and characteristics of hormone-responsive neuroblastoma X glioma hybrid cells. *Methods Enzymol* **109,** 316-41.

Haugland, R. P. (2002). "Handbook of fluorescent probes and research products." Molecular Probes, Inc., Eugene, OR.

Hays, W. L. (1994). "Statistics." Wadsworth Publishing, Fort Worth.

Holm, A., Sundqvist, T., Oberg, A., and Magnusson, K. E. (1999). Mechanical manipulation of polymorphonuclear leukocyte plasma membranes with optical tweezers causes influx of extracellular calcium through membrane channels. *Med Biol Eng Comput* **37,** 410-2.

Hong, K., Nishiyama, M., Henley, J., Tessier-Lavigne, M., and Poo, M. (2000). Calcium signalling in the guidance of nerve growth by netrin-1. *Nature* **403,** 93-8.

Huglin, M. B. (1972). Light scattering from polymer solutions. In "Physical Chemistry: A Series of Monographs" (E. M. Loebl, Ed.). Academic Press, London.

James, C. D., Davis, R., Meyer, M., Turner, A., Turner, S., Withers, G., Kam, L., Banker, G., Craighead, H., Isaacson, M., Turner, J., and Shain, W. (2000). Aligned microcontact printing of micrometer-scale poly-L-lysine structures for controlled growth of cultured neurons on planar microelectrode arrays. *IEEE Trans Biomed Eng* **47,** 17-21.

Jay, D. G. (1988). Selective destruction of protein function by chromophore-assisted laser inactivation. *Proc Natl Acad Sci U S A* **85,** 5454-8.

Jay, D. G., and Keshishian, H. (1990). Laser inactivation of fasciclin I disrupts axon adhesion of grasshopper pioneer neurons. *Nature* **348,** 548-50.

Katz, M. J. (1985). Axonal branch shapes. *Brain Res* **361,** 70-6.

Katz, M. J. (1985). How straight do axons grow? *J Neurosci* **5,** 589-95.

Kirschner, M., and Mitchison, T. (1986). Beyond self-assembly: from microtubules to morphogenesis. *Cell* **45,** 329-42.

Kirschner, M. W., and Mitchison, T. (1986). Microtubule dynamics. *Nature* **324,** 621.

Kratochvíl, P. (1987). "Classical light scattering from polymer solutions." Elsevier Science Publishers, Amsterdam.

Lamoureux, P., Zheng, J., Buxbaum, R. E., and Heidemann, S. R. (1992). A cytomechanical investigation of neurite growth on different culture surfaces. *J Cell Biol* **118,** 655-61.

Langenfeld-Oster, B., Dorlochter, M., and Wernig, A. (1993). Regular and photodamage-enhanced remodelling in vitally stained frog and mouse neuromuscular junctions. *J Neurocytol* **22,** 517-30.

Lee, J., Ishihara, A., Oxford, G., Johnson, B., and Jacobson, K. (1999). Regulation of cell movement is mediated by stretch-activated calcium channels. *Nature* **400,** 382-6.

Lee, T., and Luo, L. (1999). Mosaic analysis with a repressible cell marker for studies of gene function in neuronal morphogenesis. *Neuron* **22,** 451-61.

Lee, W. L., Ostap, E. M., Zot, H. G., and Pollard, T. D. (1999). Organization and ligand binding properties of the tail of Acanthamoeba myosin-IA. Identification of an actin-binding site in the basic (tail homology-1) domain. *J Biol Chem* **274,** 35159-71.

Letourneau, P. C. (1979). Cell-substratum adhesion of neurite growth cones, and its role in neurite elongation. *Exp Cell Res* **124,** 127-38.

Letourneau, P. C. (1979). Inhibition of intercellular adhesion by concanavalin A is associated with concanavalin A-mediated redistribution of surface receptors. *J Cell Biol* **80,** 128-40.

Letourneau, P. C. (1983). Differences in the organization of actin in the growth cones compared with the neurites of cultured neurons from chick embryos. *J Cell Biol* **97,** 963-73.

Liao, J. C., Roider, J., and Jay, D. G. (1994). Chromophore-assisted laser inactivation of proteins is mediated by the photogeneration of free radicals. *Proc Natl Acad Sci U S A* **91,** 2659-63.

Lin, C. H., and Forscher, P. (1993). Cytoskeletal remodeling during growth cone-target interactions. *J Cell Biol* **121,** 1369-83.

Maingret, F., Fosset, M., Lesage, F., Lazdunski, M., and Honore, E. (1999). TRAAK is a mammalian neuronal mechano-gated K^+ channel. *J Biol Chem* **274,** 1381-7.

Mansfield, E. (1986). "Basic Statistics with Applications." W. W. Norton & Company, Inc., New York.

McCaig, C. D., and Stewart, R. (1992). The effects of melanocortins and electrical fields on neuronal growth. *Exp Neurol* **116,** 172-9.

Mellon, P. L., Windle, J. J., Goldsmith, P. C., Padula, C. A., Roberts, J. L., and Weiner, R. I. (1990). Immortalization of hypothalamic GnRH neurons by genetically targeted tumorigenesis. *Neuron* **5,** 1-10.

Mikhailov, A. V., and Gundersen, G. G. (1998). Relationship between microtubule dynamics and lamellipoduim formation revealed by direct imaging of microtubules in cells treated with nocodazole or taxol. *Cell Motility & the Cytoskeleton* **41,** 325-340.

Ming, G., Song, H., Berninger, B., Inagaki, N., Tessier-Lavigne, M., and Poo, M. (1999). Phospholipase C-gamma and phosphoinositide 3-kinase mediate cytoplasmic signaling in nerve growth cone guidance. *Neuron* **23,** 139-48.

Munck, S., Bedner, P., Bottaro, T., and Harz, H. (2004). Spatiotemporal properties of cytoplasmic cyclic AMP gradients can alter the turning behaviour of neuronal growth cones. *Eur J Neurosci* **19,** 791-7.

Nisenbaum, E. S., Wilson, C. J., Foehring, R. C., and Surmeier, D. J. (1996). Isolation and characterization of a persistent potassium current in neostriatal neurons. *J Neurophysiol* **76,** 1180-1194.

Odde, D. J., Tanaka, E. M., Hawkins, S. S., and Buettner, H. M. (1996). Stochastic dynamics of the nerve growth cone and its microtubules during neurite outgrowth. *Biotechnology and Bioengineering* **50,** 452-461.

Oliva, A. A., Jr., James, C. D., Kingman, C. E., Craighead, H. G., and Banker, G. A. (2003). Patterning axonal guidance molecules using a novel strategy for microcontact printing. *Neurochem Res* **28,** 1639-48.

Patel, N. B., and Poo, M. M. (1984). Perturbation of the direction of neurite growth by pulsed and focal electric fields. *J Neurosci* **4,** 2939-47.

Paves, H., and Saarma, M. (1997). Neurotrophins as *in vitro* growth cone guidance molecules for embryonic sensory neurons. *Cell Tissue Res* **290,** 285-97.

Pellegrini, M., Menconi, M. C., and Pellegrino, M. (2001). Stretch-activated cation channels of leech neurons exhibit two activity modes. *Eur J Neurosci* **13,** 503-511.

Peterman, E. J., Gittes, F., and Schmidt, C. F. (2003). Laser-induced heating in optical traps. *Biophys J* **84,** 1308-16.

Rajnicek, A., Britland, S., and McCaig, C. (1997). Contact guidance of CNS neurites on grooved quartz: influence of groove dimensions, neuronal age and cell type. *J Cell Sci* **110** (Pt 23), 2905-13.

Rajnicek, A., and McCaig, C. (1997). Guidance of CNS growth cones by substratum grooves and ridges: effects of inhibitors of the cytoskeleton, calcium channels and signal transduction pathways. *J Cell Sci* **110** (Pt 23), 2915-24.

Ramón y Cajal, S. (1890). A quelle époque apparaissent les expansions des cellules nerveuses de la moelle épinière du poulet. *Anat. Anz.* **5,** 609-613, 631-639.

Rivas, R. J., Burmeister, D. W., and Goldberg, D. J. (1992). Rapid effects of laminin on the growth cone. *Neuron* **8,** 107-15.

Rochlin, M. W., Dailey, M. E., and Bridgman, P. C. (1999). Polymerizing microtubules activate site-directed F-actin assembly in nerve growth cones. Molecular Biology of the *Cell* **10,** 2309-2327.

Rochlin, M. W., Wickline, K. M., and Bridgman, P. C. (1996). Microtubule stability decreases axon elongation but not axoplasm production. *J Neurosci* **16,** 3236-46.

Rogers, S. L., Letourneau, P. C., Palm, S. L., McCarthy, J., and Furcht, L. T. (1983). Neurite extension by peripheral and central nervous system neurons in response to substratum-bound fibronectin and laminin. *Dev Biol* **98,** 212-20.

Rosania, G. R., and Swanson, J. A. (1996). Microtubules can modulate pseudopod activity from a distance inside macrophages. *Cell Motility & the Cytoskeleton* **34,** 230-245.

Sachs, F. (1986). Biophysics of mechanoreception. *Membr Biochem* **6,** 173-95.

Schmidt, C. E., Shastri, V. R., Vacanti, J. P., and Langer, R. (1997). Stimulation of neurite outgrowth using an electrically conducting polymer. *Proc Natl Acad Sci U S A* **94,** 8948-53.

Schmitt, K. E. (2003). Optical neuronal guiding on the hypothalamic GnRH cell line GT1. Thesis (M.A.), University of Texas at Austin, Austin, TX.

Schuessler, H. A., Mershin, A., Kolomenskii, A. A., and Nanopoulos, D. V. (2003). Surface plasmon resonance study of the actin-myosin sarcomeric complex and tubulin dimers. *Journal of Modern Optics* **50,** 2381-2391.

Sigurdson, W. J., and Morris, C. E. (1989). Stretch-activated ion channels in growth cones of snail neurons. *J Neurosci* **9,** 2801-8.

Sive, H. L., Grainger, R. M., and Harland, R. M. (2000). "Early development of Xenopus laevis: A Laboratory Manual." Cold Spring Harbor Laboratory Press, New York.

Smalheiser, N. R. (1989). Analysis of slow-onset neurite formation in NG108-15 cells: implications for a unified model of neurite elongation. *Brain Res Dev Brain Res* **45,** 49-57.

Smalheiser, N. R. (1989). Morphologic plasticity of rapid-onset neurites in NG108-15 cells stimulated by substratum-bound laminin. *Brain Res Dev Brain Res* **45,** 39-47.

Smalheiser, N. R. (1990). Cell attachment and neurite stability in NG108-15 cells: effects of 5'-deoxy, 5'-methyl thioadenosine (MTA) compared with laminin, kinase inhibitor H-7, and Mn^{2+} ions. *Brain Res Dev Brain Res* **51,** 153-60.

Smalheiser, N. R. (1991). Role of laminin in stimulating rapid-onset neurites in NG108-15 cells: relative contribution of attachment and motility responses. *Brain Res Dev Brain Res* **62,** 81-9.

Smalheiser, N. R. (1993). Monensin-sensitive cellular events modulate neurite extension on laminin: an example of higher-order regulation of cell motility. *Cell Motil Cytoskeleton* **24,** 256-63.

Smalheiser, N. R., Crain, S. M., and Reid, L. M. (1984). Laminin as a substrate for retinal axons *in vitro*. *Brain Res* **314,** 136-40.

Smith, S. J. (1988). Neuronal cytomechanics: the actin-based motility of growth cones. *Science* **242,** 708-715.

Song, H., Ming, G., He, Z., Lehmann, M., McKerracher, L., Tessier-Lavigne, M., and Poo, M. (1998). Conversion of neuronal growth cone responses from repulsion to attraction by cyclic nucleotides. *Science* **281,** 1515-8.

Song, H. J., Ming, G. L., and Poo, M. M. (1997). cAMP-induced switching in turning direction of nerve growth cones. *Nature* **388,** 275-9.

Song, H. J., and Poo, M. M. (1999). Signal transduction underlying growth cone guidance by diffusible factors. *Curr Opin Neurobiol* **9,** 355-63.

Spitzer, N. C., and Lamborghini, J. E. (1976). The development of the action potential mechanism of amphibian neurons isolated in culture. *Proc Natl Acad Sci U S A* **73,** 1641-5.

Stenger, D. A., Hickman, J. J., Bateman, K. E., Ravenscroft, M. S., Ma, W., Pancrazio, J. J., Shaffer, K., Schaffner, A. E., Cribbs, D. H., and Cotman, C. W. (1998). Microlithographic determination of axonal/dendritic polarity in cultured hippocampal neurons. *J Neurosci Methods* **82,** 167-73.

Stepien, E., Stanisz, J., and Korohoda, W. (1999). Contact guidance of chick embryo neurons on single scratches in glass and on underlying aligned human skin fibroblasts. *Cell Biol Int* **23,** 105-16.

Stracke, R., Bohm, K. J., Wollweber, L., Tuszynski, J. A., and Unger, E. (2002). Analysis of the migration behaviour of single microtubules in electric fields. *Biochem Biophys Res Commun* **293,** 602-9.

Stuhrmann, B. (2002). Optical control of neuronal growth. Thesis (M.A.), University of Texas at Austin, Austin, TX.

Suter, D. M., Errante, L. D., Belotserkovsky, V., and Forscher, P. (1998). The Ig superfamily cell adhesion molecule, apCAM, mediates growth cone steering by substrate-cytoskeletal coupling. *J Cell Biol* **141,** 227-40.

Suter, D. M., and Forscher, P. (1998). An emerging link between cytoskeletal dynamics and cell adhesion molecules in growth cone guidance. *Curr Opin Neurobiol* **8,** 106-16.

Suter, D. M., and Forscher, P. (2000). Substrate-cytoskeletal coupling as a mechanism for the regulation of growth cone motility and guidance. *Journal of Neurobiology* **44,** 97-113.

Tanaka, E., Ho, T., and Kirschner, M. W. (1995). The role of microtubule dynamics in growth cone motility and axonal growth. *J Cell Biol* **128,** 139-55.

Tanaka, E., and Kirschner, M. W. (1995). The role of microtubules in growth cone turning at substrate boundaries. *J Cell Biol* **128,** 127-37.

Tanaka, E. M., and Kirschner, M. W. (1991). Microtubule behavior in the growth cones of living neurons during axon elongation. *J Cell Biol* **115,** 345-63.

Taylor, J. R. (1982). "An Introduction to Error Analysis." University Science Books, Mill Valley, CA.

Tessier-Lavigne, M., and Goodman, C. S. (1996). The molecular biology of axon guidance. *Science* **274,** 1123-33.

Vitalis, E. A., Costantin, J. L., Tsai, P. S., Sakakibara, H., Paruthiyil, S., Iiri, T., Martini, J. F., Taga, M., Choi, A. L., Charles, A. C., and Weiner, R. I. (2000). Role of the cAMP signaling pathway in the regulation of gonadotropin-releasing hormone secretion in GT1 cells. *Proc Natl Acad Sci U S A* **97,** 1861-6.

Vogt, A. K., Stefani, F. D., Best, A., Nelles, G., Yasuda, A., Knoll, W., and Offenhausser, A. (2004). Impact of micropatterned surfaces on neuronal polarity. *J Neurosci Methods* **134,** 191-8.

Weiner, R. I., and Martinez de la Escalera, G. (1993). Pulsatile release of gonadotrophin releasing hormone (GnRH) is an intrinsic property of GT1 GnRH neuronal cell lines. *Hum Reprod* **8 Suppl 2,** 13-7.

Weiner, R. I., and Charles, A. (2001). Regulation of gonadotropin-releasing hormone release by cyclic AMP signalling pathways. *Growth Horm IGF Res* **11 Suppl A,** S9-15.

Williamson, T., Gordon-Weeks, P. R., Schachner, M., and Taylor, J. (1996). Microtubule reorganization is obligatory for growth cone turning. *Proc Natl Acad Sci U S A* **93,** 15221-6.

Yu, W., and Baas, P. W. (1995). The growth of the axon tip is not dependent upon net microtubule assembly at its distal tip. *Journal of Neuroscience* **15,** 6827-6833.

Zakharenko, S., and Popov, S. (1998). Dynamics of axonal microtubules regulate the topology of new membrane insertion into the growing neurites. *J Cell Biol* **143,** 1077-86.

Zeck, G., and Fromherz, P. (2001). Noninvasive neuroelectronic interfacing with synaptically connected snail neurons immobilized on a semiconductor chip. *Proc Natl Acad Sci U S A* **98,** 10457-62.

Zheng, J., Buxbaum, R. E., and Heidemann, S. R. (1994). Measurements of growth cone adhesion to culture surfaces by micromanipulation. *J Cell Biol* **127,** 2049-60.

Zheng, J., Lamoureux, P., Santiago, V., Dennerll, T., Buxbaum, R. E., and Heidemann, S. R. (1991). Tensile regulation of axonal elongation and initiation. *J Neurosci* **11,** 1117-25.

Zheng, J. Q. (2000). Turning of nerve growth cones induced by localized increases in intracellular calcium ions. *Nature* **403,** 89-93.

Zheng, J. Q., Felder, M., Connor, J. A., and Poo, M. M. (1994). Turning of nerve growth cones induced by neurotransmitters. *Nature* **368,** 140-4.

Zheng, J. Q., Zheng, Z., and Poo, M. (1994). Long-range signaling in growing neurons after local elevation of cyclic AMP-dependent activity. *J Cell Biol* **127,** 1693-701.

Zhou, F. Q., and Cohan, C. S. (2001). Growth cone collapse through coincident loss of actin bundles and leading edge actin without actin depolymerization. *J Cell Biol* **153,** 1071-84.

Zhou, F. Q., Waterman-Storer, C. M., and Cohan, C. S. (2002). Focal loss of actin bundles causes microtubule redistribution and growth cone turning. *J Cell Biol* **157,** 839-849.

Zhou, Q., Xiao, M., and Nicoll, R. A. (2001). Contribution of cytoskeleton to the internalization of AMPA receptors. *PNAS U S A* **98,** 1261-6.

Vita

Samantha A. Moore was born on April 4, 1975, to Vassilia S. Moore and Robert J. Moore, in New York, NY, and moved to Texas as soon as possible. In the intervening years, she completed secondary school at St. Andrew's-Sewanee School (St. Andrews, TN), and attended Oberlin College (Oberlin, OH) before earning a baccalaureate degree in physics from Eckerd College (St. Petersburg, FL). Her undergraduate research (1998-2000), characterizing the beam produced by a pulsed arc cluster ion source, was conducted under the supervision of Anne J. Cox, and her preliminary graduate work (2000-2002), under the supervision of Josef A. Käs, involved measuring the laser-induced deformation of viscoelastic biological dielectrics. Her dissertation research (2002-2004), on the dynamics of laser-induced neuron guidance, has been supervised by Mark G. Raizen, and her future plans involve an attempt to survive four more years of postgraduate education before embarking on a professional career. She now lives with her husband in Texas and flosses daily.

Permanent address: 2002-A Guadalupe Street #259
Austin, Texas 78705 USA

This dissertation was typed by the author.